

Low Order Multivariable Adaptive Control

by

Rienk Bakker

M.S., Mechanical Engineering
University of Twente (1989)

Submitted to the Department of Mechanical Engineering
in partial fulfillment of the requirements for the degree of

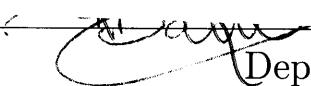
Doctor of Philosophy

at the

Massachusetts Institute of Technology

February 1996

© Massachusetts Institute of Technology 1996. All rights reserved.

Author  _____
Department of Mechanical Engineering
December 11, 1995

Certified by _____
Anuradha M. Annaswamy
Assistant Professor
Thesis Supervisor

Accepted by  _____
Ain. A. Sonin
Chairman, Department Graduate Committee
Eng.

MASSACHUSETTS INSTITUTE
OF TECHNOLOGY

MAR 19 1996

[Handwritten signature]

Low Order Multivariable Adaptive Control

by

Rienk Bakker

Submitted to the Department of Mechanical Engineering
on December 11, 1995, in partial fulfillment of the
requirements for the degree of
Doctor of Philosophy

Abstract

Adaptive control refers to the control of systems that have poorly known parameters but a well modeled structure. The adaptive control of linear, time-invariant systems is well understood. However, for systems with multiple inputs and multiple outputs the adaptive controller is of high order and complex making the approach inapplicable in a number of practical problems.

In this thesis a new approach to adaptive control of multivariable plants is proposed. The proposed controller is of lower order and contains fewer on-line adjustable parameters than other adaptive control methods. For designing the multivariable adaptive controller, the order of the plant is not required to be known. The minimum row relative degrees of the plant transfer function matrix are assumed not to exceed two. A stability proof based on positive realness of the underlying system dynamics is given. Since in practice unmodeled dynamics may be present, a robustified adaptive control algorithm is presented. A proof is given that shows that loop signals remain bounded when unmodeled dynamics are excited.

The control approach is well suited to the control of distributed systems which have a high modal density and use multiple inputs and outputs. Two applications are discussed, flexible structures and combustion. In the flexible structure application it is shown that tracking can be achieved in the presence of on-line introduced parametric uncertainties. Using an adaptive version of the internal model principle, attenuation of external disturbances of unknown frequency is accomplished as well. In the combustion application it is shown that unstable pressure modes can be stabilized in the presence of parametric uncertainties in the model and changes in the operating point.

Thesis Supervisor: Anuradha M. Annaswamy
Title: Assistant Professor

Acknowledgments

I would like to express my sincere gratitude to my thesis advisor, Professor Anaswamy. Her inspiration, persistence and appreciation of rigor have contributed significantly to this dissertation. These last three and a half years, during which I worked with her, have been a great learning experience. In addition, I thank Professors Asada, Hardt and Athans for their time and effort in serving on my thesis committee. Their comments raised in the committee meetings made me look at my work from different viewpoints.

My thanks go to students of the adaptive control laboratory, Ssu-Hsin Yu, Fredrik Skantze, Steingrimur Karason and Kathy Misovec, who have made my stay in the lab truly enjoyable. Also, I would like to acknowledge the moral support of Ali Taalebi and Nate Delson during the first years of my stay at MIT.

I am forever grateful to my dear wife Aya for her continuous support and encouragements. It is because of her that I have been able to successfully complete this endeavour.

Contents

Nomenclature	9
1 Introduction	11
1.1 Motivation	11
1.2 Contribution of Thesis	13
1.3 Previous Work	14
1.4 Synopsis of Thesis	14
2 Mathematical Preliminaries	15
2.1 Introduction	15
2.2 Definitions and Results	15
2.3 Parameterization of Closed Loop Dynamics	19
3 Low Order Controller Structures	35
3.1 Introduction	35
3.2 Singlevariable Systems	36
3.2.1 Compensator Design	37
3.2.2 Disturbance Rejection	38
3.3 Multivariable Systems	39
3.4 Structure for Feedforward Control	47
3.5 Summary	52
4 The Low Order Adaptive Controller	53
4.1 Introduction	53

4.2	The Adaptive Control Algorithm	54
4.3	The Robustified Adaptive Control Algorithm	63
4.4	Summary	74
5	Application to Vibration Systems	75
5.1	Introduction	75
5.2	Flexible Structures	78
5.2.1	Introduction	78
5.2.2	Motivation	78
5.2.3	Dynamic Model	80
5.2.4	Sample Structure	81
5.2.5	Tracking Example	82
5.2.6	Disturbance Rejection Example	97
5.2.7	Unmodeled Dynamics Example	106
5.2.8	Discussion	112
5.3	Control of an unstable Combustion System	115
5.3.1	Introduction	115
5.3.2	Motivation	115
5.3.3	Dynamic Model	117
5.3.4	Example	127
5.3.5	Discussion	138
5.4	Summary	139
6	Conclusion	141
	References	145
A	Discretization of the Combustor Equations	151
A.1	Introduction	151
A.2	Discretization	151
A.3	Reduced Mode Superposition	158
A.4	Mean Heat and Mean Flow	161

Nomenclature

\mathbb{C}^-	Open left half complex plane
$\mathcal{R}^{m_1 \times m_2}(s)$	Set of $m_1 \times m_2$ matrices whose elements are rational functions of s
$\lambda(A)$	Spectrum of a square matrix A
$\bar{\lambda}(A)$	$\lambda(A) \setminus \{0\}$
$\lambda_i(A)$	i^{th} eigenvalue of a square matrix A
K	High frequency gain matrix of $G(s) \in \mathcal{R}^{m \times m}(s)$
E	If E is non-singular then $E = K \in \mathbb{R}^{m \times m}$
$r_i = r_i[G(s)]$	Minimal relative degree in the i^{th} row of $G(s) \in \mathcal{R}^{m \times m}(s)$
ν	Observability index
$ x _2$	Euclidean norm of $x \in \mathbb{R}^n$
$ A _F$	Frobenius norm of a matrix $A \in \mathbb{R}^{n \times m}$
$\ f\ = \ f\ _\infty$	Infinity norm of $f : \mathbb{R}^+ \rightarrow \mathbb{R}^n$

Chapter 1

Introduction

1.1 Motivation

Adaptive control refers to the automatic control of partially known systems. When controlling a physical process, the control design engineer rarely knows the process characteristics exactly. The characteristics of the process can change with time due to a variety of factors and there may also be unforeseen changes in the environment in which the system operates. Conventional control design methods may not be able to achieve satisfactory performance in the entire range over which the characteristics of the process may vary. Adaptive control methods are developed to accommodate this uncertainty in the plant and environment explicitly.

A significant part of the field of adaptive control addresses dynamic systems that have parametric uncertainties. These uncertainties are due to for example errors in the model parameters, on-line changes in the plant parameters or changes in the operating conditions. The adaptive control of linear, single-input single-output (SISO), time-invariant (LTI) systems with unknown plant parameters but known structure is currently well understood [24, 47]. Several extensions to adaptive control theory have been attempted to include time-variations, unmodeled dynamics and nonlinearities in the plant. These extensions are known as robust adaptive control. The development of adaptive control emphasized initially SISO systems and it was only later that a theory for multi-input multi-output (MIMO) systems was developed.

Adaptive control of multivariable, square, LTI plants usually requires that the following assumptions are satisfied [47, 59]:

- (I) An upperbound on the observability index ν of the plant is known.
- (II) The right Hermite normal form of the plant is known.
- (III) The transmission zeros of the plant lie in \mathbb{C}^- .
- (IV) An adaptation gain matrix Γ can be found such that $K_p\Gamma = (K_p\Gamma)^T > 0$, where K_p is the high frequency gain matrix of the plant.

These conditions are similar to the assumptions made in the SISO case. The assumptions for the MIMO case are more restrictive however, and it was recognized early on that the main issues in multivariable adaptive control are the reduction of the prior knowledge of the system while keeping good convergence and stability properties, and the reduction of the number of parameters to be estimated [18, 19]. For certain applications, assumptions (II) and (IV) imply significant prior information regarding the plant structure and its parameters, and considerable research effort has been spent in trying to relax these assumptions (see for example [15, 45, 62]). On the other hand, for high order plants, assumption (I) implies that the requisite adaptive controller will be of high order, and complex. For example, the number of adjustable parameters for a Model Reference Adaptive Control (MRAC) scheme is at least $2nm$ where n is the order of the plant and m is the number of inputs and outputs. The order of the adaptive controller is at least $2(n - m)$. Also, the complexity of MRAC control algorithms increases if plants are considered whose Hermite normal form contains terms of order higher than one. In applications such as the control of distributed systems, assumption (I) may never be satisfied since the true system is infinite-dimensional. Even if based on bandwidth considerations an estimate of the observability index is used, this estimate can be high so that the complexity of the requisite controller becomes too large making it infeasible to implement. Furthermore, using this estimate, stability of the adaptive controller can not be guaranteed beforehand. As in the SISO case, modifications for robustness of MIMO adaptive control algorithms have been

developed as well [59]. However, the additional complexity introduced in the modified adaptation algorithm compounds the feasibility problem considerably.

1.2 Contribution of Thesis

The main contribution of this thesis is that it provides an alternate approach to the design of adaptive controllers for multivariable systems. The controller developed is of lower order and has fewer on-line adjustable parameters than other multivariable adaptive control methods making the approach practically viable. Compared to other multivariable adaptive control schemes, the method provides more insight into the adaptive control design. Selected parameters can be tuned on-line resulting in better transient performance. The theory underlying the adaptive control design is presented. Conditions for which the underlying passivity properties hold are derived rigorously. This derivation is based on the properties multivariable root-loci, and the analysis of the associated input-output properties.

Another contribution of this thesis is the stability-robustness of the adaptive control algorithm. A modification of the adaptive laws such that bounded signals are obtained in case unmodeled dynamics are excited is given. The modifications are such that they are practically feasible, also for the multivariable case. A rigorous robust-stability proof is given.

A third contribution is the application of the proposed low order adaptive controller to distributed systems. Two examples are given. The first example is the control of a flexible structure. Tracking can be accomplished in the presence of significant on-line introduced parametric uncertainties. Also, attenuation of band limited, uncertain external disturbances can be accomplished. The second example is the control of a combustion process. In the presence of parametric modeling errors and over a wide range of operating points, open loop unstable pressure modes can be stabilized.

1.3 Previous Work

The development of low order adaptive controllers for SISO plants was considered in [13, 26, 43]. The nature of these controllers is such that they can not be put in a broader framework that addresses the design of low order adaptive controllers. Furthermore, robustness characteristics of these controllers are extremely difficult, if not impossible, to establish. Multivariable extensions of these controllers have been reported in [7, 31]. However, these multivariable controllers are restricted to plants with no unmodeled dynamics, for which the Hermite normal form is diagonal with order one transfer functions on the diagonal, or require prior knowledge of the range in which the plant parameter values lie. The latter requirement implies significant prior information regarding the plant to be controlled. The class of plants that will be considered in this thesis is significantly larger than that in [7, 31], and the adaptive control algorithm requires less prior information.

1.4 Synopsis of Thesis

In Chapter 2 mathematical preliminaries are given that summarize the stability concepts used throughout the thesis, and some preliminary derivations are given whose result will be used in Chapter 3. In Chapter 3 the fixed controller underlying the adaptive controller is discussed. In Chapter 4 the low order adaptive controller is presented, and its stability proof is given. In Chapter 4 a modification for robustness of the adaptive algorithm is presented as well. In Chapter 5 the applicability of the control method to vibration systems is investigated, and simulation results are presented. Conclusions are given in Chapter 6.

Chapter 2

Mathematical Preliminaries

2.1 Introduction

In this chapter the mathematical tools used in the following chapters are presented. The literature on the analysis and design of adaptive systems is extensive, see for example [24, 47]. It is not the objective of this Chapter to review this literature, but rather to present known results that are most relevant to the work presented in this thesis. These results are presented in section 2.2. In section 2.3 a new parameterization of a linear time-invariant dynamic system is presented. This parameterization is crucial in determining the assumptions for which the adaptive control algorithm presented in Chapter 4 will be stable.

2.2 Definitions and Results

The adaptive control theory presented in this thesis is based primarily on Lyapunov stability theory and the concept of positive dynamic systems. For a discussion of Lyapunov theory, see for example [47, 57, 60]. Here we will focus on positive dynamic systems. A positive dynamic system is an extension to dynamic systems of the concept of positivity. Positivity is a necessary and sufficient condition for a mathematical object to be factorizable as a product. The theory of positive systems can be used to establish links between the time and frequency domains. In what follows,

first frequency domain definitions of positive dynamic systems will be given, then a well known result that relates the frequency domain conditions to the time domain description of a dynamic system will be presented.

Definition 1 [49] $H(s) \in \mathcal{R}^{m \times m}(s)$ is Positive Real (PR) if

1. The elements of $H(s)$ are analytic in $Re[s] > 0$,
2. $H^*(s) = H^T(s^*)$,
3. $H(s) + H^*(s) \geq 0$ in $Re[s] > 0$,

where $*$ denotes the complex conjugate transpose. •

The first condition requires the input-output relation described by $H(s)$ to be stable. The second condition says that $H(s)$ must be physically realizable. For example, condition 2 requires that the coefficients of s on the diagonal of $H(s)$ are real. The second condition implies that $H(s) + H^*(s)$ is Hermitian ¹. In what follows we will assume that this realizability condition is always satisfied. The third condition refers to the positivity of $H(s)$. Historically, Definition 1 is motivated by electrical networks consisting of only resistors, capacitors and inductances. $H(s)$ is then the admittance or impedance matrix of an electrical N-port. It can be shown that the energy output of $H(s)$ is never larger than the energy input. The following definition of strict positive realness is stronger than the concept of positive realness.

Definition 2 [48] A rational matrix $H(s)$ is Strictly Positive Real (SPR) if $H(s - \epsilon)$ is PR for some $\epsilon > 0$. •

For an electrical network, this stronger notion of positivity is obtained when each capacitor is replaced by a parallel connection of a capacitor and a (large) resistor, and when each inductance is replaced by a series combination of an inductance with a (small) resistance. It can be shown that the energy output of $H(s)$ is always strictly

¹ $A(s) \in \mathcal{R}^{m \times m}(s)$ is Hermitian if $A(s) = A^*(s)$. A Hermitian matrix is square and its diagonal values are real. The eigenvalues of a Hermitian matrix are always real. If x is a complex valued vector, then x^*Ax is real.

less than the energy input to $H(s)$. Definition 2 is sometimes referred to as a strong definition of SPRness [38].

Definition 2 requires evaluation of $H(s)$ over the closed right half plane, and is therefore not practical for analysis purposes. This motivates the following result.

Lemma 1 [58, 63] $H(s) \in \mathcal{R}^{m \times m}(s)$ is SPR if

1. the elements of $H(s)$ are analytic in $\text{Re}[s] \geq 0$,
2. there exists a scalar $\delta > 0$ such that $H(j\omega) + H^*(j\omega) \geq \delta I \forall \omega \in \mathbb{R}$. •

It is worth noting that these conditions are sufficient only. For both necessary and sufficient conditions for SPR multivariable systems see [58].

Next the frequency domain positivity properties of $H(s)$ are related to the time domain description of $H(s)$. Let the minimal state-space representation of $H(s) \in \mathcal{R}^{m \times m}(s)$ be given by

$$\begin{aligned} \dot{x} &= Ax + Bu \\ y &= Cx + Du \end{aligned}$$

where $A \in \mathbb{R}^{n \times n}$, $B \in \mathbb{R}^{n \times m}$, $C \in \mathbb{R}^{m \times n}$ and $D \in \mathbb{R}^{m \times m}$.

Lemma 2 (Lefschetz-Kalman-Yakubovich Lemma) [35, 58, 63] $H(s)$ is SPR, and the elements of $H(s)$ are analytic in $\text{Re}[s] > -\rho$ iff there exist matrices $P = P^T > 0$, L , K and a scalar $\nu > 0$ such that

$$\begin{aligned} A^T P + PA &= -LL^T - 2\rho P \\ B^T P + K^T L^T &= C \\ K^T K &= D + D^T. \end{aligned}$$

The importance of this Lemma is not only that it provides the choice of the Lyapunov function, $V(x(t)) = x(t)^T P x(t)$, but it also relates the input matrix B to the output matrix C . This fact is essential to the adaptive control design presented in Chapter 4. This ends the discussion on positivity of linear dynamic systems. In the remaining part of this section definitions and results are given that pertain specifically to adaptive control theory. •

In SISO adaptive control system design the relative degree plays a crucial role. In generalizing the notion of relative degree of a SISO transfer function to the multi-variable case, the right Hermite normal form is used [47]. By performing elementary column operations, a non-singular ² matrix $G(s) \in \mathcal{R}^{m \times m}(s)$ can be transformed into a canonical lower triangular structure called the right Hermite normal form. This operation is equivalent to multiplying $G(s)$ from the right by an unimodular ³ matrix $U(s)$ such that

$$G(s)U(s) = H(s).$$

The matrix $H(s)$ is lower triangular and is of the form

$$H(s) = \begin{bmatrix} \frac{1}{(s+a)^{r_1}} & & & \\ h_{21}(s) & \frac{1}{(s+a)^{r_2}} & & \\ \vdots & \vdots & \ddots & \\ h_{m1}(s) & h_{m2}(s) & \dots & \frac{1}{(s+a)^{r_m}} \end{bmatrix},$$

where $h_{ij}(s) = \frac{\delta_{ij}(s)}{(s+a)^{r_i}}$ is proper, $\delta_{ij}(s)$ depends on the parameters of $G(s)$.

Closely associated with the relative degree of a SISO transfer function $g(s)$ is the notion of the high frequency gain defined as

$$k \triangleq \lim_{s \rightarrow \infty} s^r g(s), \quad k \in \mathbb{R},$$

where r denotes the relative degree of $g(s)$. The multivariable generalization of the high frequency gain is the high frequency gain matrix defined as

$$K \triangleq \lim_{s \rightarrow \infty} H^{-1}(s)G(s), \quad K \in \mathbb{R}^{m \times m}.$$

In general, the high frequency gain matrix depends in a complex fashion on the parameters of $G(s)$. The following Lemma gives a condition which simplifies the expression for the high frequency gain matrix considerably. Let $E \in \mathbb{R}^{m \times m}$ where

² $G(s)$ non-singular means that $\det(G(s))$ is not identically zero for all s .

³A matrix $U(s) \in \mathcal{R}^{m \times m}(s)$ is unimodular if it is non-singular and its determinant does not depend on s .

the i^{th} row E_i of $E = E[G(s)]$ is determined as $E_i = \lim_{s \rightarrow \infty} s^{r_i} G_i(s)$ where $G_i(s)$ is the i^{th} row in $G(s)$.

Lemma 3 [47] If E is non-singular then $K = E$ and $H(s)$ is diagonal. •

Hence, if E is non-singular then the high-frequency gain matrix K depends only on the minimum relative degrees in the rows of $G(s)$ and the associated scalar high frequency gains.

2.3 Parameterization of Closed Loop Dynamics

The dynamics underlying the adaptive systems that are considered in this thesis are described by

$$\begin{aligned}\dot{x} &= Ax + Bu \\ y &= Cx,\end{aligned}$$

where $A \in \mathbb{R}^{n \times n}$, $B \in \mathbb{R}^{n \times m}$ and $C \in \mathbb{R}^{m \times n}$, or $y(s) = G(s)u(s)$ where

$$G(s) = C(sI - A)^{-1}B. \quad (2.1)$$

We will assume that the control inputs are independent, i.e. $\text{rank}(B) = m$. Similarly, we assume that the measurements are independent, $\text{rank}(C) = m$.

Using static output feedback of the form $u = -\theta\Theta y + r$ where $\theta \in \mathbb{R}$, $\Theta \in \mathbb{R}^{m \times m}$ and $r : \mathbb{R}^+ \rightarrow \mathbb{R}^m$ is a reference signal, the closed loop dynamics is given by

$$\begin{aligned}\dot{x} &= (A - B\theta\Theta C)x + Br \\ y &= Cx,\end{aligned} \quad (2.2)$$

or $y(s) = \overline{W}_m(s)Kr(s)$ where K denotes the high frequency gain matrix of $G(s)$, and

$$\overline{W}_m(s) = C(sI - A + B\theta\Theta C)^{-1}BK^{-1}. \quad (2.3)$$

The transfer function matrix given in Eq. (2.3) appears as one of the subsystems in the overall adaptive control system discussed in this thesis. In this section an alternate

parameterization of $\overline{W}_m(s)$ in Eq. (2.3) is given. The parameterization that follows is tied in a large measure to the spectral decomposition of $B\theta\Theta C$. In [32, 33, 39] the decomposition of $B\theta\Theta C$ is used to analyze the root-locus of MIMO systems, similar to the root-locus analysis for SISO systems due to W. R. Evans. The contribution of the parameterization derived below is that it not only considers the closed loop pole locations, but also the input-output relation of the closed loop system. The specific properties of the closed loop input-output map are derived in Chapter 3.

The parameterization will be derived under the assumption that $r_i[G(s)] = 1$ or 2 ($i = 1, 2, \dots, m$) and $E[G(s)]$ is non-singular. This implies that the zero eigenvalues of $CB\Theta$ appear in diagonal form for a suitably chosen Θ . It then follows that if $CB\Theta$ is rank deficient by d degrees then $CB\Theta$ has d zero eigenvalues. The spectral decomposition of $B\Theta C$ is then given by the following Theorem.

Theorem 1 Let $\text{rank}(CB\Theta) = (m - d)$. The spectral decomposition of $B\theta\Theta C$ is then given by

$$B\theta\Theta C = \begin{bmatrix} U_1 & U_2 & M_1 \end{bmatrix} \begin{bmatrix} \theta J_1 & & \\ & \theta J_2 & \\ & & 0_{(n-m-d) \times (n-m-d)} \end{bmatrix} \begin{bmatrix} V_1 \\ V_2 \\ N_1 \end{bmatrix}. \quad (2.4)$$

$J_1 \in \mathbb{R}^{(m-d) \times (m-d)}$ is a Jordan block with the nonzero eigenvalues of $B\Theta C$. The Jordan block $J_2 \in \mathbb{R}^{2d \times 2d}$ contains the zero eigenvalues of $B\Theta C$ in Jordan form and is described by

$$J_2 = \text{diag}(J^1 \quad J^2 \quad \dots \quad J^d) \quad \text{where} \quad J^i = \begin{bmatrix} 0 & 1 \\ 0 & 0 \end{bmatrix} \quad i = 1, \dots, d.$$

The columns of $U_1, V_1^T \in \mathbb{R}^{n \times (m-d)}$ are the right and left eigenvectors associated with J_1 . $U_2, V_2^T \in \mathbb{R}^{n \times 2d}$ are associated with J_2 and are given by

$$\begin{aligned} U_2 &= [u_1^0 \quad u_1^1 \quad u_2^0 \quad u_2^1 \quad \dots \quad u_d^0 \quad u_d^1] \\ V_2 &= [v_1^1 \quad v_1^0 \quad v_2^1 \quad v_2^0 \quad \dots \quad v_d^1 \quad v_d^0]^T. \end{aligned} \quad (2.5)$$

The true eigenvectors associated with J_2 are

$$\begin{aligned} M_2 &= [u_1^0 \quad u_2^0 \quad \dots \quad u_d^0] \\ N_2 &= [v_1^0 \quad v_2^0 \quad \dots \quad v_d^0]^T, \end{aligned} \tag{2.6}$$

and the pseudo eigenvectors associated with J_2 are

$$\begin{aligned} U &= [u_1^1 \quad u_2^1 \quad \dots \quad u_d^1] \\ V &= [v_1^1 \quad v_2^1 \quad \dots \quad v_d^1]^T. \end{aligned} \tag{2.7}$$

The true and pseudo eigenvectors are related by

$$\begin{aligned} B\Theta C U &= M_2 \\ V B\Theta C &= N_2. \end{aligned} \tag{2.8}$$

The columns of $M_1, N_1^T \in \mathbb{R}^{n \times (n-m-d)}$ are the right and left null vectors associated with the $(n-m-d)$ zero eigenvalues in diagonal form. •

Proof: It is easy to show that $\bar{\lambda}(CB\Theta) = \bar{\lambda}(B\Theta C)$. Since $\text{rank}(CB\Theta) = (m-d)$, we have that $\lambda_i(CB\Theta) = \lambda_i(B\Theta C)$ for $\lambda_i \neq 0$ and $i = 1, \dots, (m-d)$. Hence, $B\Theta C$ has $(m-d)$ independent right and left eigenvectors associated with these nonzero eigenvalues which are described by U_1 and V_1 . Also, if $\mathcal{U}_1, \mathcal{V}_1, \mathcal{B}$ and \mathcal{C} denote the range space of respectively U_1, V_1^T, B and C^T it follows that

$$\mathcal{U}_1 \subset \mathcal{B}, \quad \mathcal{V}_1 \subset \mathcal{C}.$$

Because $CB\Theta$ is rank deficient by d degrees, $B\Theta C$ must have a $(n-m+d)$ dimensional nullspace. The kernel $M \in \mathbb{R}^{n \times (n-m+d)}$ and left nullspace $N \in \mathbb{R}^{(n-m+d) \times n}$ of $B\Theta C$ satisfy

$$B\Theta C M = 0, \quad N B\Theta C = 0. \tag{2.9}$$

The range spaces of M and N^T we will denote by \mathcal{M} and \mathcal{N} , respectively. We have that $\mathcal{U}_1 \cap \mathcal{M} = 0$ and $\mathcal{V}_1 \cap \mathcal{N} = 0$, but $\mathcal{B} \cap \mathcal{M} \neq 0$ and $\mathcal{C} \cap \mathcal{N} \neq 0$. Hence $\mathcal{B} \oplus \mathcal{M}$ and $\mathcal{C} \oplus \mathcal{N}$ do not span $\mathbb{R}^{n \times n}$ completely. In fact, \mathcal{B} and \mathcal{M} , and \mathcal{C} and \mathcal{N} have a

d -dimensional intersection as will be shown next. Since $CB\Theta$ is rank deficient by d degrees there exists a kernel $\widetilde{M} \in \mathbb{R}^{m \times d}$ of $CB\Theta$ so that $CB\Theta\widetilde{M} = 0$. Because $B\Theta$ has full rank this implies that there exists a kernel $M_2 \in \mathbb{R}^{n \times d}$ of C such that

$$M_2 = B\Theta\widetilde{M}. \quad (2.10)$$

The range space of M_2 we will denote by \mathcal{M}_2 . Since $CM_2 = 0$, $\mathcal{M}_2 \subset \mathcal{M}$. Eq. (2.10) implies that $\mathcal{M}_2 \subset \mathcal{B}$, hence $\mathcal{M}_2 = \mathcal{B} \cap \mathcal{M}$. It then follows that \mathcal{M} can be partitioned into a d -dimensional subspace \mathcal{M}_2 and a $(n - m - d)$ dimensional subspace \mathcal{M}_1 where $\mathcal{M}_1 \cap \mathcal{B} = 0$. If the columns of M_1 span \mathcal{M}_1 , we may order M such that

$$M = [M_2 \quad M_1]. \quad (2.11)$$

Using similar arguments N can be partitioned into

$$N = \begin{bmatrix} N_2 \\ N_1 \end{bmatrix} \quad (2.12)$$

such that \mathcal{N}_1 , the subspace spanned by the columns of N_1^T , lies outside \mathcal{C} , while \mathcal{N}_2 , defined by the columns of N_2^T , lies in \mathcal{C} . The decomposition into M_1 and N_1 in Eq. (2.4) follows from Eqs. (2.9)–(2.12). Furthermore, since $B\Theta C$ has $(m - d)$ nonzero eigenvalues and the rank of $B\Theta C$ is m , the spectral decomposition of $B\Theta C$ has a Jordan block $J_2 \in \mathbb{R}^{2d \times 2d}$ with zero eigenvalues and $\text{rank}(J_2) = d$. The corresponding right and left eigenvectors are denoted by U_2 and V_2^T . The structure of J_2 can be specified further by considering the nullspaces M_2 and N_2 . Since $M_2 = B\Theta\widetilde{M}$, there are d vectors which lie in the range space of B and in the kernel of $B\Theta C$. Hence, there exists a $U \in \mathbb{R}^{n \times d}$ such that Eq. (2.8) is satisfied. Similar for $V \in \mathbb{R}^{d \times n}$. It follows that the $2d \times 2d$ Jordan block J_2 can be divided into d 2×2 Jordan blocks. Since M_2 is the kernel of C , the columns of M_2 are the true right eigenvectors. Similarly, the true left eigenvectors are the columns of N_2^T . With the eigenvectors associated with J_2 defined as in Eq. (2.5), the particular structure of J_2 implies that M_2 and N_2 are given by Eq. (2.6) and U and V are given by Eq. (2.7). \square

Before presenting the new parameterization of $\overline{W}_m(s)$, the following Lemmas are needed. In these Lemmas the high frequency gain matrix and the transmission zeros of $G(s)$ are expressed in terms of the left nullspaces of B , M_i ($i = 1, 2$), the right nullspaces of C , N_i ($i = 1, 2$), and the left nullspace of CB , $N^{(1)}$.

Lemma 4 If $G(s)$ in Eq. (2.1) is such that $r_i[G(s)] = 1$ or 2 and $E[G(s)]$ is non-singular, then

$$\begin{aligned} E[G(s)] &= K = CB + N^p CAB \\ &= CB + CUN_2AB \\ &= [CU_1 \quad CU] \begin{bmatrix} I_{d \times d} & 0 \\ N_2AU_1 & N_2AM_2 \end{bmatrix} \begin{bmatrix} V_1B \\ VB \end{bmatrix}, \end{aligned}$$

where $N^p = N^{(1)T}(N^{(1)}N^{(1)T})^{-1}N^{(1)}$. •

Proof: (i) $E[G(s)] = CB + N^p CAB$

Using Newton's Binomial Theorem, we have

$$\lim_{s \rightarrow \infty} G(s) = \lim_{s \rightarrow \infty} C(sI - A)^{-1}B = \lim_{s \rightarrow \infty} C \left[\frac{1}{s}(I + \frac{1}{s}A + \frac{1}{s^2}A^2 + \dots) \right] B, \quad (2.13)$$

so that $E[G(s)] = CB + X$ where X is a constant matrix with zero rows where CB has nonzero rows. Since $E[G(s)]$ is non-singular the zero eigenvalues of CB appear in diagonal form only. Let CB be rank deficient by d degrees, the spectral decomposition of CB is then given by

$$CB = [U^{(1)} \quad M^{(1)}] \begin{bmatrix} \Lambda_{1(m-d) \times (m-d)} & \\ & 0_{d \times d} \end{bmatrix} \begin{bmatrix} V^{(1)} \\ N^{(1)} \end{bmatrix}$$

where Λ_1 is the Jordan block with nonzero eigenvalues of CB . We can rearrange the inputs and outputs so that we have

$$CB = \begin{bmatrix} (CB)_1_{(m-d) \times m} \\ 0_{d \times m} \end{bmatrix} \quad \text{and} \quad CAB = \begin{bmatrix} (CAB)_1_{(m-d) \times m} \\ (CAB)_2_{d \times m} \end{bmatrix}. \quad (2.14)$$

Since $rank(CB)_1 = m - d$, it is not hard to see that $N^{(1)} = [0_{d \times (m-d)} \quad N_2^{(1)}]$ where

$N_2^{(1)} \in \mathbb{R}^{d \times d}$ is non-singular. Hence

$$N^p = \begin{bmatrix} \mathbf{0}_{(m-d) \times (m-d)} & \\ & I_{d \times d} \end{bmatrix},$$

so that

$$CB + N^p CAB = \begin{bmatrix} (CB)_1 \\ (CAB)_2 \end{bmatrix}.$$

Also, using Eqs. (2.13) and (2.14), we have that

$$E[G(s)] = \lim_{s \rightarrow \infty} \begin{bmatrix} (CB)_1 + \frac{1}{s}(CAB)_1 \\ (CAB)_2 \end{bmatrix} = \begin{bmatrix} (CB)_1 \\ (CAB)_2 \end{bmatrix}.$$

(ii) $E[G(s)] = CB + CUN_2AB$

Since $N^{(1)}CB = 0$ and C has full rank we have that $N^{(1)}C = N_2$. Furthermore, since $VB\Theta C = N_2$ and $VB\Theta CU = I$, we also have $N_2U = I_{d \times d}$ and $N^{(1)}CU = I$. Let $N^{(1)}$ be such that

$$CU = N^{(1)T} (N^{(1)}N^{(1)T})^{-1},$$

then

$$\begin{aligned} E[G(s)] &= CB + N^p CAB \\ &= CB + N^{(1)T} (N^{(1)}N^{(1)T})^{-1} N^{(1)} CAB \\ &= CB + CUN_2AB. \end{aligned}$$

(iii) $E[G(s)] = [CU_1 \quad CU] \begin{bmatrix} I_{d \times d} & 0 \\ N_2AU_1 & N_2AM_2 \end{bmatrix} \begin{bmatrix} V_1B \\ VB \end{bmatrix}.$

Define the permutation matrices $T_v \in \mathbb{R}^{2d \times 2d}$ and $T_u \in \mathbb{R}^{2d \times 2d}$ such that

$$T_v V_2 = \begin{bmatrix} V \\ N_2 \end{bmatrix}, \quad U_2 T_u = [U \quad M_2]. \quad (2.15)$$

It is not hard to show that

$$T_v T_u = \begin{bmatrix} 0 & I_{d \times d} \\ I_{d \times d} & 0 \end{bmatrix}.$$

The orthogonality of the eigenvectors in the decomposition, Theorem 1, implies that

$$\begin{aligned} I = U_1V_1 + U_2V_2 + M_1N_1 &= U_1V_1 + U_2T_u(T_vT_u)^{-1}T_vV_2 + M_1N_1 \\ &= U_1V_1 + UN_2 + M_2V + M_1N_1. \end{aligned} \quad (2.16)$$

By expanding $E[G(s)]$ we have that

$$\begin{aligned} E[G(s)] &= CU_1V_1B + CUN_2A(U_1V_1 + M_2V)B \\ &= C(I - UN_2 + M_2V + M_1N_1)B + CUN_2A(I - UN_2 + M_1N_1)B \\ &= CB + CUN_2AB. \end{aligned}$$

□

It follows from Lemma 4 that if $E[G(s)]$ is non-singular then N_2AM_2 is invertible. The transmission zeros of the system can then be expressed using the decomposition as well, which is done in Lemma 5.

Lemma 5 Let the transmission zeros of $G(s)$ be defined as $\lambda(A_z)$. If $G(s)$ in Eq. (2.1) is such that $r_i[G(s)] = 1$ or 2 and $E[G(s)]$ is non-singular, then

1. $A_z = N_1AM_1$ when $\text{rank}(CB) = m$.
2. $A_z = N_1AM_1 - N_1AM_2(N_2AM_2)^{-1}N_2AM_1$ when $\text{rank}(CB) \leq (m - 1)$. •

Proof: Let z be a multivariable zero. By definition $\text{rank}(S(z)) < (n + m)$ where

$$S(z) = \begin{bmatrix} zI - A & -B \\ C & 0 \end{bmatrix}.$$

Define

$$L = \begin{bmatrix} N & 0 \\ (B^TB)^{-1}B^T & 0 \\ 0 & I_{d \times d} \end{bmatrix}, \quad R = \begin{bmatrix} M & C^T(CC^T)^{-1} & 0 \\ 0 & 0 & I_{d \times d} \end{bmatrix}.$$

Both $L \in \mathbb{R}^{(n+m) \times (n+m)}$ and $R \in \mathbb{R}^{(n+m) \times (n+m)}$ have full rank. The matrix $LS(z)R$

loses rank iff

$$|N(zI - A)M| = \begin{vmatrix} -N_2AM_2 & -N_2AM_1 \\ -N_1AM_2 & zI - N_1AM_1 \end{vmatrix} = 0.$$

If CB has full rank it follows immediately that $\lambda_i(A_z) = \lambda_i(N_1AM_1)$ define the multivariable zeros. If CB is rank deficient the multivariable zeros are the eigenvalues of $A_z = N_1AM_1 - N_1AM_2(N_2AM_2)^{-1}N_2AM_1$ using Schur's formula [23]. \square

The spectral decomposition given in Theorem 1, together with the alternative expressions for the high frequency gain matrix of $G(s)$ in Lemma 4 and the transmission zeros of $G(s)$ in Lemma 5, can be used in similarity transforms that lead to a new parameterization of the closed loop transfer function matrix $\bar{W}_m(s)$. This parameterization is given in Theorem 2.

Theorem 2 Let $\bar{W}_m(s)$ be given by Eq. (2.3), if $G(s)$ in Eq. (2.1) is such that $r_i[G(s)] = 1$ or 2 and $E[G(s)]$ is non-singular then an alternate parameterization of $\bar{W}_m(s)$ is given by

$$\bar{W}_m(s) = [sI - CU_1V_1AU_1(CU_1)^{-1} + \theta K\Theta - V_1AM_1(sI - A_z)^{-1}N_1AU_1]^{-1} \quad (2.17)$$

when $\text{rank}(CB) = m$, and by

$$\begin{aligned} \bar{W}_m(s) = & [CUA_2s^2 + (CU_1A_1 + \mathcal{D} + R_1)s + \theta K\Theta + R_2 + \\ & (R_3 + R_4s)(sI - A_z)^{-1}(R_5 + R_6s)]^{-1} \end{aligned} \quad (2.18)$$

when $\text{rank}(CB) \leq (m - 1)$. •

Proof: The minimal state-space representation of $y(s) = \bar{W}_m(s)Kr(s)$ is given by Eq. (2.2). We need θJ_1 and θJ_2 in Eq. (2.4) to appear explicitly in the state equations. This can be accomplished if we pre- and postmultiply Eq. (2.2) with the left- and right eigenvectors and make use of the fact that the eigenvectors are orthogonal,

$$\begin{bmatrix} V_1 \\ V_2 \\ N_1 \end{bmatrix} [U_1 \quad U_2 \quad M_1] = I_{n \times n}.$$

Hence, transform the closed loop dynamics by substituting $x = Tv$ in Eq. (2.2) where

$$T = [U_1 \quad U_2 \quad M_1] \quad \text{and} \quad T^{-1} = \begin{bmatrix} V_1 \\ V_2 \\ N_1 \end{bmatrix}. \quad (2.19)$$

The similarity transform of Eq. (2.2) is then given by

$$\begin{aligned} \dot{v} &= T^{-1}(A - \theta B\Theta C)Tv + T^{-1}Br \\ y &= CTv \end{aligned} \quad (2.20)$$

or using Theorem 1, Eq. (2.4),

$$\begin{aligned} \begin{bmatrix} \dot{v}_1 \\ \dot{v}_2 \\ \dot{v}_3 \end{bmatrix} &= \begin{bmatrix} V_1AU_1 - \theta J_1 & V_1AU_2 & V_1AM_1 \\ V_2AU_1 & V_2AU_2 - \theta J_2 & V_2AM_1 \\ N_1AU_1 & N_1AU_2 & N_1AM_1 \end{bmatrix} \begin{bmatrix} v_1 \\ v_2 \\ v_3 \end{bmatrix} + \begin{bmatrix} V_1B \\ V_2B \\ 0 \end{bmatrix} r \\ y &= [CU_1 \quad CU_2 \quad 0] \begin{bmatrix} v_1 \\ v_2 \\ v_3 \end{bmatrix}. \end{aligned} \quad (2.21)$$

Starting from Eq. (2.21), we will present the two cases $\text{rank}(CB) = m$ and $\text{rank}(CB) \leq (m - 1)$.

Case (i) $\text{rank}(CB) = m$

Since CB , and therefore $CB\Theta$, has full rank, the assumption that the zero eigenvalues of $CB\Theta$ appear in diagonal form is trivially satisfied. Eq. (2.21) can then be reduced to

$$\begin{aligned} \begin{bmatrix} \dot{v}_1 \\ \dot{v}_3 \end{bmatrix} &= \begin{bmatrix} V_1AU_1 - \theta J_1 & V_1AM_1 \\ N_1AU_1 & A_z \end{bmatrix} \begin{bmatrix} v_1 \\ v_3 \end{bmatrix} + \begin{bmatrix} V_1B \\ 0 \end{bmatrix} r \\ y &= [CU_1 \quad 0] \begin{bmatrix} v_1 \\ v_3 \end{bmatrix}. \end{aligned}$$

This can be transformed further by choosing $v = T_w w$ where

$$v = \begin{bmatrix} v_1 \\ v_3 \end{bmatrix}, \quad T_w = \begin{bmatrix} (CU_1)^{-1} & 0 \\ 0 & I \end{bmatrix} \quad \text{and} \quad w = \begin{bmatrix} w_1 \\ w_2 \end{bmatrix}.$$

This results in

$$\begin{bmatrix} \dot{w}_1 \\ \dot{w}_2 \end{bmatrix} = \begin{bmatrix} CU_1V_1AU_1(CU_1)^{-1} - \theta CB\Theta & V_1AM_1 \\ N_1AU_1 & A_z \end{bmatrix} \begin{bmatrix} w_1 \\ w_2 \end{bmatrix} + \begin{bmatrix} I \\ 0 \end{bmatrix} CBr$$

$$y = [I \ 0] \begin{bmatrix} w_1 \\ w_2 \end{bmatrix}.$$

With $y(s) = \bar{W}_m(s)CBr(s)$, $\bar{W}_m(s)$ is given by Eq. (2.17).

Case (ii) $rank(CB) \leq (m-1)$

If CB hence $CB\Theta$ is rank deficient by d degrees, a subsequent manipulation of Eq. (2.21) rearranges the $2d \times 2d$ Jordan block J_2 into a $d \times d$ identity matrix and into a $d \times d$ zero matrix. This rearrangement is accomplished by using the permutation matrices T_v and T_u , defined in Eq. (2.15), in the transformation matrices defined as

$$F_v = \text{diag}(I_{(m-d) \times (m-d)}, T_v, I_{(n-m-d) \times (n-m-d)}),$$

$$F_u = \text{diag}(I_{(m-d) \times (m-d)}, T_u, I_{(n-m-d) \times (n-m-d)}).$$

Let $v = F_u u$ in Eq. (2.20) and premultiply the system equation with F_v . The system in Eq. (2.20) becomes

$$\begin{bmatrix} I & 0 & 0 & 0 \\ 0 & 0 & I & 0 \\ 0 & I & 0 & 0 \\ 0 & 0 & 0 & I \end{bmatrix} \begin{bmatrix} \dot{u}_1 \\ \dot{u}_2 \\ \dot{u}_3 \\ \dot{u}_4 \end{bmatrix} = \begin{bmatrix} V_1AU_1 - \theta J_1 & V_1AU & V_1AM_2 & V_1AM_1 \\ VAU_1 & VAU - \theta I & VAM_2 & VAM_1 \\ N_2AU_1 & N_2AU & N_2AM_2 & N_2AM_1 \\ N_1AU_1 & N_1AU & N_1AM_2 & N_1AM_1 \end{bmatrix} \begin{bmatrix} u_1 \\ u_2 \\ u_3 \\ u_4 \end{bmatrix} + \begin{bmatrix} V_1B \\ VB \\ 0 \\ 0 \end{bmatrix} r \quad (2.22)$$

$$y = [CU_1 \ CU \ 0 \ 0] \begin{bmatrix} u_1 \\ u_2 \\ u_3 \\ u_4 \end{bmatrix}.$$

Next, we introduce a transformation $u = G_\tau p$ which results in a matrix A_z represent-

ing the transmission zeros on the lower diagonal of the system matrix. G_r is given by

$$G_r = \begin{bmatrix} I_{(m-d) \times (m-d)} & 0 & 0 & 0 \\ 0 & I_{d \times d} & 0 & 0 \\ 0 & 0 & (N_2 A M_2)^{-1} & -(N_2 A M_2)^{-1} N_2 A M_1 \\ 0 & 0 & 0 & I_{(n-m-d) \times (n-m-d)} \end{bmatrix}.$$

If we substitute $u = G_r p$ in Eq. (2.22), we obtain

$$\begin{bmatrix} I & 0 & 0 & 0 \\ 0 & 0 & (N_2 A M_2)^{-1} & -(N_2 A M_2)^{-1} N_2 A M_1 \\ 0 & I & 0 & 0 \\ 0 & 0 & 0 & I \end{bmatrix} \begin{bmatrix} \dot{p}_1 \\ \dot{p}_2 \\ \dot{p}_3 \\ \dot{p}_4 \end{bmatrix} = \begin{bmatrix} V_1 A U_1 - \theta J_1 & V_1 A U \\ V A U_1 & V A U - \theta I \\ N_2 A U_1 & N_2 A U \\ N_1 A U_1 & N_1 A U \end{bmatrix} + \begin{bmatrix} V_1 A M_2 (N_2 A M_2)^{-1} & V_1 A M_1 - V_1 A M_2 (N_2 A M_2)^{-1} N_2 A M_1 \\ V A M_2 (N_2 A M_2)^{-1} & V A M_1 - V A M_2 (N_2 A M_2)^{-1} N_2 A M_1 \\ I & 0 \\ N_1 A M_2 (N_2 A M_2)^{-1} & A_z \end{bmatrix} \begin{bmatrix} p_1 \\ p_2 \\ p_3 \\ p_4 \end{bmatrix} + \begin{bmatrix} V_1 B \\ V B \\ 0 \\ 0 \end{bmatrix} r \quad (2.23)$$

$$y = [C U_1 \quad C U \quad 0 \quad 0] \begin{bmatrix} p_1 \\ p_2 \\ p_3 \\ p_4 \end{bmatrix}. \quad (2.24)$$

To obtain the high frequency gain in the input matrix and an identity in the output matrix, we perform two additional transformations. First, we premultiply Eq. (2.23) with G_l where

$$G_l = \begin{bmatrix} I_{(m-d) \times (m-d)} & 0 & 0 & 0 \\ N_2 A U_1 & N_2 A M_2 & 0 & 0 \\ 0 & 0 & I_{d \times d} & 0 \\ 0 & 0 & 0 & I_{(n-m-d) \times (n-m-d)} \end{bmatrix}.$$

We then obtain

$$\begin{aligned}
& \begin{bmatrix} I & 0 & 0 & 0 \\ N_2AU & 0 & I & -N_2AM_2 \\ 0 & I & 0 & 0 \\ 0 & 0 & 0 & I \end{bmatrix} \begin{bmatrix} \dot{p}_1 \\ \dot{p}_2 \\ \dot{p}_3 \\ \dot{p}_4 \end{bmatrix} = \begin{bmatrix} V_1AU_1 - \theta J_1 & V_1AU \\ Q_1 & Q_2 \\ N_2AU_1 & N_2AU \\ N_1AU_1 & N_1AU \\ V_1AM_2(N_2AM_2)^{-1} & V_1AM_1 - V_1AM_2(N_2AM_2)^{-1}N_2AM_1 \\ Q_3 & Q_4 \\ I & 0 \\ N_1AM_2(N_2AM_2)^{-1} & A_z \end{bmatrix} \begin{bmatrix} p_1 \\ p_2 \\ p_3 \\ p_4 \end{bmatrix} \\
& + \begin{bmatrix} V_1B \\ N_2AU_1V_1B + N_2AM_2VB \\ 0 \\ 0 \end{bmatrix} r. \tag{2.25}
\end{aligned}$$

where

$$\begin{aligned}
Q_1 &= N_2AU_1(V_1AU_1 - \theta J_1) + N_2AM_2VAU_1 \\
Q_2 &= N_2AU_1V_1AU + N_2AM_2(VAU - \theta I) \\
Q_3 &= N_2AU_1V_1AM_2(N_2AM_2)^{-1} + N_2AM_2VAM_2(N_2AM_2)^{-1} \\
Q_4 &= N_2AU_1(V_1AM_1 - V_1AM_2(N_2AM_2)^{-1}N_2AM_1) + \\
& \quad N_2AM_2(VAM_1 - VAM_2(N_2AM_2)^{-1}N_2AM_1).
\end{aligned}$$

Next, we define

$$[CU_1 \quad CU]^{-1} = \begin{bmatrix} A_1 \\ A_2 \end{bmatrix} \quad \text{and} \quad \begin{bmatrix} V_1B \\ VB \end{bmatrix}^{-1} = [B_1 \quad B_2]$$

where $A_1 \in \mathbb{R}^{(m-d) \times m}$, $A_2 \in \mathbb{R}^{d \times m}$, $B_1 \in \mathbb{R}^{m \times (m-d)}$ and $B_2 \in \mathbb{R}^{m \times d}$, and substitute

$p = T_w w$ in Eq. (2.25) and Eq. (2.24) where

$$T_w = \begin{bmatrix} A_1 & 0 & 0 \\ A_2 & 0 & 0 \\ 0 & I_{d \times d} & 0 \\ 0 & 0 & I_{(n-m-d) \times (n-m-d)} \end{bmatrix} \quad \text{and} \quad w = \begin{bmatrix} w_1 \\ w_2 \\ w_3 \end{bmatrix}.$$

Eqs. (2.25) and (2.24) become

$$\begin{bmatrix} CU_1 A_1 + CUN_2 AUA_1 & CU & -CUN_2 AM_2 \\ A_2 & 0 & 0 \\ 0 & 0 & I \end{bmatrix} \begin{bmatrix} \dot{w}_1 \\ \dot{w}_2 \\ \dot{w}_3 \end{bmatrix} = \begin{bmatrix} Q_5 & Q_6 & Q_7 \\ N_2 AU_1 A_1 + N_2 AUA_2 & I & 0 \\ N_1 AU_1 A_1 + N_1 AUA_2 & N_1 AM_2 (N_2 AM_2)^{-1} & A_z \end{bmatrix} \begin{bmatrix} w_1 \\ w_2 \\ w_3 \end{bmatrix} + \begin{bmatrix} CU_1 V_1 B + CUN_2 AU_1 V_1 B + CUN_2 AM_2 VB \\ 0 \\ 0 \end{bmatrix} r$$

$$y = [I \quad 0 \quad 0] \begin{bmatrix} w_1 \\ w_2 \\ w_3 \end{bmatrix}$$

where

$$\begin{aligned} Q_5 &= CU_1(V_1 AU_1 - \theta J_1)A_1 + CU_1 V_1 AUA_2 + \\ &\quad CU\{N_2 AU_1(V_1 AU_1 - \theta J_1) + N_2 AM_2 V AU_1\}A_1 + \\ &\quad CU\{N_2 AU_1 V_1 AU + N_2 AM_2(V AU - \theta I)\}A_2 \\ Q_6 &= CU_1 V_1 AM_2 (N_2 AM_2)^{-1} + CUN_2 AU_1 V_1 AM_2 (N_2 AM_2)^{-1} + \\ &\quad CUN_2 AM_2 V AM_2 (N_2 AM_2)^{-1} \\ Q_7 &= (CU_1 + CUN_2 AU_1)(V_1 AM_1 - V_1 AM_2 (N_2 AM_2)^{-1} N_2 AM_1) + \\ &\quad CUN_2 AM_2 (V AM_1 - V AM_2 (N_2 AM_2)^{-1} N_2 AM_1). \end{aligned}$$

We note that the first term in the input matrix can be written as

$$CU_1V_1B + CUN_2AU_1V_1B + CUN_2AM_2VB = CB + CUN_2AB = K$$

from Lemma 4 and Eq. (2.16). If we differentiate w_1 twice and eliminate w_2 and \dot{w}_2 , then the input r appears in a second order differential equation in w_1 given by

$$\begin{aligned} CUA_2\ddot{w}_1 + (CU_1A_1 + \mathcal{D} + R_1)\dot{w}_1 + [\theta K\Theta + R_2]w_1 + R_3w_3 + R_4\dot{w}_3 &= Kr \\ \dot{w}_3 - A_2w_3 - R_5w_1 - R_6\dot{w}_1 &= 0 \\ y &= w_1, \end{aligned} \tag{2.26}$$

where

$$\begin{aligned} \mathcal{D} &= -K \begin{bmatrix} B_1 & B_2 \end{bmatrix} \begin{bmatrix} V_1AM_2(N_2AM_2)^{-1} \\ VAM_2(N_2AM_2)^{-1} \end{bmatrix} A_2 \\ R_1 &= CU \begin{bmatrix} N_2AU - N_2AU_1 & N_2AU \end{bmatrix} \begin{bmatrix} A_1 \\ A_2 \end{bmatrix} \\ R_2 &= K \begin{bmatrix} B_1 & B_2 \end{bmatrix} R_2^m \begin{bmatrix} A_1 \\ A_2 \end{bmatrix} \\ R_2^m &= \begin{bmatrix} V_1AM_2(N_2AM_2)^{-1}N_2AU_1 - V_1AU_1 & V_1AM_2(N_2AM_2)^{-1}N_2AU - V_1AU \\ VAM_2(N_2AM_2)^{-1}N_2AU_1 - VAU_1 & VAM_2(N_2AM_2)^{-1}N_2AU - VAU \end{bmatrix} \\ R_3 &= K \begin{bmatrix} B_1 & B_2 \end{bmatrix} \begin{bmatrix} V_1AM_1 - V_1AM_2(N_2AM_2)^{-1}N_2AM_1 \\ VAM_1 - VAM_2(N_2AM_2)^{-1}N_2AM_1 \end{bmatrix} \\ R_4 &= -CUN_2AM_2 \\ R_5 &= (N_1AU_1 - N_1AM_2(N_2AM_2)^{-1}N_2AU_1)A_1 + \\ &\quad (N_1AU - N_1AM_2(N_2AM_2)^{-1}N_2AU)A_2 \\ R_6 &= N_1AM_2(N_2AM_2)^{-1}A_2. \end{aligned} \tag{2.27}$$

If the input-output representation of Eq. (2.26) is $y(s) = \overline{W}_m(s)Kr(s)$, then $\overline{W}_m(s)$ is given by Eq. (2.18). \square

Remarks:

1. A geometric interpretation of Lemma 4 is that N^p projects the column space of CAB onto the left nullspace of CB . $N^{(1)T}$ is the orthogonal complement of $U^{(1)}$, the column space of CB , in \mathbb{R}^m . Since $E[G(s)]$ is non-singular, CB and $N^p CAB$ span $\mathbb{R}^{m \times m}$.
2. It is known that the non-singularity of E implies that $G(s)$ can be decoupled by state feedback [47]. Using Lemmas 4 and 5 another interpretation of the singularity of $E[G(s)]$, $r_i[G(s)] = 1$ or 2 , can be given. If $E[G(s)]$ is non-singular, a total of $n - m - d$ transmission zeros exist. The excess of poles over zeros is $m + d$. Lemmas 4 and 5 imply that if E becomes nonsingular, then some of the $n - m - d$ finite transmission zeros move to infinity. How many of the $n - m - d$ finite zeros move to infinity depends on the particular structure of the system considered. Hence, the non-singularity of E refers to a loss in the nominal number of transmission zeros.

Chapter 3

Low Order Controller Structures

3.1 Introduction

In this Chapter the linear, non-adaptive controller structure that would be used if all plant parameters were known is discussed. The MIMO LTI plants that will be considered are described by

$$\begin{aligned} \dot{x}_p &= A_p x_p + B_p u + L_d d \\ y_p &= C_p x_p, \end{aligned} \tag{3.1}$$

where $x_p : \mathbb{R}^+ \rightarrow \mathbb{R}^n$ is the state vector, $u : \mathbb{R}^+ \rightarrow \mathbb{R}^m$ is the control input, $d : \mathbb{R}^+ \rightarrow \mathbb{R}^s$ is a bounded input disturbance and $y_p : \mathbb{R}^+ \rightarrow \mathbb{R}^m$ is the measured output. We will assume throughout the thesis that the control inputs and output measurements are not redundant, i.e. $\text{rank}(B_p) = m \leq n$ and $\text{rank}(C_p) = m \leq n$. The input-output representation of Eq. (3.1) is given by $y_p = G_p(s)u + G_d(s)d$, where

$$G_p(s) = C_p(sI - A_p)^{-1}B_p \tag{3.2}$$

$$G_d(s) = C_p(sI - A_p)^{-1}L_p. \tag{3.3}$$

The high frequency gain matrix of $G_p(s)$ will be denoted by $K_p \in \mathbb{R}^{m \times m}$.

The organization of the Chapter is as follows. In section 3.2 the feedback con-

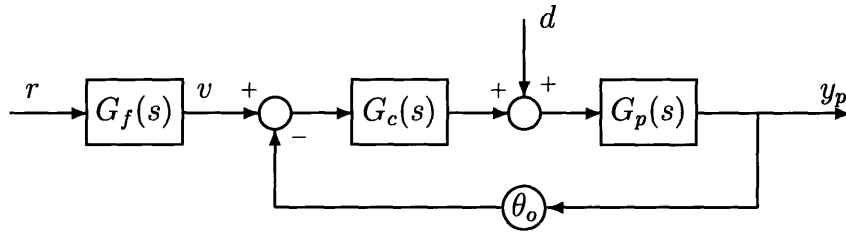


Figure 3-1: Controller Structure

troller structure for SISO systems is described, and extensions of the basic controller structure are discussed. In section 3.3 the controller structure for the MIMO case is presented. A feedforward control strategy as to accomplish output tracking is discussed in section 3.4. The contributions of this Chapter are summarized in section 3.5.

3.2 Singlevariable Systems

The control objective of the controllers developed in this thesis is to stabilize the plant, and for the plant output to track a reference trajectory. The fixed, non-adaptive controller structure underlying the adaptive controller that will be used to accomplish this is shown in Fig. 3-1. In Fig. 3-1, $G_p(s)$ denotes the plant to be controlled, $G_c(s)$ and $G_f(s)$ are compensators to be designed. The basic idea behind the controller is to design a low-order compensator $G_c(s)$ such that $\bar{W}_m(s) = (1 + \theta_o G_p(s) G_c(s))^{-1} G_p(s) G_c(s)$ is asymptotically stable and has desirable properties. The feedforward compensator $G_f(s)$ is then designed such that the desired tracking objective is realized.

A plethora of techniques is available to design $G_c(s)$ and $G_f(s)$ as to realize the control objective. However, only a limited number of parameterizations of $G_c(s)$ and $G_f(s)$ will lead to a stable analytical solution that assures the boundedness and convergence of the adaptive controllers presented in Chapter 4. As will become clear in Chapter 4, to be able to design a stable adaptive controller positivity of the underlying dynamics is needed. In this thesis, this positivity is achieved by requiring

that a compensator $G_c(s)$ can be found such that $\overline{W}_m(s)$ is strictly positive real. The strict positive realness of $\overline{W}_m(s)$ is obtained by choosing $G_c(s)$ appropriately and by exploiting the relative degree of $G_p(s)$. For example, if $G_p(s)$ is minimum phase, the relative degree of $G_p(s)$ is 1 and the high frequency gain k_p of $G_p(s)$ is positive, then it is sufficient to choose $G_c(s) = 1$. It follows from standard root-locus arguments that $\overline{W}_m(s) = (1 + \theta_o G_p(s))^{-1} G_p(s)$ is SPR for sufficiently large θ_o . Clearly, if the relative degree of $G_p(s)$ is greater than 1, positive realness can not be established using a causal $G_c(s)$. However, with the adaptive control method discussed in Chapter 4 it is possible to recover an input-output map of the form $W_m(s) = \overline{W}_m(s)(s + a)$ where $a \in \mathbb{R}^+$ is a design parameter to be chosen. Hence, relative degree two plants can also be considered.

In the following two sections we will discuss how $G_c(s)$ can be chosen when the relative degree of $G_p(s)$ is either one or two and the zeros of $G_p(s)$ lie in \mathbb{C}^- . The design of $G_f(s)$ is addressed in section 3.4 for both the SISO and MIMO case.

3.2.1 Compensator Design

The basic structure of $G_c(s)$ that will be used is a phase lead compensator of the form

$$G_c(s) = \frac{s + a_o}{s + b_o}$$

where $0 < a_o < b_o$. Lead compensation increases the bandwidth, improving the speed of response. Furthermore, from standard root-locus arguments it follows that for any given $a > 0$, the parameters a_o , b_o and θ_o can be chosen such that $\overline{W}_m(s)$ is asymptotically stable, and $W_m(s) = \overline{W}_m(s)(s + a)$ is SPR. A formal proof of this can be found in [6].

A phase lead compensator is the lowest order compensator needed to stabilize a relative degree two, minimum phase plant, independent of the order of the plant $G_p(s)$. Furthermore, the phase lead compensator can be used to obtain a SPR input-output map $W_m(s)$. The disadvantage of using such a low order compensator may be that as to obtain the SPR input-output map, the required loop gain θ_o may be

too high making the system susceptible to actuator saturation, unmodeled dynamics and sensor noise. To lower the gain it might therefore be desirable to employ a more sophisticated, minimum phase, compensator of the form

$$G_c(s) = \frac{s^q + a_{q-1}s^{q-1} + \dots + a_1s + a_o}{s^q + b_{q-1}s^{q-1} + \dots + b_1s + b_o}.$$

For example, $G_c(s)$ can be chosen to obtain a desirable pole-zero interleaving of $G_p(s)G_c(s)$. The choice of the order q of the compensator depends on the the richness of the dynamics of $G_p(s)$ in the bandwidth over which tracking is desired.

3.2.2 Disturbance Rejection

In the discussion of the control design we have so far neglected the presence of external, not measurable disturbances d as shown in Fig. 3-1. In case it is desired that exact tracking is accomplished in the presence of exogenous, low frequency, disturbances, the internal model principle may be applied. The idea of the internal model principle is to supply closed loop zeros which cancel the poles of the disturbance [20]. For this reason, the only disturbances that can be rejected exactly are constants and sinusoids. The internal model principle implies that the poles of the compensator $G_c(s)$ must contain the frequencies of the disturbance. For example, rejection of a constant disturbance requires the compensator to contain a pure integrator, so that the compensator is of the form

$$G_c(s) = \frac{s + a_o}{s + b_o} \frac{s + c_o}{s}$$

where $c_o > 0$. Similarly, a sinusoidal disturbance of frequency ω_d can be rejected by using a compensator of the form

$$G_c(s) = \frac{s + a_o}{s + b_o} \frac{s^2 + c_1s + c_o}{s^2 + \omega_d^2}$$

where c_1 and c_o are chosen so that $s^2 + c_1s + c_o$ is Hurwitz. In case the disturbance is not limited to a countable number of frequencies, but still band limited, this approach

may still be used to improve the tracking performance. Exact disturbance rejection will not be accomplished, however.

3.3 Multivariable Systems

The design of non model-based compensators for multivariable systems is generally much harder than for singlevariable systems because of the cross-coupling between the input and output channels, and the multitude of controller parameters that can be chosen. The discussion in this section is therefore limited to provide sufficient control structures to stabilize the plant described by Eq. (3.1) , and achieve positive input-output relations that are needed in the adaptive control design discussed in Chapter 4. In contrast to the single-variable case, the conditions under which a positive input-output map exists had to be derived formally. The results are stated compactly in Lemmas 6 and 7. Variations on these lemmas for the special case that $K_p > 0$ are given in Corollaries 1 and 2.

The following Lemma gives the conditions under which static output feedback of the form

$$u = -\theta_o \Theta_o y_p + v \tag{3.4}$$

where $\theta_o \in \mathbb{R}$, $\Theta_o \in \mathbb{R}^{m \times m}$ and $v : \mathbb{R}^+ \rightarrow \mathbb{R}^m$ is a reference signal, can be used to stabilize $G_p(s)$ and achieve a SPR input-output map.

Lemma 6 If the transmission zeros of $G_p(s)$ in Eq. (3.2) lie in \mathbb{C}^- and $\text{rank}(C_p B_p) = m$ then there exist $\theta_o^* \in \mathbb{R}^+$ and $\Theta_o^* \in \mathbb{R}^{m \times m}$ such that

$$\overline{W}_m(s) = C_p (sI - A_p + \theta_o B_p \Theta_o C_p)^{-1} B_p (C_p B_p)^{-1} \tag{3.5}$$

is SPR for $\theta_o = \theta_o^*$, $\Theta_o = \Theta_o^*$. •

Proof: The control input given in Eq. (3.4) applied to the the plant described

by Eq. (3.1) results in the closed loop dynamics given by

$$\begin{aligned} \dot{x}_p &= (A_p - \theta_o B_p \Theta_o C_p) x_p + B_p v \\ y_p &= C_p x_p. \end{aligned} \quad (3.6)$$

Since $\text{rank}(C_p B_p) = m$, Theorem 2 provides an alternate description of the system in Eq. (3.6):

$$\begin{aligned} \begin{bmatrix} \dot{w}_1 \\ \dot{w}_2 \end{bmatrix} &= \begin{bmatrix} C_p U_1 V_1 A_p U_1 (C_p U_1)^{-1} - \theta_o C_p B_p \Theta_o & V_1 A_p M_1 \\ N_1 A_p U_1 & A_z \end{bmatrix} \begin{bmatrix} w_1 \\ w_2 \end{bmatrix} + \begin{bmatrix} I \\ 0 \end{bmatrix} C_p B_p v \\ y_p &= [I \ 0] \begin{bmatrix} w_1 \\ w_2 \end{bmatrix}. \end{aligned} \quad (3.7)$$

We will describe Eq. (3.7) with

$$\begin{aligned} \dot{w} &= Fw + GC_p B_p v \\ y_p &= Hw. \end{aligned} \quad (3.8)$$

According to Lemma 2, with $D = 0$, Lemma 6 is proved if we find a matrix $P = P^T > 0$ and a matrix $Q = Q^T > 0$ such that $\{F, G, H\}$ in Eq. (3.8) satisfy

$$F^T P + PF = -Q \quad (3.9)$$

$$PG = H^T. \quad (3.10)$$

Since the transmission zeros of $G_p(s)$ lie in \mathbb{C}^- , $A_z \in \mathbb{R}^{(n_p - m) \times (n_p - m)}$ is exponentially stable. Hence, there exists a $(n_p - m) \times (n_p - m)$ matrix $P_z = P_z^T > 0$ and a $(n_p - m) \times (n_p - m)$ matrix $Q_z = Q_z^T > 0$ which satisfy the Lyapunov equation

$$A_z^T P_z + P_z A_z = -Q_z. \quad (3.11)$$

If we choose

$$P = \begin{bmatrix} I_{m \times m} & 0 \\ 0 & P_z \end{bmatrix}, \quad (3.12)$$

we will show that Eq. (3.10) is satisfied and that we can find a Q in Eq. (3.9) such that $Q = Q^T > 0$ for a large enough gain θ_o . First, if we substitute Eq. (3.12) in Eq. (3.10) we get

$$\begin{bmatrix} I & 0 \\ 0 & P_z \end{bmatrix} \begin{bmatrix} I \\ 0 \end{bmatrix} = \begin{bmatrix} I \\ 0 \end{bmatrix}.$$

The equality given by Eq. (3.10) is therefore trivially satisfied. Next, we substitute Eq. (3.12) in Eq. (3.9) and find that

$$Q = \begin{bmatrix} \theta_o Q_\theta - C_p A_p U_1 (C_p U_1)^{-1} - (C_p A_p U_1 (C_p U_1)^{-1})^T & -(N_1 A_p U_1)^T P_z - V_1 A_p M_1 \\ -(V_1 A_p M_1)^T - P_z N_1 A_p U_1 & Q_z \end{bmatrix}$$

where $Q_\theta = (C_p B_p \Theta_o)^T + C_p B_p \Theta_o$. It is easy to see that $Q = Q^T$. What remains to be shown is that Q is positive definite as well. Hence consider $x^T Q x$, where $x^T = [x_1^T \quad x_2^T]$, $x_1 : \mathbb{R}^+ \rightarrow \mathbb{R}^m$ and $x_2 : \mathbb{R}^+ \rightarrow \mathbb{R}^{n_p - m}$. Then

$$\begin{aligned} x^T Q x &= \theta_o x_1^T Q_\theta x_1 - x_1^T [C_p A_p U_1 (C_p U_1)^{-1} + (C_p A_p U_1 (C_p U_1)^{-1})^T] x_1 \\ &\quad - 2x_1^T [(N_1 A_p U_1)^T P_z + V_1 A_p M_1] x_2 + x_2^T Q_z x_2. \end{aligned}$$

If $x_1 \equiv 0$ then $x^T Q x > 0$ since $Q_z > 0$. If $x_1 \neq 0$ then we can always find a θ_o large enough such that $x^T Q x > 0$ provided

$$Q_\theta = (C_p B_p \Theta_o)^T + C_p B_p \Theta_o > 0. \quad (3.13)$$

If we choose $\Theta_o = \Theta_o^* = (C_p B_p)^{-1}$, then Eq. (3.13) is indeed satisfied. It follows that Q will be positive definite, and symmetric, for $\theta_o = \theta_o^*$ where θ_o^* is a large enough scalar, which proves Lemma 6. \square

If the high frequency gain matrix $K_p = C_p B_p$ is positive definite Lemma 6 can be simplified. This simplification will be useful for the robust adaptive control algorithm presented in Chapter 4.

Corollary 1 If the transmission zeros of $G_p(s)$ in Eq. (3.2) lie in \mathbb{C}^- and $C_p B_p > 0$

then there exist $\theta_o^* \in \mathbb{R}^+$ and $\Theta_o^* \in \mathbb{R}^{m \times m}$ such that

$$\overline{W}_m(s) = C_p(sI - A_p + \theta_o B_p \Theta_o C_p)^{-1} B_p$$

is SPR for $\theta_o = \theta_o^*$, $\Theta_o = \Theta_o^*$. •

Proof: The proof follows along the same lines as the proof of Lemma 6. □

If $\text{rank}(C_p B_p) < m$ then a dynamic output feedback will have to be used. Motivated by the singlevariable phase lead compensator, the multivariable compensator is chosen as

$$\begin{aligned} u &= \Theta_1 \omega_1 + I \tilde{e} \\ \dot{\omega}_1 &= -\Lambda \omega_1 + I u \end{aligned} \tag{3.14}$$

where $\omega_1 : \mathbb{R}^+ \rightarrow \mathbb{R}^m$, and $\tilde{e} = -\theta_o \Theta_o y_p + v$. Combining Eqs. (3.1) and (3.14), the loop dynamics is given by

$$\begin{aligned} \dot{x} &= Ax + B \tilde{e} \\ y_p &= Cx, \end{aligned} \tag{3.15}$$

where

$$x = \begin{bmatrix} x_p \\ \omega_1 \end{bmatrix}, \quad A = \begin{bmatrix} A_p & B_p \Theta_1 \\ 0 & \Theta_1 - \Lambda \end{bmatrix}, \quad B = \begin{bmatrix} B_p \\ I \end{bmatrix}, \quad \text{and} \quad C = [C_p \quad 0], \tag{3.16}$$

so that $n = n_p + m$. The following Theorem states the conditions under which a SPR input-output map is obtained.

Lemma 7 Let $\{A, B, C\}$ be defined as in Eq. (3.16), and let $G_p(s)$ be given by Eq. (3.2). If the transmission zeros of $G_p(s)$ lie in \mathbb{C}^- , $G_p(s)$ satisfies $r_i[G_p(s)] = 1$ or 2 ($i = 1, 2, \dots, m$) and $E[G_p(s)]$ is nonsingular, then for any $\Lambda > 0$ there exist $\theta_o^* \in \mathbb{R}$, $\Theta_o^* \in \mathbb{R}^{m \times m}$ and $\Theta_1^* \in \mathbb{R}^{m \times m}$ such that

$$W_m(s) = [(s + a)I] C(sI - A + \theta_o B \Theta_o C)^{-1} B K_p^{-1}, \quad a \in \mathbb{R}^+ \tag{3.17}$$

is SPR for $\theta_o = \theta_o^*$, $\Theta_o = \Theta_o^*$ and $\Theta_1 = \Theta_1^*$. •

Proof: Before actually proving the Lemma, relations between properties of $B \Theta_o C$

and $B_p\Theta_oC_p$ are needed. The following relations can be established.

Relation between the Jordan Blocks in the Decompositions:

Let the rank deficiency of CB be denoted by d . Since $CB = C_pB_p$, the rank deficiency of C_pB_p is d as well. Hence, Theorem 1 implies that $J_1 \in \mathbb{R}^{(m-d) \times (m-d)}$ and $J_2 \in \mathbb{R}^{2d \times 2d}$ are identical for both decompositions:

$$B_p\Theta_oC_p = [U_1^p \quad U_2^p \quad M_1^p] \begin{bmatrix} J_1 & & \\ & J_2 & \\ & & 0_{(n-m-d) \times (n-m-d)} \end{bmatrix} \begin{bmatrix} V_1^p \\ V_2^p \\ N_1^p \end{bmatrix} \quad (3.18)$$

where

$$B_p\Theta_oC_pU_p = M_2^p, \quad V_pB_p\Theta_oC_p = N_2^p, \quad (3.19)$$

and

$$B\Theta_oC = [U_1 \quad U_2 \quad M_1] \begin{bmatrix} J_1 & & \\ & J_2 & \\ & & 0_{(n-d) \times (n-d)} \end{bmatrix} \begin{bmatrix} V_1 \\ V_2 \\ N_1 \end{bmatrix} \quad (3.20)$$

where

$$B\Theta_oCU = M_2, \quad VB\Theta_oC = N_2. \quad (3.21)$$

Relation between Eigenvectors:

Using the orthogonality of the eigenvectors and Eqs. (3.18) – (3.21), the eigenvectors of $B_p\Theta_oC_p$ and $B\Theta_oC$ can be related as

$$\begin{aligned} U_1 &= \begin{bmatrix} U_1^p \\ U_1^c \end{bmatrix} & V_1 &= [V_1^p \quad 0_{d \times m}] \\ U &= \begin{bmatrix} U_p \\ (B_p^T B_p)^{-1} B_p^T U_p \\ M_2^p \end{bmatrix} & V &= [V_p \quad 0_{d \times m}] \\ M_2 &= \begin{bmatrix} M_2^p \\ \Theta_o C_p U_p \end{bmatrix} & N_2 &= [N_2^p \quad 0_{d \times m}] \\ M_1 &= \begin{bmatrix} M_1^p & 0 \\ (B_p^T B_p)^{-1} B_p^T M_1^p & I \end{bmatrix} & N_1 &= \begin{bmatrix} N_1^p & 0 \\ -(B_p^T B_p)^{-1} B_p^T & I \end{bmatrix} \end{aligned} \quad (3.22)$$

where $U_1^c \in \mathbb{R}^{m \times (m-d)}$ and satisfies $B_p U_1^c = U_1^p$.

Relation between High Frequency Gains:

From Eq. (3.22) and Lemma 4, we have that the high frequency gain matrix of the cascaded dynamics is the same as the high frequency gain matrix of the plant since

$$K_p = CB + CUN_2AB = C_pB_p + C_pU_pN_2^pA_pB_p.$$

With the above relations we can establish the Strict Positive Real result for $W_m(s)$ by showing that $W_m(s)^{-1}$ is SPR. We will use Lemma 1 to show that $W_m(s)^{-1}$ is SPR.

1. Since the transmission zeros of the plant lie in \mathbb{C}^{-1} , $\Lambda > 0$ and $a > 0$, $W_m^{-1}(s)$ is analytic in the closed right half plane.

2. We will consider two cases, $K_p = CB$ and $K_p = CB + N^pCAB$:

Case (i) $K_p = CB$

From Theorem 2 we have that Eq. (3.17) can be represented by

$$W_m(s) = [(s+a)I] \left[sI - CU_1V_1AU_1(CU_1)^{-1} + \theta_o K_p \Theta_o - V_1AM_1(sI - A_z)^{-1}N_1AU_1 \right]^{-1}.$$

Define

$$\begin{aligned} W_1(s) &= [(s+a)I] [sI + \theta_o K_p \Theta_o]^{-1} \\ W_2(s) &= -[(s+a)I] \left[CU_1V_1AU_1(CU_1)^{-1} + V_1AM_1(sI - A_z)^{-1}N_1AU_1 \right]^{-1} \end{aligned}$$

so that $W_m^{-1}(s) = W_1^{-1}(s) + W_2^{-1}(s)$. We have that

$$W_1^{-1}(j\omega) + W_1^{-1}(j\omega)^* = (\omega^2 + a^2)^{-1} \left[a\theta_o(K_p\Theta_o + (K_p\Theta_o)^T) + 2\omega^2 I \right].$$

From (a) we have that $A_z < 0$, hence $(j\omega I - A_z)^{-1}$ exists $\forall \omega \in (-\infty, \infty)$ so that

$$\begin{aligned} W_2^{-1}(j\omega) &= -(\omega^2 + a^2)^{-1} [(a - j\omega)I] \\ &\quad \left[CU_1V_1AU_1(CU_1)^{-1} + V_1AM_1(j\omega I - A_z)^{-1}N_1AU_1 \right]^{-1}. \end{aligned}$$

Let Θ_1^* be bounded, then for $\Theta_1 = \Theta_1^*$ we have that $\exists \delta = \delta(\Theta_1) > 0$ such that

$$-\frac{\delta}{a^2 + \omega^2}I \leq W_2^{-1}(j\omega) + W_2^{-1}(j\omega)^* \leq \frac{\delta}{a^2 + \omega^2}I.$$

Let

$$\theta_o^* = (2a)^{-1}(\delta + \epsilon), \epsilon > 0, \quad \Theta_o^* = K_p^{-1},$$

then, for $\theta_o = \theta_o^*$ and $\Theta_o = \Theta_o^*$, we have that

$$W_m^{-1}(j\omega) + W_m^{-1}(j\omega)^* \geq \frac{\epsilon + 2\omega^2}{a^2 + \omega^2}I \geq \min\left(\frac{\epsilon}{a^2}, 2\right)I > 0.$$

Note that $CB\Theta_o^* = I$ has no zero eigenvalues so that use of Theorem 2 is justified.

Case (ii) $K_p = CB + N^pCAB$

From Theorem 2 we have that Eq. (3.17) can now be written as

$$W_m(s) = [(s+a)I] \left[CUA_2s^2 + (CU_1A_1 + \mathcal{D} + R_1)s + \theta_o K_p \Theta_o + R_2 + (R_3 + R_4s)(sI - A_z)^{-1}(R_5 + R_6s) \right]^{-1}.$$

Define

$$\begin{aligned} W_1(s) &= [(s+a)I] \left[CUA_2s^2 + (CU_1A_1 + \mathcal{D})s + \theta_o K_p \Theta_o \right]^{-1} \\ W_2(s) &= [(s+a)I] \left[R_2 + R_3(sI - A_z)^{-1}R_5 + \right. \\ &\quad \left. sR_3(sI - A_z)^{-1}R_6 + sR_4(sI - A_z)^{-1}R_5 \right]^{-1} \\ W_3(s) &= [(s+a)I] s^{-2} \left[R_4(sI - A_z)^{-1}R_6 \right]^{-1} \end{aligned}$$

so that $W_m^{-1}(s) = W_1^{-1}(s) + W_2^{-1}(s) + W_3^{-1}(s)$. Since $A_z < 0$, $(j\omega I - A_z)^{-1}$ exists $\forall \omega \in (-\infty, \infty)$. Also $\exists \delta_2 = \delta_2(\Theta_1) > 0$ for any bounded Θ_1 , and $\exists \delta_3 > 0$ such that

$$\begin{aligned} -\frac{\delta_2}{a^2 + \omega^2}I &\leq W_2^{-1}(j\omega) + W_2^{-1}(j\omega)^* \leq \frac{\delta_2}{a^2 + \omega^2}I \\ -\frac{\delta_3\omega^2}{a^2 + \omega^2} (CUA_2 + (CUA_2)^T) &\leq \end{aligned}$$

$$W_3^{-1}(j\omega) + W_3^{-1}(j\omega)^* \leq \frac{\delta_3\omega^2}{a^2 + \omega^2} (CUA_2 + (CUA_2)^T).$$

Let

$$\begin{aligned}\theta_o^* &= (2a)^{-1}(\delta_2 + \epsilon), \\ \Theta_o^* &= K_p^{-1}, \\ \theta_1^* &= a + \delta_3 + 1, \\ \Theta_1^* &= -\theta_1^* K_p^{-1} C_p U^p N_2^p A_p M_2^p V^p B_p - \{B_1^p V_1^p + B_2^p V^p\} A_p M_2^p V^p B_p.\end{aligned}$$

where $\epsilon > 0$. For $\Theta_1 = \theta_1^* \Theta_1^*$ we find that, using Eq. (2.27),

$$\begin{aligned}\mathcal{D} &= -K_p \{B_1 V_1 + B_2 V\} A M_2 (N_2 A M_2)^{-1} A_2 \\ &= -K_p \{B_1^p V_1^p + B_2^p V^p\} A_p M_2^p (N_2^p A_p M_2^p)^{-1} A_2^p - K_p \Theta_1 \Theta_o C_p U^p (N_2^p A_p M_2^p)^{-1} A_2^p \\ &= \theta_1^* C_p U^p A_2^p = \theta_1^* C U A_2.\end{aligned}$$

With $\theta_o = \theta_o^*$, $\Theta_o = \Theta_o^*$ we have

$$\begin{aligned}W_1^{-1}(j\omega) + W_1^{-1}(j\omega)^* &= \\ &= \frac{1}{a^2 + \omega^2} \left[2a\theta_o^* I + \omega^2 \left((\theta_1^* - a) (CUA_2 + (CUA_2)^T) + CU_1 A_1 + (CU_1 A_1)^T \right) \right].\end{aligned}$$

Hence

$$\begin{aligned}W_m^{-1}(j\omega) + W_m^{-1}(j\omega)^* &\geq \frac{1}{a^2 + \omega^2} \left[(2a\theta_o^* - \delta_2) I + \omega^2 \left((\theta_1^* - a - \delta_3) \right. \right. \\ &\quad \left. \left. (CUA_2 + (CUA_2)^T) + CU_1 A_1 + (CU_1 A_1)^T \right) \right] \\ &\geq \frac{\epsilon + 2\omega^2}{a^2 + \omega^2} I \geq \min \left(\frac{\epsilon}{a^2}, 2 \right) I > 0.\end{aligned}$$

Since the zero eigenvalues of CBK_p^{-1} appear in diagonal form, use of Eq. (2.18), Theorem 2, is justified. \square

The following result will be of use in the design of the robust adaptive controller in Chapter 4.

Corollary 2 Let $\{A, B, C\}$ be defined as in Eq. (3.16) and let $G_p(s)$ be given by Eq. (3.2). If the transmission zeros of $G_p(s)$ lie in \mathbb{C}^- , $G_p(s)$ satisfies $r_i[G_p(s)] = 1$ or 2 ($i = 1, 2, \dots, m$) and $E[G_p(s)] > 0$ then for any $\Lambda > 0$ there exist $\theta_o^* \in \mathbb{R}$, $\Theta_o^* \in \mathbb{R}^{m \times m}$ and $\Theta_1^* \in \mathbb{R}^{m \times m}$ such that

$$W_m(s) = [(s + a)I]C(sI - A + \theta_o B \Theta_o C)^{-1}B, \quad a \in \mathbb{R}^+$$

is SPR for $\theta_o = \theta_o^*$, $\Theta_o = \Theta_o^*$ and $\Theta_1 = \Theta_1^*$.

Proof: The proof follows along the same lines as the proof of Lemma 7. \square

Remarks:

1. Similar to the discussion in section 3.2.1, more elaborate compensation schemes may be used. For example, if $\Lambda \in \mathbb{R}^{2m \times 2m}$ and $\Theta_1 \in \mathbb{R}^{m \times 2m}$ in Eq. (3.14), more degrees of freedom are available to shape $W_m(s)$ which may result in a lower overall gain θ_o for which strict positive realness is achieved. For the SISO case, this was accomplished by placing compensator poles and zeros such that the loop transfer function $G_c(s)G_p(s)$ has interleaving poles and zeros, for example. However, for the MIMO case it is not clear how Λ and Θ_1 should be chosen.
2. The comments made in section 3.2.2 regarding disturbance rejection can be extended to the multivariable case by augmenting each input channel with the poles of the disturbance. It is important to note that to achieve this rejection robustly it is necessary and sufficient that the pole of the disturbance is duplicated on each channel [16].

3.4 Structure for Feedforward Control

In this section the structure of $G_f(s)$ in Fig. 3-1 is discussed. Our goal is to find a feedforward controller for an asymptotically stable, minimum phase plant described by

$$\begin{aligned} \dot{x}(t) &= Ax(t) + Bv(t) \\ y_p(t) &= Cx(t) \end{aligned} \tag{3.23}$$

where $A \in \mathbb{R}^{n \times n}$, $B \in \mathbb{R}^{n \times m}$ and $C \in \mathbb{R}^{m \times n}$. The control objective is for $y_p(t)$ to track $y_m(t)$ specified by the dynamics

$$\begin{aligned} \dot{x}_m(t) &= A_m x_m(t) & x_m(0) &= x_{m0} \\ y_m(t) &= C_m x_m(t) \end{aligned} \quad (3.24)$$

where $A_m \in \mathbb{R}^{p \times p}$ and $C_m \in \mathbb{R}^{m \times p}$. The following Theorem gives the control input that will achieve the desired control objective.

Theorem 3 Let $\Theta_{pm} \in \mathbb{R}^{n \times p}$ and $\Theta_m \in \mathbb{R}^{m \times p}$. If the eigenvalues of A_m do not coincide with the transmission zeros of the system in Eq. (3.23) then the control law given by

$$v(t) = \Theta_m x_m(t) \quad (3.25)$$

where Θ_m is the solution to

$$\begin{aligned} A\Theta_{pm} - \Theta_{pm}A_m + B\Theta_m &= 0 \\ C\Theta_{pm} &= C_m, \end{aligned} \quad (3.26)$$

results in $y_p(t)$ tracking $y_m(t)$ asymptotically. •

In proving the Theorem, the following Lemmas will be helpful.

Lemma 8 Let $A \in \mathbb{R}^{n \times n}$, $B \in \mathbb{R}^{m \times m}$ and $C \in \mathbb{R}^{n \times m}$ be given. Then

$$\int_0^t e^{A(t-\tau)} C e^{B\tau} d\tau = \Theta e^{Bt} - e^{At} \Theta,$$

where $\Theta \in \mathbb{R}^{n \times m}$ is the solution of the generalized Lyapunov equation

$$A\Theta - \Theta B + C = 0. \quad (3.27)$$

Proof: The proof follows by premultiplying Eq. (3.27) by $e^{A(t-\tau)}$ and postmultiplying with $e^{B\tau}$, and integration by parts. □

Lemma 9 Let $A \in \mathbb{R}^{n \times n}$, $B \in \mathbb{R}^{m \times m}$ with $C \in \mathbb{R}^{n \times m}$ be given. If $\lambda_i(A)\lambda_k(B) \neq 1$ ($i = 1, \dots, n$, $k = 1, \dots, m$) then the solution X of the discrete time Lyapunov equation

$$AXB + C = X$$

exists for any C , and is unique. •

Proof: See [29]. □

Proof of Theorem 3: Since Eqs. (3.23) and (3.24) describe LTI systems, we have

$$\begin{aligned} x(t) &= e^{At}x(0) + \int_0^t e^{A(t-\tau)}Bv(\tau)d\tau \\ x_m(t) &= e^{A_m t}x_{m0}. \end{aligned}$$

Using Eq. (3.25) and applying Lemma 8 we find

$$\begin{aligned} x(t) &= e^{At}x(0) + \int_0^t e^{A(t-\tau)}B\Theta_m e^{A_m \tau}x_{m0}d\tau \\ &= e^{At}x(0) + (\Theta_{pm}e^{A_m t} - e^{At}\Theta_{pm})x_{m0} \\ &= e^{At}(x(0) - \Theta_{pm}x_{m0}) + \Theta_{pm}e^{A_m t}x_{m0}, \end{aligned}$$

where Θ_{pm} is given by Eq. (3.26). It follows that tracking is achieved exponentially since

$$\begin{aligned} e_1(t) &= y(t) - y_m(t) \\ &= Cx(t) - C_mx_m(t) \\ &= Ce^{At}(x(0) - \Theta_{pm}x_{m0}) \end{aligned} \tag{3.28}$$

using Eq. (3.26).

Next we will show that solutions Θ_{pm} and Θ_m to Eq. (3.26) do indeed exist. For this purpose we first need some results regarding the transmission zeros of the plant.

Define

$$S(s) = \begin{bmatrix} sI - A & -B \\ -C & 0 \end{bmatrix}$$

where s is a complex variable. Since the plant has no transmission zeros at the origin, it follows that $\Omega = -S(0)^{-1}$ exists. Let Ω be partitioned as

$$\Omega = \begin{bmatrix} \Omega_{11}^{n \times n} & \Omega_{12}^{n \times m} \\ \Omega_{21}^{m \times n} & \Omega_{22}^{m \times m} \end{bmatrix}.$$

If z is a transmission zero, then

$$\begin{aligned} 0 &= \det(S(z)) \\ &= \det(S(0)^{-1}) \det(S(z)) \\ &= \det(S(0)^{-1}) \det(z \operatorname{diag}(I_n, 0_m) + S(0)) \\ &= \det(z \Omega \operatorname{diag}(I_n, 0_m) - I_{n+m}) \\ &= \det(z \Omega_{11} - I_n). \end{aligned}$$

Hence, the transmission zeros of the plant in Eq. (3.23) are given by the inverse of the nonzero eigenvalues of Ω_{11} . To solve Eq. (3.26), we rewrite the equations in matrix form as

$$-S(0) \begin{bmatrix} \Theta_{pm} \\ \Theta_m \end{bmatrix} = \begin{bmatrix} \Theta_{pm} A_m \\ C_m \end{bmatrix},$$

or

$$\Theta_{pm} = \Omega_{11} \Theta_{pm} A_m + \Omega_{12} C_m \tag{3.29}$$

$$\Theta_m = \Omega_{21} \Theta_{pm} A_m + \Omega_{22} C_m.$$

Since the eigenvalues of A_m do not coincide with the transmission zeros of the plant we have that $\lambda_i(\Omega_{11}) \lambda_k(A_m) \neq 1$. From Lemma 9 it follows that in Eq. (3.29) a unique Θ_{pm} can be found, and hence a Θ_m which results in $y_p(t)$ tracking $y_m(t)$ exponentially, exists. \square

Remarks:

1. If the plant outputs are to follow a class of desired trajectories, as in Eq. (3.24), the problem is referred to as a servo problem [1, 16]. The result stated in Theorem 3 is valid without any conditions on A_m , except that the eigenvalues of A_m should not coincide with the transmission zeros of the (closed loop) plant. A_m can be asymptotically stable, marginally stable or unstable and in all of these cases tracking can be achieved asymptotically. In other words, $y_m(t)$ can be a linear combination of constants, sinusoids, polynomials, exponentials, and any filtered versions thereof, which encompasses a large class of continuous functions of time.

2. When the outputs of the plant are to follow the response of another plant (or model), the problem is referred to as a model-following problem [1]. This is the problem solved in Model Reference Adaptive Control (MRAC) [47]. In MRAC the underlying fixed controller structure is chosen such that, when all parameters are known, the plant with the controller matches a reference model over all frequencies. That approach allows the plant output to track the output of the reference model for arbitrary (piecewise continuous) reference inputs. The scheme proposed here can be augmented to accomplish model-following by generating x_m as

$$\begin{aligned}\dot{x}_m &= A_m x_m + B_m r \\ y_m &= C_m x_m\end{aligned}$$

and by selecting the feedforward input as

$$v = \Theta_m x_m + \Theta_r r.$$

Θ_m and Θ_r are the solution to

$$\begin{aligned}A\Theta_{pm} - \Theta_{pm} \begin{bmatrix} A_m & B_m \\ 0_{m \times p} & 0_{m \times m} \end{bmatrix} + B [\Theta_m \quad \Theta_r] &= 0 \\ C [\Theta_m \quad \Theta_r] &= C_m.\end{aligned}$$

In this case, over a bandwidth determined by A_m , the tracking error as described by Eq. (3.28) is small if $\{A_m, B_m, C_m\}$ contains the same zeros as $\{A, B, C\}$, and if the number of states of A_m is equal to the number of states of A .

3. This feedforward control scheme was proposed in [50] although a less rigorous proof was given there.

3.5 Summary

In this Chapter the fixed controller structure underlying the adaptive controller has been discussed. Several results dealing with the existence of positive multi-input multi-output maps have been presented. The results are valid for arbitrary linear plants satisfying two conditions: the plant has to be minimum phase and the matrix $E[G_p(s)]$, $r_i[G_p(s)] = 1$ or 2 has to be non-singular. Using the controller structures discussed in this Chapter, three control objectives can be achieved: regulation, tracking of the plant output and attenuation of band limited disturbances.

Chapter 4

The Low Order Adaptive Controller

4.1 Introduction

In this Chapter the low order adaptive controller will be presented. The MIMO LTI plant that will be considered is described by

$$\begin{aligned}\dot{x}_p &= A_p x_p + B_p u \\ y_p &= C_p x_p.\end{aligned}\tag{3.1}$$

where $x_p : \mathbb{R}^+ \rightarrow \mathbb{R}^n$, $u : \mathbb{R}^+ \rightarrow \mathbb{R}^m$ and $y_p : \mathbb{R}^+ \rightarrow \mathbb{R}^m$. The input-output representation of Eq. (3.1) is given by $y_p = G_p(s)u$, where

$$G_p(s) = C_p(sI - A_p)^{-1}B_p.\tag{3.2}$$

The control objective is for $y_p(t)$ to follow a reference trajectory as discussed in section 3.4. The reference trajectory is given by

$$\begin{aligned}\dot{x}_m &= A_m x_m \\ y_m &= C_m x_m\end{aligned}\tag{3.24}$$

where $x_m : \mathbb{R}^+ \rightarrow \mathbb{R}^p$ and $y_m : \mathbb{R}^+ \rightarrow \mathbb{R}^m$. $A_m \in \mathbb{R}^{p \times p}$ is a stable matrix ¹ and $C_m \in \mathbb{R}^{m \times p}$.

This Chapter is organized as follows. In section 4.2 the assumptions on the plant are given, and the low order adaptive control algorithm is presented. Then, in section 4.3, a modified adaptive algorithm that guarantees boundedness in the presence of unmodeled dynamics is presented. The contributions of this Chapter are summarized in section 4.4.

4.2 The Adaptive Control Algorithm

The adaptive controller will be developed under the following assumptions regarding the plant given in Eq. (3.1):

(A1) (i) $r_i[G_p(s)] = 1$ or 2 ($i = 1, 2, \dots, m$) and, (ii) $E[G_p(s)]$ is nonsingular.

(A2) The transmission zeros of $G_p(s)$ lie in \mathbb{C}^- .

(A3) An adaptation gain matrix Γ can be found such that $K_p\Gamma = (K_p\Gamma)^T > 0$.

Also, we will assume that the reference trajectory is chosen such that:

(M1) The eigenvalues of A_m do not coincide with the zeros of the plant.

Below the adaptive control algorithm that can will achieve the described control objective is described. This adaptive controller is based on the fixed feedback controller presented in Lemma 7. Define (Fig. 4-1)

$$e_1(t) = y_p(t) - y_m(t), \quad \Theta(t) = [\Theta_o(t) \quad \Theta_1(t) \quad \Theta_m(t)], \quad (4.1)$$

$$\omega^T(t) = [y_p^T(t) \quad \omega_1^T(t) \quad x_m^T(t)], \quad \bar{\omega}(t) = \left[\frac{1}{s+a} I \right] \omega(t), \quad a \in \mathbb{R}^+.$$

The control input is given by

$$u(t) = \Theta(t)\omega(t) + \dot{\Theta}(t)\bar{\omega}(t) \quad (4.2)$$

¹A matrix A is a stable matrix if all the eigenvalues of A_m have non-positive real parts and those with zero parts are simple zeros of the minimal polynomial of A .

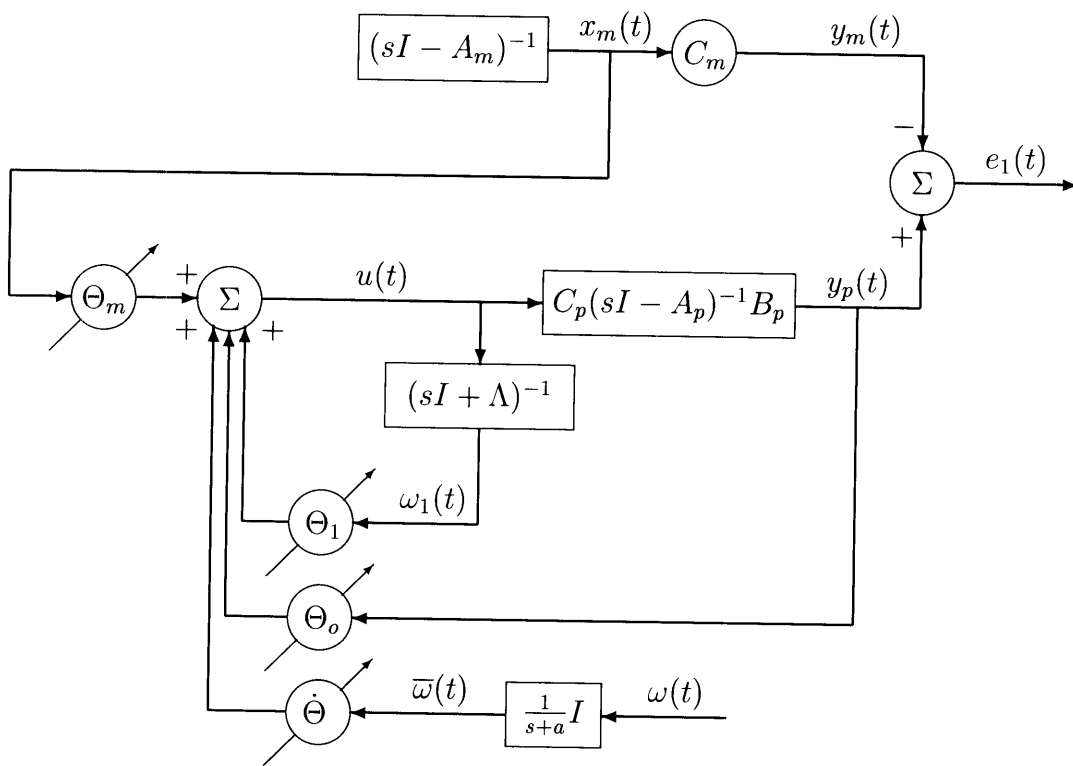


Figure 4-1: The Low Order Adaptive Control Scheme.

where $\omega_1(t)$ is generated as

$$\dot{\omega}_1(t) = -\Lambda\omega_1(t) + u(t), \quad \lambda(-\Lambda) \cap \lambda(A_m) = \emptyset, \Lambda > 0. \quad (4.3)$$

The adaptive law for adjusting $\Theta(t)$ is given by

$$\dot{\Theta}(t) = -\Gamma e_1(t)\bar{\omega}^T(t). \quad (4.4)$$

The following Theorem states a main result.

Theorem 4 When $G_p(s)$ satisfies assumptions (A1), (A2) and (A3), and the desired trajectory $y_m(t)$ is given by Eq. (3.24) satisfying assumption (M1), then the adaptive controller given by Eqs. (4.2) – (4.4) ensures that all signals in the loop are globally bounded and that $e_1(t)$ tends to zero asymptotically. •

Proof: Based on the discussion in Chapter 3, the control input is chosen as

$$u(t) = \Theta(t)\omega(t) + \dot{\Theta}(t)\bar{\omega}(t), \quad (4.2)$$

where $\Theta(t)$ is a time-varying gain. The second term in Eq. (4.2) is needed since $r_i[G_p(s)]$ may be one or two. Define $\Theta^* = [\Theta_o^* \ \Theta_1^* \ \Theta_m^*]$. Note that if $\Theta(t) \equiv \Theta^*$ then the controller reduces to the controller discussed in Lemma 7. With the controller in Eq. (4.2), the closed loop dynamics is given by

$$\begin{aligned} \begin{bmatrix} \dot{x}_p \\ \dot{\omega}_1 \end{bmatrix} &= \begin{bmatrix} A_p & B_p\Theta_1(t) \\ 0 & \Theta_1(t) - \Lambda \end{bmatrix} \begin{bmatrix} x_p \\ \omega_1 \end{bmatrix} + \begin{bmatrix} B_p \\ I \end{bmatrix} (\Theta_o(t)y_p(t) + \Theta_m(t)x_m(t) + \dot{\Theta}(t)\bar{\omega}(t)) \\ y_p &= [C_p \ 0] \begin{bmatrix} x_p \\ \omega_1 \end{bmatrix}. \end{aligned}$$

Define the parameter error matrix $\Phi(t)$ as $\Phi(t) = \Theta(t) - \Theta^*$, we then obtain the following closed loop equation:

$$\begin{aligned} \dot{x} &= \bar{A}x + B[\Theta_m^*x_m(t) + \Phi(t)\omega(t) + \dot{\Phi}(t)\bar{\omega}(t)] \\ y_p &= Cx, \end{aligned}$$

with $\{\bar{A}, B, C\}$ defined as in Eq. (3.16). The input-output relation is given by

$$y_p(t) = \bar{W}_m(s)K_p \left[\Theta_m^* x_m(t) + \Phi(t)\omega(t) + \dot{\Phi}(t)\bar{\omega}(t) \right].$$

From the discussion in Chapter 3 we have that the reference signal can be represented as

$$y_m(t) = \bar{W}_m(s)K_p \Theta_m^* x_m(t),$$

neglecting exponentially decaying initial conditions, so that the error equation is

$$e_1(t) = \bar{W}_m(s)K_p [\Phi(t)\omega(t) + \dot{\Phi}(t)\bar{\omega}(t)].$$

Since $\Phi(t)\omega(t) + \dot{\Phi}(t)\bar{\omega}(t) = [(s+a)I]\Phi(t)\bar{\omega}(t)$, the error equation can be simplified as

$$e_1(t) = W_m(s)K_p \Phi(t)\bar{\omega}(t) \tag{4.5}$$

where $W_m(s) = [(s+a)I]\bar{W}_m(s)$ is SPR from Lemma 7. Neglecting exponentially decaying initial conditions, the state-space representation of Eq. (4.5) is given by

$$\begin{aligned} \dot{e} &= \bar{A}e + BK_p^{-1}\{K_p\Phi(t)\bar{\omega}(t)\} \\ e_1 &= [(s+a)I]Ce = [aC + C\bar{A}]e + CBK_p^{-1}\{K_p\Phi(t)\bar{\omega}(t)\}. \end{aligned} \tag{4.6}$$

Since $W_m(s)$ is SPR, Lemma 2 assures that there exist a matrix $P = P^T > 0$, matrices K and L and a scalar $\rho > 0$ such that

$$\begin{aligned} \bar{A}^T P + P\bar{A} &= -LL^T - 2\rho P \\ (BK_p^{-1})^T P + K^T L^T &= aC + C\bar{A} \\ K^T K &= CBK_p^{-1} + (CBK_p^{-1})^T. \end{aligned} \tag{4.7}$$

Choose a Lyapunov function of the form

$$V(e, \Phi) = e^T P e + \text{tr}(\Phi^T K_p^T (K_p \Gamma)^{-1} K_p \Phi).$$

The derivative evaluated along the trajectories of Eqs. (4.4) and (4.6) is given by

$$\dot{V}(e, \Phi) = -e^T(LL^T + 2\rho P)e + 2e^T PB\Phi\bar{\omega} - 2e_1^T K_p \Phi\bar{\omega}.$$

Since $B^T P e = e_1 - CB\Phi\bar{\omega} - K^T L^T e$, we have

$$\dot{V}(e, \Phi) = -2\rho e^T P e - e_2^T e_2 \leq 0,$$

where $e_2 = L^T e + K K_p \Phi\bar{\omega}$. This implies that e and Φ are bounded, and that $e, e_2 \in \mathcal{L}^2$. Since ω_1 is a part of e , we have that $\bar{\omega}_1 \in \mathcal{L}^\infty$. Also, $\bar{y}_p - \bar{y}_m = C e$, and hence \bar{y}_p is bounded. As a result, $\bar{\omega} \in \mathcal{L}^\infty$. Since \bar{A} is exponentially stable and $\Phi, \bar{\omega}, e \in \mathcal{L}^\infty$ we have that $\dot{e} \in \mathcal{L}^\infty$. Since $e \in \mathcal{L}^\infty \cap \mathcal{L}^2$ and $\dot{e} \in \mathcal{L}^\infty$, Barbalat's Lemma [47] gives that $\lim_{t \rightarrow \infty} e(t) = 0$. Also, $e_1 = C(\dot{e} + a e)$ is bounded. Hence, all signals in the loop are bounded.

We shall now show that $\lim_{t \rightarrow \infty} e_1(t) = 0$ as well. Since $\dot{e} \in \mathcal{L}^\infty$, it follows that $\dot{\bar{y}}_p$ and $\dot{\bar{\omega}} \in \mathcal{L}^\infty$. Hence, since $\dot{e}_2 = L^T \dot{e} + K K_p \dot{\Phi}\bar{\omega} + K K_p \Phi\dot{\bar{\omega}}$, $\dot{e}_2 \in \mathcal{L}^\infty$ as well, Barbalat's Lemma gives that $\lim_{t \rightarrow \infty} e_2 = 0$ and hence

$$\lim_{t \rightarrow \infty} K K_p \Phi(t)\bar{\omega}(t) = 0.$$

We note that, using Lemma 4, $K_p^T C B$ can be simplified as

$$K_p^T C B = (C B)^T C B + (C A B)^T N^p C B = (C B)^T C B.$$

Hence, using Eq. (4.7), $K = \sqrt{2} C B K_p^{-1}$. Therefore, we have that

$$\lim_{t \rightarrow \infty} C B K_p^{-1} \{K_p \Phi(t)\bar{\omega}(t)\} = 0,$$

hence $\lim_{t \rightarrow \infty} e_1(t) = 0$. □

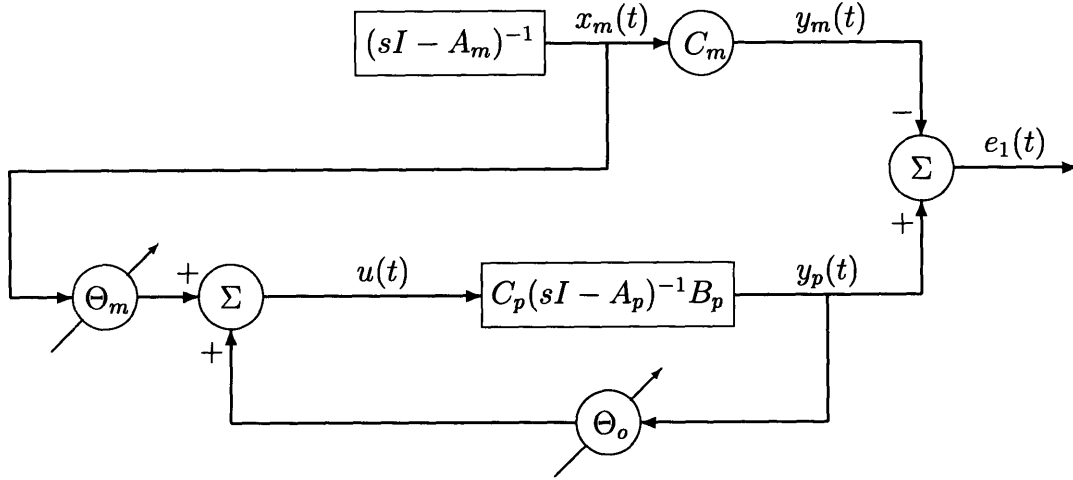


Figure 4-2: Simplified Low Order Adaptive Control Scheme when $\text{rank}(C_p B_p) = m$

If it is known *a priori* that $\text{rank}(C_p B_p) = m$ so that in assumption (A1) $r_i[G_p(s)] = 1 \forall i$, then the controller can be simplified as described below. Define (Fig. 4-2)

$$e_1(t) = y_p(t) - y_m(t), \quad \Theta(t) = [\Theta_o(t) \quad \Theta_m(t)], \quad \omega^T(t) = [y_p^T(t) \quad x_m^T(t)]. \quad (4.8)$$

The control input is given by

$$u(t) = \Theta(t)\omega(t), \quad (4.9)$$

and the adaptive law for adjusting Θ is given by

$$\dot{\Theta}(t) = -\Gamma e_1(t)\omega^T(t). \quad (4.10)$$

Then we have the following result.

Theorem 5 When $G_p(s)$ is such that $\text{rank}(C_p B_p) = m$ and assumptions (A2) and (A3) are satisfied, and the desired trajectory $y_m(t)$ is given by Eq. (3.24) satisfying assumption (M1), then the adaptive controller given by Eqs. (4.9) – (4.10) ensures that all signals in the loop are globally bounded and that $e_1(t)$ tends to zero asymptotically. •

Proof: Using Lemma 6, the proof follows along similar lines as the proof of Theorem 4. □

Remarks:

1. In assumption (A1), knowledge of the relative degrees, together with a nonsingular $E[G_p(s)]$, implies that the Hermite normal form of the plant is diagonal where the transfer functions on the diagonal are of order one or two. This essentially replaces assumption (II) discussed in Chapter 1.
2. It is worth noting that in contrast to many multivariable adaptive control algorithms, the observability index ν is not required to be known for designing the adaptive controller (assumption (I) in Chapter 1). Furthermore, the adaptive control algorithm presented here is of significantly lower order than most other MIMO adaptive schemes (Table 4.1).
3. One of the most important parameters in designing the adaptive controller given in Theorem 4 is the filter parameter a in Eq. (4.1). a determines indirectly how large a loop gain θ_o is needed to achieve the desired strictly positive real transfer function $W_m(s) = [(s + a)I](1 - \theta_o G_p(s)G_c(s)\Theta_o)^{-1}G_p(s)G_c(s)$. In general, if a is chosen to be large with respect to the open loop bandwidth a high gain θ_o^* is required to make $W_m(s)$ SPR. The benefit of the high gain is that $W_m(s)$ will have a high bandwidth and a fast speed of response. For the tracking problem, this implies that the effect of initial conditions diminishes quickly. The disadvantage of a large gain θ_o^* is that unmodeled dynamics may get excited, that actuator saturation can occur and that the controller becomes more sensitive to measurement noise.
4. The controllers presented in Theorem 4 and Theorem 5 are based on the non-adaptive phase-lead and static output feedback controllers discussed in Chapter 3. Tracking is achieved using an adaptive version of the feedforward controller discussed in section 3.4. Naturally, the comments made in section 3.2.1 regarding the use of more sophisticated compensator structures apply here as well.

Λ can be chosen, based on prior information, such that $W_m(s)$ becomes SPR for lower gain. Also, Λ can be chosen close to stable open loop poles so that tracking can be achieved using fewer states in the feedforward model A_m .

When constant or sinusoidal disturbances are present then the internal model principle as discussed in section 3.2.2 can be applied here as well. In the singlevariable case for example, if a sinusoidal disturbance is present the term ω_d in

$$G_c(s) = \frac{s + a_o}{s + b_o} \frac{s^2 + c_1 s + c_o}{s^2 + \omega_d^2}.$$

can be assumed unknown, and the control algorithm can be modified to include an estimate of ω_d . The adaptation algorithm then ensures that exact tracking is achieved. In case the disturbance is known not to be constant or sinusoidal, exact tracking cannot be achieved. If the disturbance is band limited, the augmented algorithm can still be used to achieve disturbance attenuation. However, the modified adaptive algorithm presented in section 4.3 will have to be used to guarantee boundedness of the loop signals.

5. When $r_i[G_p(s)] = 1 \forall i$ and $E[G_p(s)]$ is non-singular, and all $r_{ij}[G_p(s)]$ are known ($i, j = 1, \dots, m$) then $G_p(s)$ can be augmented with a precompensator $W_c(s) \in \mathcal{R}^{m \times m}(s)$ so that for $\overline{G}_p(s) = G_p(s)W_c(s)$ satisfies $r_i[\overline{G}_p(s)] = 1$ or 2 and $E[\overline{G}_p(s)]$ is almost always nonsingular [56]. If $r_i[G_p(s)] = 2 \forall i$, even though a compensator can be found for which $E[\overline{G}_p(s)]$ is almost always nonsingular, $r_i[\overline{G}_p(s)]$ exceeds 2 and therefore Theorem 4 is not directly applicable.
6. Assumption (M1) is included for ease of exposition as well as to allow better tracking of slowly decaying exponentials.

	MRAC	Low Order Controller
Number of on-line adjustable parameters	$2\nu m^2 \geq 2nm$	$2m^2 + mp$
Order of the underlying fixed controller	$2m(\nu - 1) + p \geq 2(n - m) + p$	$m + p$
Order of the adaptive controller	$2m(\nu - 1) + 2\nu m + p \geq 2(n - m) + 2n + p$	$3m + 2p$
Total number of controller states	$2\nu m^2 + 2m(\nu - 1) + 2\nu m + p \geq 2nm + 2(n - m) + 2n + p$	$2m^2 + mp + 3m + 2p$

Table 4.1: Comparison of the order of the MRAC and the Low Order Adaptive Controller. (MIMO MRAC for a plant satisfying assumption (A1) with $r_i[G_p(s)] = 2 \forall i$. For the MRAC, p denotes the order of the reference model. For the Low Order Controller, p denotes the dimension of A_m .)

4.3 The Robustified Adaptive Control Algorithm

The adaptive controller presented in section 4.2 is developed assuming that (A1), (A2) and (A3) are satisfied. Furthermore, the analysis assumes that no unexpected external disturbances are present. In any practical application these assumptions will not always be valid. The modified algorithm presented in this section guarantees boundedness of the loop signals in the case that these assumptions are violated. The non-ideal MIMO LTI system that will be considered in this section is described by

$$y_p = G(s)u + G_d(s)d = \{G_p(s)[I + \mu\Delta_i(s)] + \mu\Delta_a(s)\}u + G_d(s)d \quad (4.11)$$

where the minimal representations of $G_p(s)$ and $G_d(s)$ are given by

$$G_p(s) = C_p(sI - A_p)^{-1}B_p \quad (3.2)$$

$$G_d(s) = C_p(sI - A_p)^{-1}L_p. \quad (3.3)$$

$G_p(s) \in \mathcal{R}^{m \times m}(s)$ is the nominal plant for which the adaptive controller described in section 4.2 is developed, $G_d(s) \in \mathcal{R}^{m \times s}(s)$ shows how the bounded disturbance $d : \mathbb{R}^+ \rightarrow \mathbb{R}^s$ enters the system. The violation of assumptions (A1) and (A2) is reflected by $\Delta_a(s)$ and $\Delta_i(s)$. Without loss of generality, we weight $\Delta_a(s)$ and $\Delta_i(s)$ by the same positive scalar μ .

The following assumptions regarding the nominal plant are needed.

(A1) (i) $r_i[G_p(s)] = 1$ or 2 ($i = 1, 2, \dots, m$) and, (ii) $E[G_p(s)]$ is nonsingular.

(A2) The transmission zeros of $G_p(s)$ lie in \mathbb{C}^- .

(A4) K_p is sign definite, and $\Gamma = \text{sgn}(K_p)\gamma I$ where $\text{sgn}(K_p)$ is known.

(A5) An upperbound θ_{max}^* on the desired control parameter matrix is known,

where $|\Theta^*|_F < \theta_{max}^*$,

and $|A|_F^2 \triangleq \text{trace}(A^T A)$.

In describing the assumptions on Δ_a and Δ_i , and in the proof of Theorem 6, the following notation will be used. If $f : \mathbb{R}^+ \rightarrow \mathbb{R}^n$ and $T \in \mathbb{R}^+$, $\|f\| = \|f\|_\infty \triangleq \text{ess sup}_{t \geq 0} |f(t)|_2$ and $f_T(t) = f(t)$ for $t \leq T$ and $f_T(t) = 0$ for $t > T$. Let H be a MIMO, LTI operator such that $H : \mathcal{L}^\infty \rightarrow \mathcal{L}^\infty$ where $\mathcal{L}^\infty = \{f : \mathbb{R}^+ \rightarrow \mathbb{R}^n \mid \|f\|_\infty < \infty\}$. The \mathcal{L}^∞ induced operator norm of H is denoted by $\|H\|_1$, and is defined as (see [14], for example)

$$\|H\|_1 \triangleq \sup_{x \neq 0} \frac{\|Hx\|}{\|x\|}.$$

The assumptions on the plant perturbations are as follows:

Δ_m and Δ_a are assumed to be LTI, and

(U1) $\|\Delta_m\|_1$ is bounded,

(U2) $\|\bar{\Delta}_a\|_1$ is bounded,

where the Laplace transform of $\bar{\Delta}_a$ is defined as $\bar{\Delta}_a(s) \triangleq \Delta_a(s)[I(s + \epsilon)]$ for some $\epsilon \in \mathbb{R}^+$. Δ_m and Δ_a are allowed to be infinite dimensional.

The adaptive control algorithm is described below. Let e_1 , Θ , ω and $\bar{\omega}$ be defined as in Eq. (4.1). Define

$$\bar{\Theta}(t) = [\bar{\Theta}_o(t) \quad \bar{\Theta}_1(t) \quad \bar{\Theta}_m(t)].$$

The control law remains unchanged as

$$u(t) = \Theta(t)\omega(t) + \dot{\Theta}(t)\bar{\omega}(t), \quad (4.2)$$

and the control parameters Θ are determined as projection of $\bar{\Theta}$ given by

$$\Theta(t) = \begin{cases} \bar{\Theta}(t) & \text{if } |\bar{\Theta}(t)|_F \leq \theta_{max}^* \\ \frac{\theta_{max}^*}{|\bar{\Theta}(t)|_F} \bar{\Theta}(t) & \text{if } |\bar{\Theta}(t)|_F > \theta_{max}^*, \end{cases} \quad (4.12)$$

and Θ is adjusted according to the adaptive law

$$\dot{\Theta}(t) = -\Gamma e_1(t)\bar{\omega}^T(t) - \sigma(\bar{\Theta}(t) - \Theta(t)), \quad \sigma > 0. \quad (4.13)$$

The following Theorem states the boundedness result.

Theorem 6 When $G_p(s)$ in Eq. (3.1) satisfies assumptions (A1), (A2), (A4), and (A5), the uncertainties $\Delta_a(s)$ and $\Delta_i(s)$ satisfy assumptions (U1) and (U2), the disturbance d is bounded and the desired trajectory is given by Eq. (3.24) satisfying assumption (M1), then a $\mu^* > 0$ exists such that for all $\mu \in [0, \mu^*)$ the adaptive controller given by Eqs. (4.2), (4.12) and (4.13) ensures that all the signals in the loop are globally bounded. If $\mu = 0$ and $d(t) \equiv 0$ then the adaptive controller ensures that the output error $e_1(t)$ tends to zero asymptotically. •

Proof: In what follows, let $\xi_i(t)$ ($i = 1, \dots, 4$) denote exponentially decaying signals of appropriate dimension due to initial conditions. Define the parameter error $\Phi(t) = \Theta(t) - \Theta^*$ and define the nonminimal state error

$$e \triangleq x - x^*,$$

where $x \in \mathbb{R}^n$ is given by

$$\begin{aligned} \dot{x} &= \bar{A}e + B(\Theta_m^* x_m + \Phi\omega + \dot{\Phi}\bar{\omega}) + B\Theta_o^* \mu \Delta_a[u] + B_1 \mu \Delta_m[u] + L_d d \\ y_p &= Cx + \Delta_a[u], \end{aligned}$$

where \bar{A} , B and C are defined by Eq. (3.16), $B_1^T = [B_p^T \ 0]$, $L_d^T = [L_p^T \ 0]$. Δ_a and Δ_m denote LTI operators. $x^* \in \mathbb{R}^n$ is the state in the nonminimal state-space representation of

$$y_m = \widetilde{W}_m(s) \text{sgn}(K_p) \Theta_m^* x_m - \xi_1$$

where, from the discussion in section 3.4, $\xi_1(t) = Ce^{\bar{A}t}(x(0) - \Theta_{pm}^* x_{m0})$. It follows that the nonminimal state error representation is given by

$$\begin{aligned} \dot{e} &= \bar{A}e + B(\Phi\omega + \dot{\Phi}\bar{\omega}) + B\Theta_o^* \mu \Delta_a[u] + B_1 \mu \Delta_m[u] + L_d d \\ e_1 &= Ce + \Delta_a[u] + \xi_1, \end{aligned} \tag{4.14}$$

From Corollary 2 it is known that $\widetilde{W}_m(s)$ is SPR, hence Lemma 2 implies there exist

a matrix $P = P^T > 0$, a vector L , a scalar k and a positive scalar ρ such that

$$\begin{aligned}\bar{A}^T P + P \bar{A} &= -LL^T - 2\rho P \\ \text{sgn}(K_p)B^T P + kL^T &= aC + C\bar{A} \\ \text{sgn}(K_p)K^T K &= CB + (CB)^T.\end{aligned}\tag{4.15}$$

Define the fictitious state \bar{e} as

$$\bar{e} = \begin{bmatrix} 1 \\ s+a \end{bmatrix} e,\tag{4.16}$$

then \bar{e} evolves as

$$\begin{aligned}\dot{\bar{e}} &= \bar{A}\bar{e} + B\Phi\bar{w} + B\Theta_o^*\mu\Delta_a[\Theta\bar{w}] + B_1\mu\Delta_m[\Theta\bar{w}] + L_d\bar{d} + \xi_2 \\ e_1 &= (aC + C\bar{A})\bar{e} + CB\Phi\bar{w} + CB\Theta_o^*\mu\Delta_a[\Theta\bar{w}] + \mu H\bar{\Delta}_a[\Theta\bar{w}] + CB_1\mu\Delta_m[\Theta\bar{w}] + \\ &\quad CL_d\bar{d} + C\xi_2 + \xi_1 + \xi_3.\end{aligned}\tag{4.17}$$

In Eq. (4.17), $\bar{\Delta}_a$ and H denote MIMO LTI operators. $\bar{\Delta}_a$ is defined as in assumption (U2), the Laplace transform of H is defined as $H(s) = [I \frac{s+a}{s+\epsilon}]$, $\epsilon \in \mathbb{R}^+$. $\bar{d} \in \mathbb{R}^s$ is an equivalent input disturbance defined as $\bar{d}(t) = \int_0^t e^{-aI(t-\tau)} d(\tau) d\tau$. We choose a Lyapunov function candidate of the form

$$V(\bar{e}, \bar{\Theta}) = \bar{e}^T P \bar{e} + \gamma^{-1} \text{tr}(\Phi^T \Phi) + 2\gamma^{-1} \text{tr}(\Phi^T (\bar{\Theta} - \Theta)).\tag{4.18}$$

Since

$$\text{tr}(\Phi^T (\bar{\Theta} - \Theta)) \geq (|\bar{\Theta}|_F - \theta_{max}^*)(\theta_{max}^* - |\Theta^*|_F) > 0 \quad \text{if } |\bar{\Theta}|_F > \theta_{max}^*,$$

it follows that $V(\bar{e}, \bar{\theta})$ is continuous, positive definite, and radially unbounded (Fig 4-3). Also, V has continuous first partial derivatives with respect to the elements of \bar{e} and $\bar{\Theta}$. Evaluating \dot{V} along the trajectories of (4.12), (4.13) and (4.17), together with the definition of P as in Eq. (4.15) and the fact that $\text{tr}(\dot{\Phi}^T (\bar{\Theta} - \Theta)) = 0$, we

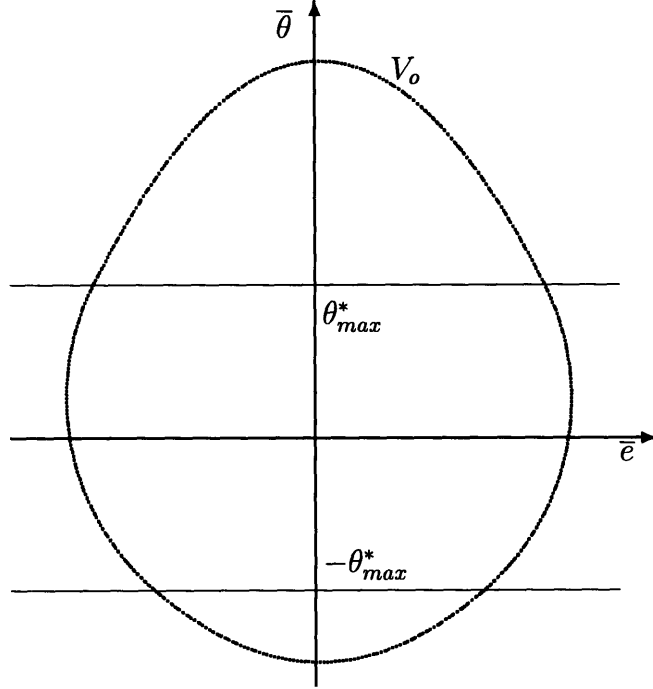


Figure 4-3: Example of a level set of V for a scalar case. $V(\bar{e}, \bar{\theta}) = \bar{e}^2 + \phi^2 + 2\phi(\bar{\theta} - \theta)$, $\theta^* = 0.5$, $\theta_{max}^* = 2$. $V_o = \{(\bar{e}, \bar{\theta}) \mid V(\bar{e}, \bar{\theta}) = 11\}$.

obtain that

$$\begin{aligned}
\dot{V}(\bar{e}, \bar{\theta}) = & -2\rho\bar{e}^T P \bar{e} - \bar{e}_2^T \bar{e}_2 + 2\bar{e}^T P(L_d \bar{d} + \xi_2) + \\
& 2(\bar{e}^T P B - \text{sgn}(K_p) \bar{\omega}^T \Phi^T C B) \Theta_o^* \mu \Delta_a[\Theta \bar{\omega}] - \\
& 2\text{sgn}(K_p) \bar{\omega}^T \Phi^T \mu H \bar{\Delta}_a[\Theta \bar{\omega}] + \\
& 2(\bar{e}^T P B_1 - \text{sgn}(K_p) \bar{\omega}^T \Phi^T C B_1) \mu \Delta_m[\Theta \bar{\omega}] - \\
& 2\text{sgn}(K_p) \bar{\omega}^T \Phi^T (C L_d \bar{d} + C \xi_2 + \xi_1 + \xi_3) - \\
& 2\sigma \gamma^{-1} \text{tr}(\Phi^T (\bar{\Theta} - \Theta))
\end{aligned} \tag{4.19}$$

where $\bar{e}_2 = L^T \bar{e} + \text{sgn}(K_p) K \Phi \bar{\omega}$. The proof of Theorem 6 is completed by considering the cases $\mu = 0$, $d \equiv 0$ and $\mu \neq 0$, $d \not\equiv 0$ separately. First we show that when $\mu = 0$, $d \equiv 0$, the closed-loop system given by Eq. (4.17) and the adaptive law in Eqs. (4.12) and (4.13) leads to globally bounded solutions and $e_1(t) \rightarrow 0$ asymptotically. When $\mu \neq 0$ and $d \not\equiv 0$, we show that all signals in the loop remain globally bounded using a small-gain type argument.

$\mu = 0, d \equiv 0$ For ease of exposition, we will neglect the effect of exponentially decaying initial conditions ξ_i ($i = 1, \dots, 3$), although the result can also be shown if they are present. Since $\text{tr}(\Phi^T(\bar{\Theta} - \Theta)) > 0$, Eq. (4.19) can be reduced to

$$\dot{V}(\bar{e}, \bar{\Theta}) \leq -2\rho\bar{e}^T P\bar{e} - \bar{e}_2^T \bar{e}_2. \quad (4.20)$$

This implies that \bar{e} and $\bar{\Theta}$ are bounded. By definition, Θ is bounded. Since $\bar{e} \in \mathcal{L}^\infty$, $\bar{\omega} \in \mathcal{L}^\infty$. It therefore follows from Eq. (4.17) that $\dot{\bar{e}} \in \mathcal{L}^\infty$. Hence $e \in \mathcal{L}^\infty$, so that all loop signals are bounded. Also, Eq. (4.20) implies that

$$\bar{e} \in \mathcal{L}^2, \quad \bar{e}_2 \in \mathcal{L}^2.$$

Therefore, $\bar{e}(t) \rightarrow 0$ as $t \rightarrow \infty$. Since

$$\dot{\Theta} = \begin{cases} \dot{\bar{\Theta}} & \text{if } |\bar{\Theta}|_F \leq \theta_{max}^* \\ \frac{\theta_{max}^*}{|\bar{\Theta}|_F} [\dot{\bar{\Theta}} - \frac{1}{|\bar{\Theta}|_F^2} \text{tr}(\bar{\Theta}^T \dot{\bar{\Theta}}) \bar{\Theta}] & \text{if } |\bar{\Theta}|_F > \theta_{max}^*. \end{cases} \quad (4.21)$$

and $\dot{\bar{\omega}} = -aI\bar{\omega} + \omega$, it follows that $\dot{\bar{e}}_2 \in \mathcal{L}^\infty$. Hence, $\bar{e}_2(t) \rightarrow 0$ as $t \rightarrow \infty$. This implies that $\Phi\bar{\omega} \rightarrow 0$ asymptotically, and as a result, $\lim_{t \rightarrow \infty} e_1(t) = 0$.

$\mu \neq 0, d \neq 0$ In what follows, let c_i ($i = 0, \dots, 15$) denote positive, finite constants. The exact definition of the c_i 's is given in Table 4.2. Substituting Eq. (4.18) in Eq. (4.19) results in

$$\dot{V} \leq -2\alpha V + 2\bar{e}^T P(L_d \bar{d} + \xi_2) - 2\text{sgn}(K_p) \bar{\omega}^T \Phi^T (CL_d \bar{d} + C\xi_2 + \xi_1 + \xi_3) + 2\alpha\gamma^{-1} \text{tr}(\Phi^T \Phi) + \delta, \quad (4.22)$$

where $\alpha = \min(\rho, \frac{\sigma}{2})$, and

$$\begin{aligned} \delta = & 2 \left(\bar{e}^T P B - \text{sgn}(K_p) \bar{\omega}^T \Phi^T C B \right) \Theta_o^* \mu \Delta_a[\Theta \bar{\omega}] - 2\text{sgn}(K_p) \bar{\omega}^T \Phi^T \mu H \bar{\Delta}_a[\Theta \bar{\omega}] \\ & + 2 \left(\bar{e}^T P B_1 - \text{sgn}(K_p) \bar{\omega}^T \Phi^T C B \right) \mu \Delta_m[\Theta \bar{\omega}]. \end{aligned}$$

The definition of e as the nonminimal state error implies that

$$\omega = \begin{bmatrix} y_p \\ \omega_1 \\ x_m \end{bmatrix} = \begin{bmatrix} C_p & 0 \\ 0 & 1 \\ 0 & 0 \end{bmatrix} e + \begin{bmatrix} C_p x_p^* \\ \omega_1^* \\ x_m \end{bmatrix} = W e + \omega^*.$$

This, together with the definition of $\bar{\omega}$ as in Eq. (4.1) and \bar{e} as in Eq. (4.16), implies that $\bar{\omega}$ can be expressed as

$$\bar{\omega}(t) = W \bar{e}(t) + \bar{\omega}^*(t) + \xi_4(t), \quad \bar{\omega}^*(t) = \int_0^t I e^{-a(t-\tau)} \omega^*(\tau) d\tau. \quad (4.23)$$

Also, using Eq. (4.18), we have

$$|\bar{e}|_2^2 \leq \frac{1}{\lambda_{\min}(P)} V. \quad (4.24)$$

Using Eqs. (4.23) and (4.24), Eq. (4.22) can be simplified as

$$\dot{V} \leq -2\alpha V + c_0 \sqrt{V} + c_1 + \delta \leq -\alpha V + c_2 + \delta. \quad (4.25)$$

Eq. (4.25) implies that

$$\|V_T\| \leq V(0) + 3\alpha^{-1} (c_2 + \|\delta_T\|). \quad (4.26)$$

Since

$$\|(\Theta \bar{\omega})_T\| = \text{ess sup}_{0 \leq t \leq T} |\Theta(t) \bar{\omega}(t)| \leq \theta_{\max}^* \|\bar{\omega}_T\|,$$

we have using Eq. (4.23) that

$$\|(\Theta \bar{\omega})_T\| \leq \theta_{\max}^* (\sigma_{\max}(W) \|\bar{e}_T\| + \|(\bar{\omega}^* + \xi_4)_T\|), \quad (4.27)$$

and, similarly,

$$\|(\Phi \bar{\omega})_T\| \leq 2\theta_{\max}^* (\sigma_{\max}(W) \|\bar{e}_T\| + \|(\bar{\omega}^* + \xi_4)_T\|). \quad (4.28)$$

Using Eqs. (4.27) and (4.28) it follows that

$$\begin{aligned}\|\delta_T\| &\leq \mu\|\bar{\Delta}_a\|_1(c_4\|\bar{e}_T\|^2 + c_5\|\bar{e}_T\| + c_6) + \mu\|\Delta_m\|_1(c_7\|\bar{e}_T\|^2 + c_8\|\bar{e}_T\| + c_9) \\ &\leq \mu\|\bar{\Delta}_a\|_1(2c_4\|\bar{e}_T\|^2 + \frac{c_5^2}{4c_4} + c_6) + \mu\|\Delta_m\|_1(2c_7\|\bar{e}_T\|^2 + \frac{c_8^2}{4c_7} + c_9).\end{aligned}\quad (4.29)$$

Also, Eq. (4.24) implies that

$$\|\bar{e}_T\|^2 \leq \frac{1}{\lambda_{\min}(P)}\|V_T\|, \quad (4.30)$$

so that, using Eqs. (4.29) and (4.30), Eq. (4.26) can be written as

$$\|V_T\| \leq c_3 + c_{10}\mu\|\bar{\Delta}_a\|_1 + c_{11}\mu\|\Delta_m\|_1 + c_{12}\mu\|\bar{\Delta}_a\|_1\|V_T\| + c_{13}\mu\|\Delta_m\|_1\|V_T\|.$$

Assumptions (U1) and (U2) imply that there exist positive, finite constants c_{14} and c_{15} such that $\|\bar{\Delta}_a\|_1 = c_{14}$, $\|\Delta_m\|_1 = c_{15}$. If we define $\mu^* = \frac{1}{c_{12}c_{14} + c_{13}c_{15}}$, then for all $\mu \in [0, \mu^*)$ we have that

$$\|V_T\| \leq \frac{c_3 + \mu(c_{10}c_{14} + c_{11}c_{15})}{1 - \mu(c_{12}c_{14} + c_{13}c_{15})}. \quad (4.31)$$

Hence, $\|V_T\|$ is bounded for all $T \in \mathbb{R}^+$. Since V is bounded, \bar{e} and $\bar{\theta}$ are bounded, which implies that all signals in the loop are bounded. \square

$$\begin{aligned}
c_0 &= 2[\lambda_{\min}(P)]^{-\frac{1}{2}} \left\{ \sigma_{\max}(PL_d)3a^{-1}\|d\| + \lambda_{\max}(P)\|\xi_2\| + \right. \\
&\quad \left. 2\theta_{\max}^* \sigma_{\max}(W)(\sigma_{\max}(CL_d)3a^{-1}\|d\| + \sigma_{\max}(C)\|\xi_2\| + \|\xi_1\| + \|\xi_3\|) \right\} \\
c_1 &= 4\theta_{\max}^* \|\bar{w}^* + \xi_4\| (\sigma_{\max}(CL_d)3a^{-1}\|d\| + \sigma_{\max}(C)\|\xi_2\| + \|\xi_1\| + \|\xi_3\|) + \\
&\quad 8\alpha\gamma^{-1}\theta_{\max}^{*2} \\
c_2 &= \frac{c_0^2}{4\alpha} + c_1 \\
c_3 &= V(0) + 3\alpha^{-1}c_2 \\
c_4 &= \theta_{\max}^* \theta_o^* 3\epsilon^{-1} \sigma_{\max}(W) (2\sigma_{\max}(PB) + 2\sigma_{\max}(CB)\theta_{\max}^* \sigma_{\max}(W)) + \\
&\quad 4\|H\|_1 \theta_{\max}^{*2} \sigma_{\max}^2(W) \\
c_5 &= 2\theta_{\max}^* \|\bar{w}^* + \xi_4\| \left\{ \theta_o^* 3\epsilon^{-1} (\sigma_{\max}(PB) + 2\sigma_{\max}(CB)\theta_{\max}^* \sigma_{\max}(W)) + \right. \\
&\quad \left. 4\theta_{\max}^* \|H\|_1 \sigma_{\max}(W) \right\} \\
c_6 &= \theta_{\max}^{*2} \|\bar{w}^* + \xi_4\|^2 (\theta_o^* 3\epsilon^{-1} 2\sigma_{\max}(CB) + 4\|H\|_1) \\
c_7 &= \theta_{\max}^* \theta_o^* \sigma_{\max}(W) (2\sigma_{\max}(PB_1) + 2\theta_{\max}^* \sigma_{\max}(CB)\sigma_{\max}(W)) \\
c_8 &= 2\theta_{\max}^* \|\bar{w}^* + \xi_4\| \theta_o^* (\sigma_{\max}(PB_1) + 2\theta_{\max}^* \sigma_{\max}(CB)\sigma_{\max}(W)) \\
c_9 &= 2\theta_{\max}^{*2} \theta_o^* \sigma_{\max}(CB) \|\bar{w}^* + \xi_4\|^2 \\
c_{10} &= 3\alpha^{-1} \left(\frac{c_5^2}{4c_4} + c_6 \right) \\
c_{11} &= 3\alpha^{-1} \left(\frac{c_8^2}{4c_7} + c_9 \right) \\
c_{12} &= 6c_4 \alpha^{-1} [\lambda_{\min}(P)]^{-1} \\
c_{13} &= 6c_7 \alpha^{-1} [\lambda_{\min}(P)]^{-1} \\
c_{14} &= \|\bar{\Delta}_a\|_1 \\
c_{15} &= \|\Delta_m\|_1
\end{aligned}$$

Table 4.2: Definition of Constants in Robustness Proof

Remarks:

1. If an estimate $\hat{\Theta}^*$ of the desired control parameters is available, then the algorithm can be modified by replacing $\Theta(t)$ in Eq. (4.2) by $\tilde{\Theta}(t) + \hat{\Theta}^*$, and by replacing $\Theta(t)$ in Eqs. (4.12) and (4.13) by $\tilde{\Theta}(t)$. Furthermore, if the magnitude of θ_{max}^* in assumption (A5) can be reduced then μ^* can be increased.
2. A projection-like algorithm is used in Eqs. (4.12) and (4.13) for guaranteeing robustness. While a similar continuous-time algorithm has been proposed in [46], Eqs. (4.12) and (4.13) are significantly simpler.
3. If it is known *a priori* that $rank(C_p B_p) = m$, then the algorithm given by Eqs. (4.2), (4.12) and (4.13) can be simplified in a manner similar to the non-robustified algorithm given in Theorem 5.
4. It follows from Eqs. (4.30) and (4.31) that

$$\|\bar{e}\| \leq \sqrt{\frac{c_3 + \mu(c_{10}c_{14} + c_{11}c_{15})}{\lambda_{min}(P) - 6\alpha^{-1}\mu(c_4c_{14} + c_7c_{15})}},$$

which together with Eq. (4.17) provides a quantitative bound on the transient performance of the adaptive controller. Since the plant parameters are unknown, this bound can not be evaluated in practice. This bound is also conservative by the very nature of the way it is derived. However, it does provide some insight as to how the system parameters affect the performance. For example, as θ_{max}^* increases the bound on $\|\bar{e}\|$ increases.

5. It should be noted that the control input u in Eq. (4.2) with Θ defined as in Eq. (4.12) is not continuous when $|\bar{\Theta}|_F = \theta_{max}^*$. This is because at $|\bar{\Theta}|_F = \theta_{max}^*$, Θ is continuous but not differentiable, i.e. $\dot{\Theta}$ in Eq. (4.21) is not continuous. For this reason, the modification of the adaptive law presented here may be more appropriate for bounding slowly drifting control parameters.
6. The Lyapunov based approach taken here to analyze the stability of the adaptive control system in the presence of unmodeled dynamics is significantly different

from the approach taken in the non-adaptive robust control literature where the stability analysis is based on the small-gain theorem. The small-gain theorem can provide powerful stability criteria for nonstructured as well as structured uncertainties. Clearly, the connection of robust adaptive control methods with non-adaptive robust control design techniques is of crucial importance for lasting success of adaptive control. Unfortunately, although the adaptive system presented in this section can be cast into the small-gain framework, the evaluation of the relevant operator norms is a non-trivial task.

7. Theorem 4.3 states that a robust adaptive controller exists for small enough plant perturbations. The robust adaptive controller synthesis problem is an open problem, although some partial results have been reported in [34, 61].
8. As was noted in [27], the characterization of the unmodeled dynamics as in assumptions (U1) and (U2) implies that the perturbations can not have a direct throughput at $\mu=0$, i.e. perturbations of the form $\mu\Delta_i = \frac{1}{\mu s+1}$ ($i = a, m$) are not allowed, whereas perturbations of the form $\mu\Delta_i = \frac{\mu}{\mu s+1}$ ($i = a, m$) are admissible. The design of adaptive controllers such that this assumption is relaxed is still an open issue.

4.4 Summary

In this Chapter the low order adaptive controller was developed in two parts. In the first part, under certain assumptions, the adaptation algorithm was presented. Using results from Chapter 3, a compact stability proof was given. The algorithm ensures that the plant output converges asymptotically to the reference trajectory.

In the second part the adaptive laws were modified to account for fast unmodeled dynamics and high frequency disturbances. When unmodeled dynamics are present, the controller is shown to result in bounded loop signals with a tracking error proportional to the size of the unmodeled dynamics, the magnitude of the exogenous input and the size of the parametric uncertainty.

Chapter 5

Application to Vibration Systems

5.1 Introduction

In this chapter the adaptive controller developed in Chapter 4 will be applied to two illustrative examples motivated by practical control problems. The Chapter is divided into two parts. In section 5.2 it is shown how the low order adaptive controller can be applied to flexible structures for tracking and disturbance rejection. In section 5.3 the controller is used to stabilize a combustion process. These applications illustrate the different aspects of the low order adaptive controller by tuning selected gains only. The mass-spring-damper example discussed in section 5.2.5 shows how by tuning the feedforward gain Θ_m , tracking can be achieved. In this case, the other control parameters remain fixed. Similarly, in section 5.2.6 it is shown how by only tuning the compensator gain Θ_1 , disturbance rejection is achieved. The combustion example in section 5.3 shows how by tuning the feedback gain Θ_o , pressure modes are stabilized.

The systems considered in this Chapter can be described by a finite-dimensional, second order matrix differential equation of the form

$$M\ddot{x} + C\dot{x} + Kx = B_{ux}u, \quad (5.1)$$

where $x : \mathbb{R}^+ \rightarrow \mathbb{R}^{n_p/2}$, n_p even, and $u : \mathbb{R}^+ \rightarrow \mathbb{R}^m$, $n_p \geq 2m$. The measurements

are given by

$$y = C_{xy}x \quad (5.2)$$

where $y : \mathbb{R}^+ \rightarrow \mathbb{R}^m$. In the applications that we will consider here we have that $M = M^T > 0$ and $K = K^T > 0$. The properties of the matrix C depend on the specifics of the system under consideration. The input-output representation of Eqs. (5.1) and (5.2) is given by $y = G_p(s)u$ where

$$G_p(s) = C_{xy} [Ms^2 + Cs + K]^{-1} B_{ux}.$$

For application of the adaptive controller to the system described by Eqs. (5.1) and (5.2), it is important to recognize when assumptions

(A1) (i) $r_i[G_p(s)] = 1$ or 2 ($i = 1, 2, \dots, m$) and, (ii) $E[G_p(s)]$ is nonsingular,

(A2) the transmission zeros of $G_p(s)$ lie in \mathbb{C}^- , and

(A3) an adaptation gain matrix Γ can be found such that $K_p\Gamma = (K_p\Gamma)^T > 0$,

are satisfied without relying on the parameters of the system. For satisfaction of assumptions (A1) and (A3), it is sufficient that the actuators and sensors are colocated, i.e. $C_{yx} = B_{ux}^T$. Namely, the high frequency gain matrix of the system is then given by

$$\begin{aligned} K_p = E &= \lim_{s \rightarrow \infty} s^2 B_{ux}^T [Ms^2 + Cs + K]^{-1} B_{ux} \\ &= B_{ux}^T M^{-1} B_{ux} \\ &> 0 \end{aligned}$$

since M is symmetric and positive definite. An adaptation gain $\Gamma = \gamma I_{m \times m}$, $\gamma > 0$ will satisfy assumption (A3). In fact, since $K_p > 0$, Corollary 2 implies that any $\Gamma = \Gamma^T > 0$ can be used. In case Eq. (5.1) represents a discretization of a continuous system, as is the case in the finite element method for example, then the colocation assumption may be weakened, and also proximally located actuator sensor pairs are

allowed. Even for colocated systems, the verification of assumption (A2) is difficult in general. Without loss of generality, Eqs. (5.1) and (5.2) can be rearranged such that the frequency domain representation is given by

$$\begin{aligned} \begin{bmatrix} M_{11}s^2 + C_{11}s + K_{11} & M_{12}s^2 + C_{12}s + K_{12} \\ M_{21}s^2 + C_{12}s + K_{12} & M_{22}s^2 + C_{22}s + K_{22} \end{bmatrix} \begin{bmatrix} x_1 \\ x_2 \end{bmatrix} &= \begin{bmatrix} B_{xu} \\ 0 \end{bmatrix} u \\ y &= [B_{xu}^T \quad 0] \begin{bmatrix} x_1 \\ x_2 \end{bmatrix} \end{aligned}$$

where $x_1 \in \mathbb{R}^m$ and $x_2 \in \mathbb{R}^{n_p/2-m}$, and B_{xu} has full rank. The transmission zero locations are therefore given by the solution of

$$\det(M_{22}s^2 + C_{22}s + K_{22}) = 0. \quad (5.3)$$

Since the principal submatrix of a positive definite matrix is itself positive definite, we have that $M_{22} = M_{22}^T > 0$ and $K_{22} = K_{22}^T > 0$ as well. Hence, there are a total of $n_p - 2m$ finite transmission zeros. If $n_p = 2m$ no transmission zeros exist and assumption (A2) is trivially satisfied. In this case, one control input is available for each mode of vibration. If $n_p > 2m$, the minimum phaseness of the transmission zeros depends on the properties of the matrix C_{22} which depends on C . The structure of C depends on the specifics of the system considered, and we will therefore address the verification of assumption (A2) separately for each of the applications considered in sections 5.2 and 5.3.

This Chapter is organized as follows. The flexible structure and combustion applications are presented in section 5.2 and section 5.3, respectively. Both these sections are divided into subsections giving an introduction to the problem, a motivation for using adaptive control, the derivation of the dynamic model, a sample system description, simulation results and a discussion. The main contributions of this Chapter are summarized in section 5.4.

5.2 Flexible Structures

5.2.1 Introduction

In this section the application of the low order adaptive controller to flexible structures is discussed. The section is organized as follows. In section 5.2.2 a motivation for using adaptive control is given. In section 5.2.3 a dynamic model of flexible structures is presented, and the assumptions required for application of the low order adaptive controller are verified. In section 5.2.4 a sample structure is given, this sample structure was used in simulations whose results are presented in sections 5.2.5 and 5.2.6. Simulation results of an example dealing with unmodeled dynamics are given in 5.2.7. A discussion of the simulation results is given in section 5.2.8.

5.2.2 Motivation

Deployment of large space structures for communications, space defense and manufacturing has motivated many investigations in the automatic control of flexible structures. For active control of flexible structures using conventional, non-adaptive, high performance control methods, a high fidelity model of the structure is required. Such models are developed using finite element analysis. However, when a controller based on a finite element model is applied to the actual structure, the closed loop system is not necessarily stable due to differences between the actual plant and the plant model. The primary cause of instability in this case is the (small) difference in the parameters that describe the plant and the model, and the low inherent damping in metal structures. The parametric uncertainties may have occurred in the modeling phase, finite element models will have errors of about 10% in modal frequencies and mode shapes [10], or may occur due to in-flight structural modifications. Another fact that complicates control design is the close spacing of the vibration modes which makes controller roll-off in the presence of the parametric uncertainty and low damping a difficult problem [28, 54].

Since conventional methods do not work well, many efforts have been undertaken

to develop more robust control methods for flexible structures. The simplest, robust control method is the use of velocity feedback. Here colocated velocity feedback is used to add damping to the structural modes [10]. This can be accomplished without requiring an accurate plant model. The disadvantage of this method is that it is difficult to find feedback gains so that selected modes have the desired amount of added damping. More recently, an approach has been suggested that enables the feedback to add more damping in a selected frequency range using impedance matching ideas [40]. These methods work well if vibration suppression is desired for broadband disturbance inputs, and are known as Low Authority Control (LAC) since they seek to modify the structural modes only slightly [3]. In case certain modes strongly influence performance, as may be the case in pointing or shape control applications, high added damping or mode shape adjustment of a few modes is desirable. This is typically accomplished using High Authority Control (HAC). Examples of such controllers are LQG , LQG/LTR and H_∞ . Since these controllers are model based, the controller order is in principle as high as that of the plant model which could make the controller practically infeasible. Also, since the controllers rely heavily on the fidelity of the plant model they can perform badly in the presence of parametric uncertainties in the plant model. Methods have been developed to guard against the adverse effects of parametric uncertainty however (real μ -analysis, for example). In HAC/LAC both control strategies are combined.

Since parametric uncertainty is a primary concern in designing high performance controllers for flexible structures, the use of adaptive control is only natural and this application was therefore the initial motivation for the development of the controller presented in this thesis. The adaptive controller can be viewed as a HAC/LAC controller. The feedback loop with Θ_o in combination with the phase-lead based compensator ensures that some damping is added to the vibration modes (LAC part). The use of a feedforward input with gain Θ_m and further augmentation of the compensator with gain Θ_1 assures that tracking and disturbance rejection are achieved at the measured outputs (HAC part). Adaptive control for flexible structures has been investigated in [7, 8, 44]. The disadvantage of these controllers is that they rely heav-

ily on the use of both position and velocity measurements while in most cases only one of the two is available. The adaptive controller presented in this thesis requires position measurements only.

5.2.3 Dynamic Model

In this section we outline briefly why flexible structures can be represented as in Eq. (5.1), and we verify assumption (A2) regarding minimum phaseness. Using finite element analysis, assuming small displacements, dynamic models of flexible structures are of the form

$$\begin{aligned} M\ddot{x} + Kx &= B_{xu}u \\ y &= C_{xy}x \end{aligned} \tag{5.4}$$

where $M = M^T > 0$ is the (consistent) mass matrix and $K = K^T > 0$ is the stiffness matrix. Here we will assume that the finite element mesh is chosen such that Eq. (5.4) is a model of the continuous structure valid in the frequency range upto 4 to 10 times the desired closed loop bandwidth ¹. From a physical point of view, it is known that any flexible structure, with no rigid body modes, will come to rest when released from any initial condition. However, the model in Eq. (5.4) implies that all system trajectories remain on the same level set ². Hence, although the model in Eq. (5.4) does capture the kinetic and potential energies of the structure, it does not capture the dissipative mechanism. The model postulated in Eq. (5.1) is the simplest linear model that captures the energy dissipative mechanism, with $C > 0$ ³. The dissipative mechanism is attributed to the presence of material damping, which is very difficult to model explicitly. Since material damping is typically very small, $\lambda_{min}(C) > \epsilon > 0$ where $\epsilon \in \mathbb{R}^+$ is small.

The properties of C are important to establish if the system described by Eqs. (5.1) and (5.2) is minimum phase. Consider Eq. (5.3). For $n_p > 2m$, since $C > 0$ it follows that $C_{22} > 0$ as well. The roots of Eq. (5.3) are then the poles of a structure

¹In section 5.3 this issue is addressed in a finite element representation of a combustion process.

²Choose a Lyapunov function of the form $V(x, \dot{x}) = \frac{1}{2}\dot{x}^T M \dot{x} + \frac{1}{2}x^T K x$, $u \equiv 0$.

³This can be shown using the same Lyapunov function and LaSalle's Invariant Set Theorem.

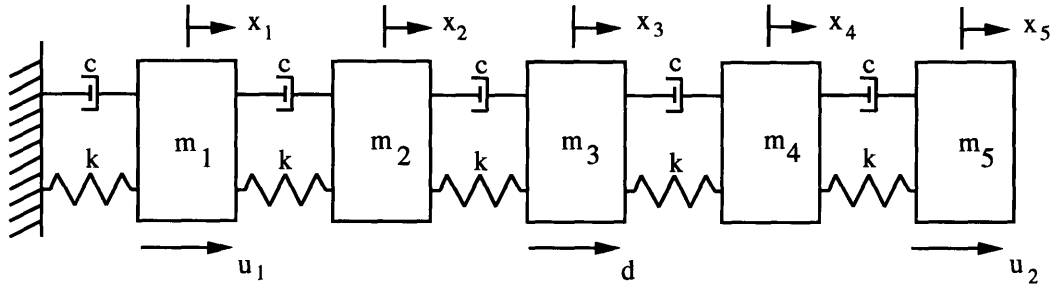


Figure 5-1: Sample flexible structure.

described by $M_{22}\ddot{z} + C_{22}\dot{z} + K_{22}z = 0$ where $z : \mathbb{R}^+ \rightarrow \mathbb{R}^{n_p/2-m}$. Since these poles are exponentially stable, it follows that the transmission zeros of the system described by Eqs. (5.1) and (5.2) are finite, and lie in \mathbb{C}^- . Assumption (A2) is therefore satisfied. In numerical simulations of the dynamic response of flexible structures, damping is typically modeled as proportional or modal with, respectively, coefficients or damping ratios chosen based on experimental observations [9]. In case proportional or modal damping is assumed, even more can be said about the locations of the transmission zeros, see [64].

5.2.4 Sample Structure

In this section a sample problem to illustrate the use of the controller for flexible structures is discussed. This sample problem has deliberately been kept simple, the underlying system dynamics is easy to understand. For application of the controller to a complex flexible structure, see [4, 5]. The sample system consists of five masses with five identical springs and dampers connected in series (Fig. 5-1). The x_i ($i = 1, \dots, 5$) denote positions of the masses with respect to a fixed reference frame. We will consider a two-input two-output case, with two collocated actuator-sensor pairs at x_1 and x_5 .

The equation of motion of the mass-spring-damper is given by

$$\begin{bmatrix} m_1 & 0 & 0 & 0 & 0 \\ 0 & m_2 & 0 & 0 & 0 \\ 0 & 0 & m_3 & 0 & 0 \\ 0 & 0 & 0 & m_4 & 0 \\ 0 & 0 & 0 & 0 & m_5 \end{bmatrix} \begin{bmatrix} \ddot{x}_1 \\ \ddot{x}_2 \\ \ddot{x}_3 \\ \ddot{x}_4 \\ \ddot{x}_5 \end{bmatrix} + \begin{bmatrix} 2c & -c & 0 & 0 & 0 \\ -c & 2c & -c & 0 & 0 \\ 0 & -c & 2c & -c & 0 \\ 0 & 0 & -c & 2c & -c \\ 0 & 0 & 0 & -c & c \end{bmatrix} \begin{bmatrix} \dot{x}_1 \\ \dot{x}_2 \\ \dot{x}_3 \\ \dot{x}_4 \\ \dot{x}_5 \end{bmatrix} +$$

$$\begin{bmatrix} 2k & -k & 0 & 0 & 0 \\ -k & 2k & -k & 0 & 0 \\ 0 & -k & 2k & -k & 0 \\ 0 & 0 & -k & 2k & -k \\ 0 & 0 & 0 & -k & k \end{bmatrix} \begin{bmatrix} x_1 \\ x_2 \\ x_3 \\ x_4 \\ x_5 \end{bmatrix} = \begin{bmatrix} 1 & 0 \\ 0 & 0 \\ 0 & 0 \\ 0 & 0 \\ 0 & 1 \end{bmatrix} \begin{bmatrix} u_1 \\ u_2 \end{bmatrix}$$

The measurements are given by

$$\begin{bmatrix} y_1 \\ y_2 \end{bmatrix} = \begin{bmatrix} 1 & 0 & 0 & 0 & 0 \\ 0 & 0 & 0 & 0 & 1 \end{bmatrix} \begin{bmatrix} x_1 \\ x_2 \\ x_3 \\ x_4 \\ x_5 \end{bmatrix}.$$

For this sample system two control objectives will be considered, tracking and disturbance rejection.

5.2.5 Tracking Example

It is the objective of this example to show how the low order adaptive controller reacts to parameter changes that occur on-line. The control objective is for the first and fifth mass to follow an up-and-down reference trajectory. During the tracking task, a parametric uncertainty is introduced. These parametric changes cause the controller to be mismatched to the actual structure, and results in a tracking error. The parameters in the adaptive controller are then tuned on-line such that this tracking error is

eliminated.

The low order adaptive controller in Theorem 4 was used. Based on the discussion in section 3.4, to achieve good tracking performance using a low gain design, one mode can be controlled per actuator. Since in this case two actuators were used, the other modes have to be either canceled using a more elaborate compensator design or they have to be such that their adverse effect on the tracking performance is small. In this example the latter case was considered. The nominal values for the masses are $m_1 = m_5 = 1$, $m_2 = m_3 = m_4 = 0.1$. The value for the stiffness is $k = 1$, and the damping is chosen as $c = 0.01$. For the selected actuator-sensor pairs, these values result in two dominant modes at the lowest frequencies ω_1 and ω_2 (Table 5.1). The remaining, higher frequency modes are less dominant. These modes can not be neglected however since they lie within 10 times the desired closed loop bandwidth of the controller, and can be destabilized in a closed loop dynamic system. The parametric uncertainty is introduced by increasing the masses to $m_1 = 2$ and $m_2 = 2$ on-line. The other masses are not changed. It is worth noting that this parameter change causes a large change in the low frequency, dominant modes (Table 5.1). Such changes are difficult to accommodate using conventional, fixed control methods.

To illustrate that tracking is primarily achieved using an (adaptive) feedforward input, only Θ_m will be tuned on-line (Fig. 5-2). Θ_o and Θ_1 are chosen *a priori* such that $W_m(s) = [(s + a)I]\bar{W}_m(s)$ is SPR for the range of values expected in m_1 and m_5 . With the filter parameters chosen as $a = 1$ rad/s and $\Lambda = 0.2I_{2 \times 2}$ rad/s, the feedback parameters that result in a SPR $W_m(s)$ are $\Theta_o(0) = -2I_{2 \times 2}$ and $\Theta_1(0) = -1.5I_{2 \times 2}$. Following the discussion in section 3.4, the reference trajectory for each output channel is chosen of third order, relative degree two:

$$\begin{aligned}
 A_m &= \begin{bmatrix} 0_{2 \times 2} & I_{2 \times 2} & 0_{2 \times 2} & 0_{2 \times 2} \\ -\omega_m^2 I_{2 \times 2} & -2\zeta_m \omega_m I_{2 \times 2} & 0_{2 \times 2} & I_{2 \times 2} \\ (a_o - b_o) I_{2 \times 2} & 0_{2 \times 2} & -b_o I_{2 \times 2} & 0_{2 \times 2} \\ 0_{2 \times 2} & 0_{2 \times 2} & 0_{2 \times 2} & 0_{2 \times 2} \end{bmatrix} \\
 C_m &= \begin{bmatrix} \frac{b_o}{a_o} I_{2 \times 2} & 0_{2 \times 2} & \frac{b_o}{a_o} I_{2 \times 2} & 0_{2 \times 2} \end{bmatrix} \\
 x_{m_o}^T &= [0_{1 \times 2} \quad 0_{1 \times 2} \quad 0_{1 \times 2} \quad [1 \quad 1]], \quad \text{or}
 \end{aligned}$$

frequency	nominal(rad/s)	perturbed (rad/s)	change (%)
ω_1	0.41	0.30	27
ω_2	1.11	0.80	28
ω_3	2.61	2.51	4
ω_4	4.53	4.50	3
ω_5	5.86	5.85	1

Table 5.1: Tracking Example. Natural Frequencies of the Sample Structure.

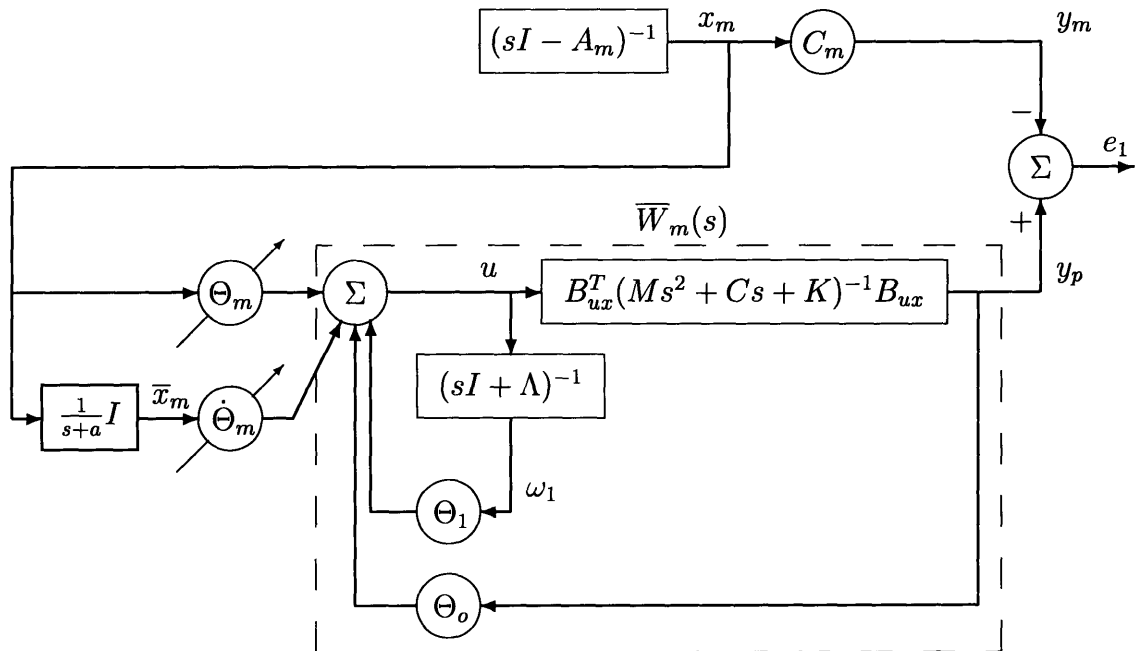


Figure 5-2: Low order adaptive control scheme for tracking. Only the feedforward parameter Θ_m is adjusted on-line.

$$x_{mo}^T = [0_{1 \times 2} \quad 0_{1 \times 2} \quad 0_{1 \times 2} \quad [0 \quad 0]].$$

A real zero at $a_o = -\Lambda(1,1) = -0.2$ rad/s is needed to eliminate initial condition effects. To cancel the effect of this zero in the reference trajectory, an almost pole-zero cancellation was created by placing a pole at $b_o = 0.21$ rad/s. Effectively, the resulting reference model is of second order of bandwidth $\omega_m = 0.5$ rad/s, damping ratio $\zeta_m = 0.707$ and unity DC-gain. The bandwidth of this reference trajectory implies that primarily the first and second mode are excited, the remaining modes are excited to a lesser degree. Based on the nominal plant values and the initial feedback gains, the initial value of Θ_m was computed using Eq. (3.26) in section 3.4 as

$$\Theta_m = \begin{bmatrix} 2.78 & -0.30 & 0.89 & 0.04 & -200.55 & 38.60 & 0.28 & 0.01 \\ -0.30 & 1.72 & 0.04 & 0.88 & 38.60 & -44.42 & 0.01 & 0.28 \end{bmatrix}.$$

Note that since all the entries in Θ_m are nonzero, there exists a cross-coupling between the two input and output channels, indicating the multivariable character of the problem. To only adjust Θ_m on-line, the adaptation gains were chosen as $\Gamma_m = I_{2 \times 2}$, $\Gamma_o = 0_{2 \times 2}$ and $\Gamma_1 = 0_{2 \times 2}$.

Simulation results are shown in Figs. 5-3–5-6. In these simulations, the masses m_1 and m_5 are increased at $t = 100s$. For comparison, the response using the underlying fixed controller, computed using the nominal parameters, is shown as well. When the adaptive control parameters are matched to those of the plant ($t < 100s$), the response of the adaptive controller is similar to that of the (matched) fixed controller (Figs. 5-3 and 5-4). When the desired trajectory undergoes a sudden step change at $t = 0s$ and $t = 50s$, there is some change in the estimated control parameters due to the effect of the higher modes, but their net effect on the parameter estimation is negligible (Fig. 5-5). Once the parameter change is introduced at $t = 100s$, the control parameters change more significantly (Fig. 5-5). For $t > 100s$, the adaptive controller improves significantly on the tracking performance of the now mismatched fixed controller (Fig. 5-3). Interestingly enough, the improvement of the tracking performance in the upward phase ($t = 100s$, $t = 200s$) is much better than the

improvement in the tracking in the downward phase ($t = 150s$, $t = 250s$). This may be due to the fact that the kinetic energy increases in the downward phase, and is more difficult to compensate for. Convergence of the trajectory in the downward phase occurs after continued excitation as well. The improvement in tracking performance is achieved with only a modest increase in control action (Fig. 5-4). Not only is the tracking performance at the measured outputs very good, the response at the other masses is acceptable (Fig. 5-6).

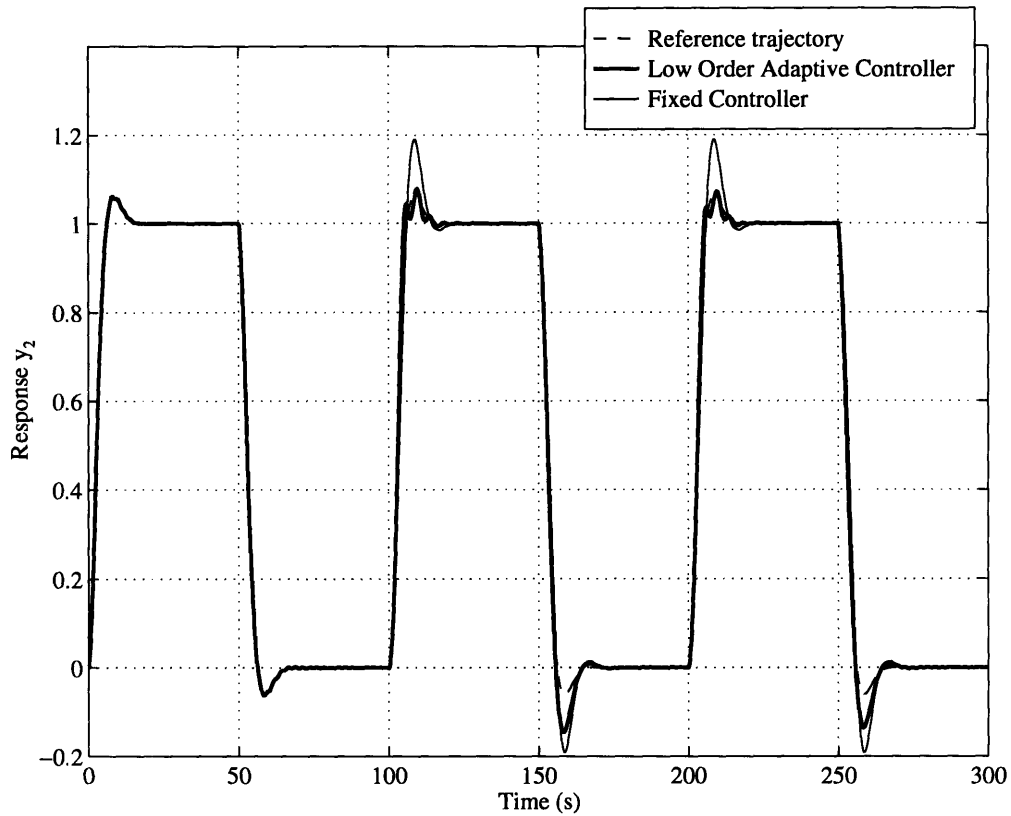


Figure 5-3: Comparison of the low order adaptive controller with the underlying fixed controller. Plant output y_2 for a tracking example. For $t < 100s$ the adaptive controller and the matched fixed controller give identical tracking performance. The adaptive controller recovers after the parameter change at $t = 100s$.

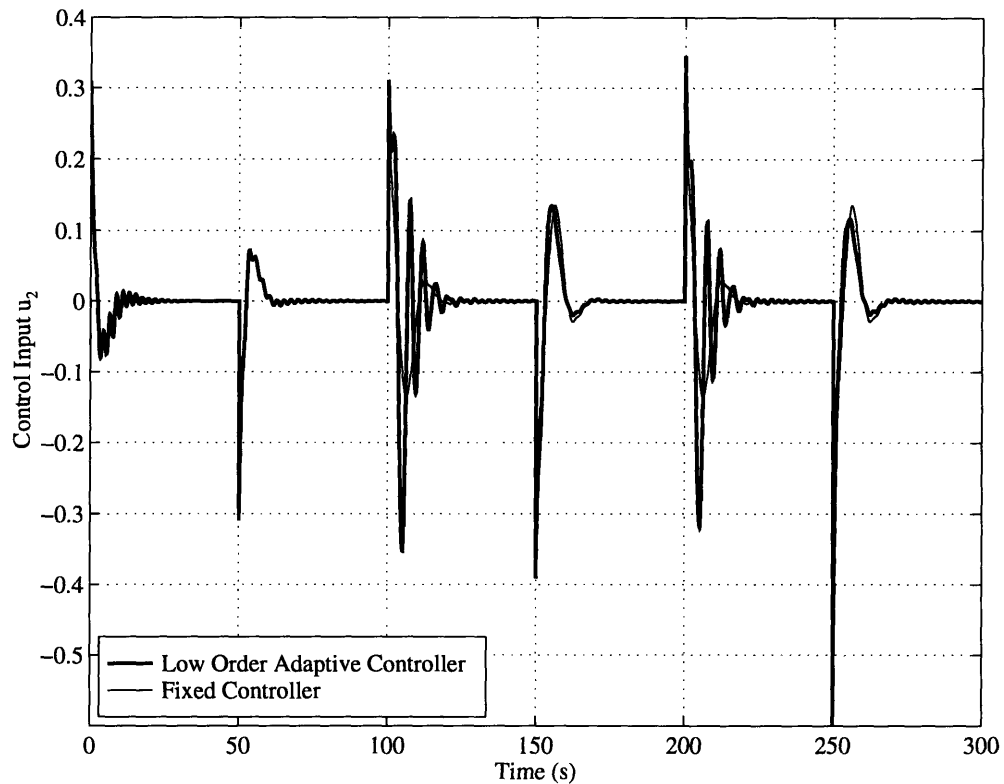


Figure 5-4: Comparison of the low order adaptive controller with the underlying fixed controller. Control input u_2 for a tracking example. For $t < 100$ s, the control input for the fixed controller is slightly smoother than that of the adaptive controller. For $t > 100$ s the control input generated by the adaptive controller is more oscillatory than that of the fixed controller due to the presence of non-linear terms in the control law.

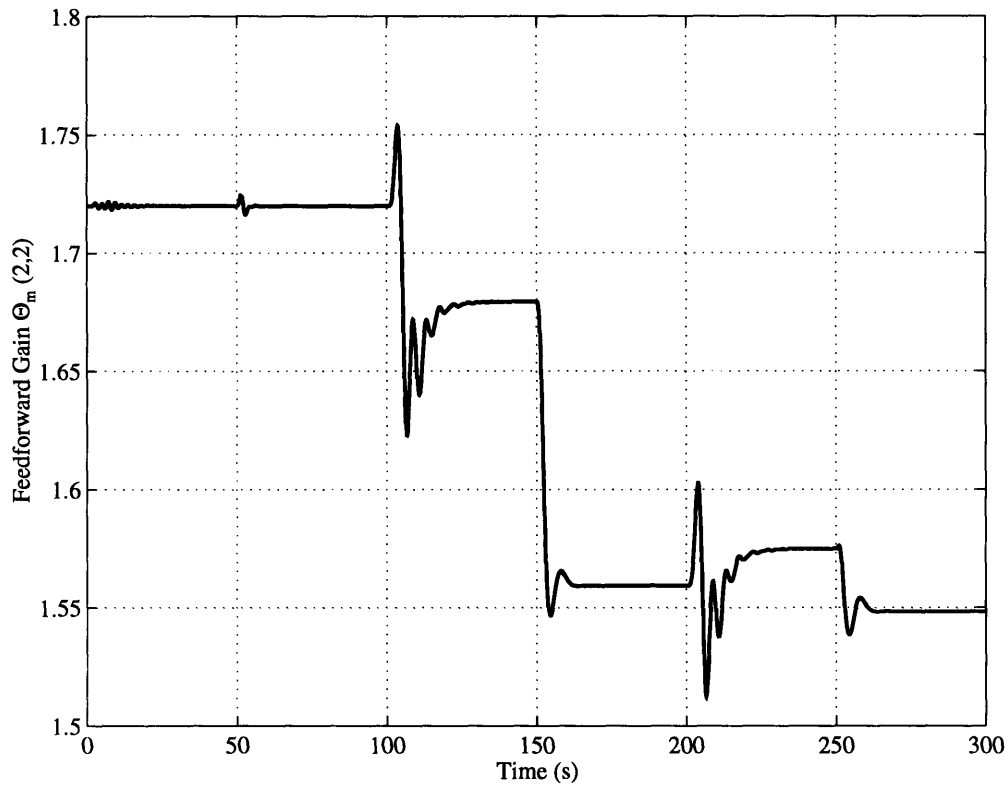


Figure 5-5: Comparison of the low order adaptive controller with the underlying Fixed Controller. Feedforward gain $\Theta_m(2, 2)(t)$ in a tracking example. For $t < 100s$ the control gain changes slightly due to the excited higher modes. For $t > 100s$ the control gain varies in such a way that tracking is achieved asymptotically.

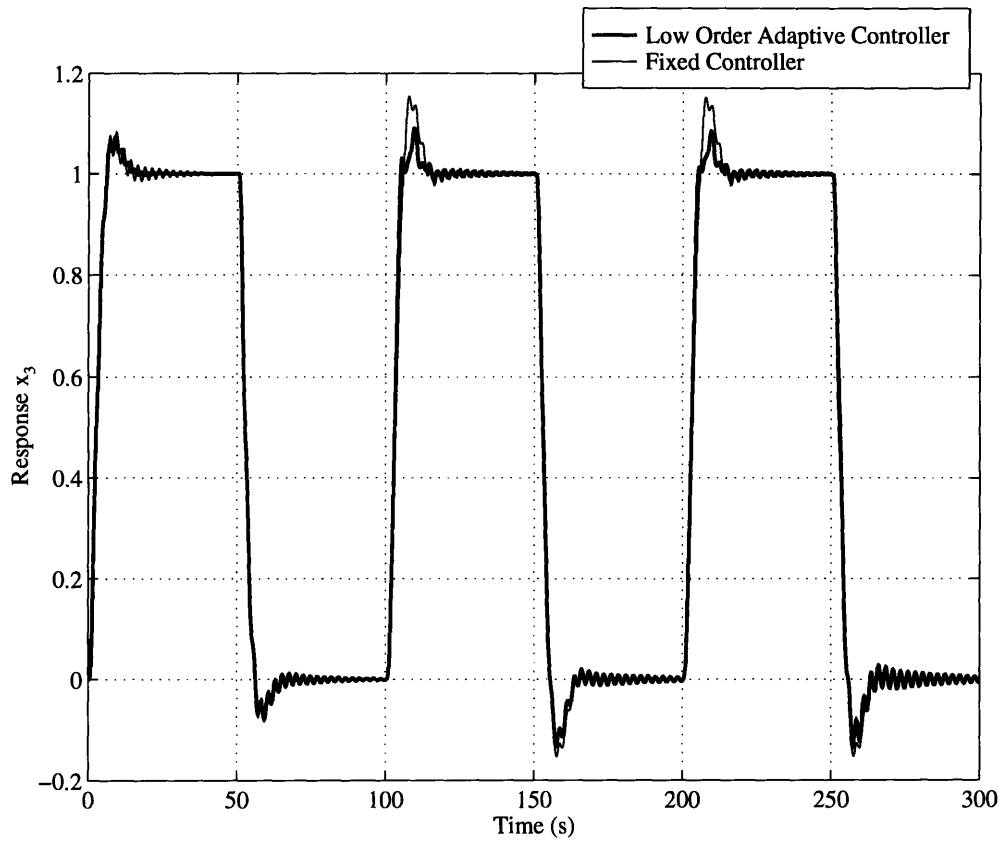


Figure 5-6: Comparison of the low order adaptive controller with the underlying fixed controller. Plant response at x_3 . For $t < 100s$ the displacement of the third mass is the same for both controllers. For $t > 100s$ the adaptive controller results in a smaller overshoot of the third mass.

Next the low order adaptive controller is compared with a standard MIMO Model Reference Adaptive Controller [47, 55]. One of the difficulties in designing the MRAC is the selection of the observability index ν (assumption (I) in Chapter 1). For this example, ν was computed numerically based on the nominal model and was found to be $\nu = 6$. It is assumed that the on-line change in mass does increase ν . Due to the lack of a state space solution in the literature for the ideal MRAC control parameters, the initial control parameters (at $t = 0s$) for the MRAC were generated by imposing the same up-and-down trajectory for a long period of time. A second order reference model for each output channel was used with bandwidth $\omega_m = 0.5$ rad/s and damping $\zeta_m = 0.707$. The adaptation gains for the MRAC were chosen such that the tracking error converged in a manner similar to the low order adaptive controller.

The simulation results are shown in Figs. 5-7-5-8. As before, the masses m_1 and m_5 are increased at $t = 100s$. From the simulations it can be concluded that the low order adaptive controller has at least as good a tracking performance as a model reference adaptive controller. This is accomplished using significantly fewer on-line adjustable parameters and with a controller that is of much lower order (Table 5.2).

	LOAC	MRAC	RO MRAC
Order of the adaptive controller	18	48	16
Number of parameters adjusted on-line	16	48	16
Total controller states	34	96	32

Table 5.2: Comparison of the order of the Low Order Adaptive Controller with that of a MRAC scheme. (Using Table 4.1. Low Order Adaptive Controller (LOAC): $m = 2, p = 8$ with a correction since Θ_o and Θ_1 are not tuned on-line. MRAC: $\nu = 6, m = 2, p = 4$. Reduced Order (RO) MRAC: $\nu = 2, m = 2, p = 4$.)

One could argue that the large difference in the controller order as given in Table 5.2 is obtained in an unfair manner because the observability index $\nu = 6$ used in designing the MRAC controller was chosen too large. After all, the structure contains only two dominant modes, and a smaller ν will result in a lower order MRAC scheme (Table 4.1). Below this issue is addressed qualitatively. Since only two dominant

modes are present in the input-output transfer function matrix, it seems reasonable to approximate the dynamics of the sample structure in Fig. 5-1 by a two mass-spring-damper system. For such a system with one actuator-sensor pair on each mass, the observability index $\nu = 2$. Namely, the observability index ν is defined as the smallest integer q such that $\text{rank}([C^T \ A^T C^T \ \dots \ (A^T)^{q-1} C^T]) = n$ where C is the output matrix, A the system matrix and n the system order. For a flexible structure we have, using Eqs. (5.1) and (5.2),

$$A = \begin{bmatrix} 0 & I \\ -M^{-1}K & -M^{-1}C \end{bmatrix}, \quad C = [C_{xy} \ 0].$$

For a two mass-spring-damper, two input-output system we have

$$\text{rank}([C^T \ A^T C^T]) = \text{rank}\left(\begin{bmatrix} C_{xy} & 0 \\ 0 & C_{xy} \end{bmatrix}\right) = \text{rank}(I_{4 \times 4}) = 4,$$

so that $\nu = 2$. The resulting order of the MRAC scheme using $\nu = 2$ as a control design parameter is given in Table 5.2. The order of the Reduced Order MRAC is lower than that of the Low Order Adaptive controller proposed in this thesis, and might therefore seem more attractive. To verify, qualitatively, whether such a Reduced Order MRAC is indeed attractive for this application, a comparison with the full order MRAC was performed (Figs. 5-9 and 5-10). The tracking objective and the on-line parameter change in the simulations was the same as before. The simulations show that the response of the Reduced Order MRAC is more oscillatory than that of the full order MRAC (Fig. 5-9). Also, the control input is larger, and more oscillatory (Fig. 5-10). Although not shown here, the parameter estimates for the Reduced Order MRAC do not seem to converge for the given reference trajectory.

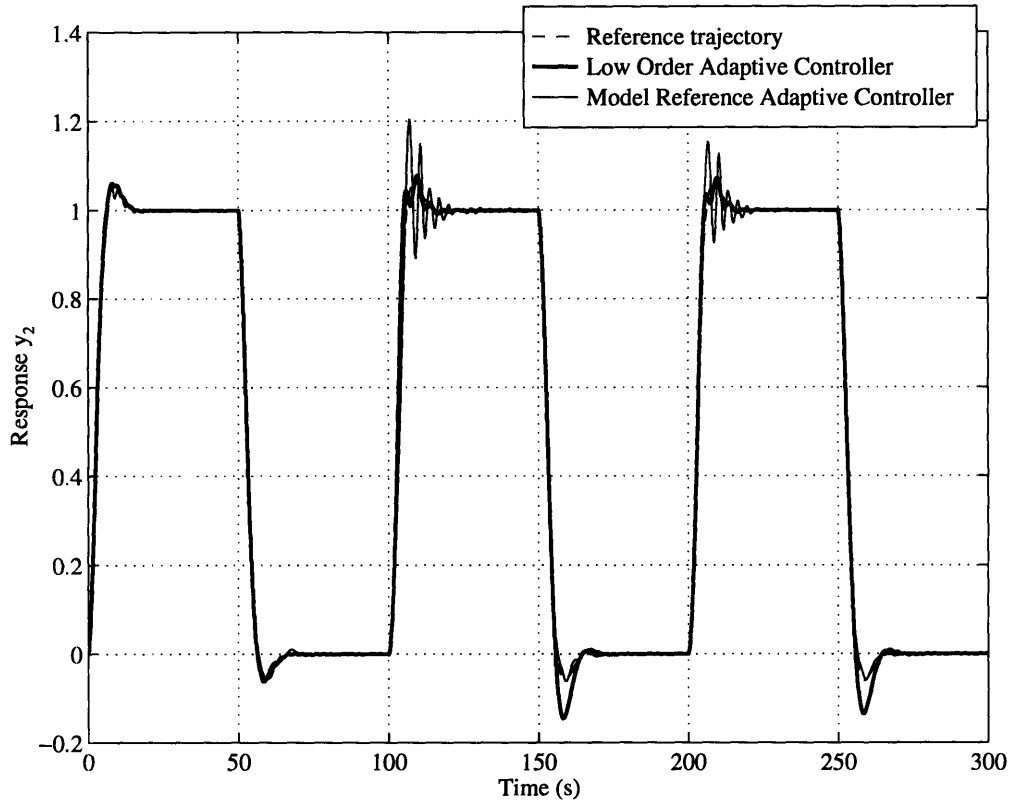


Figure 5-7: Comparison of the low order adaptive controller with a MRAC scheme. Plant output y_2 for a tracking example. For $t < 100$ s the tracking performance of both controllers is comparable. When a parameter change is introduced at $t = 100$ s, the MRAC response shows much more oscillatory behavior in the upward phase than the low order controller. The MRAC does better in the downward phase than the low order controller, although the low order controller recovers further when more excitation takes place.

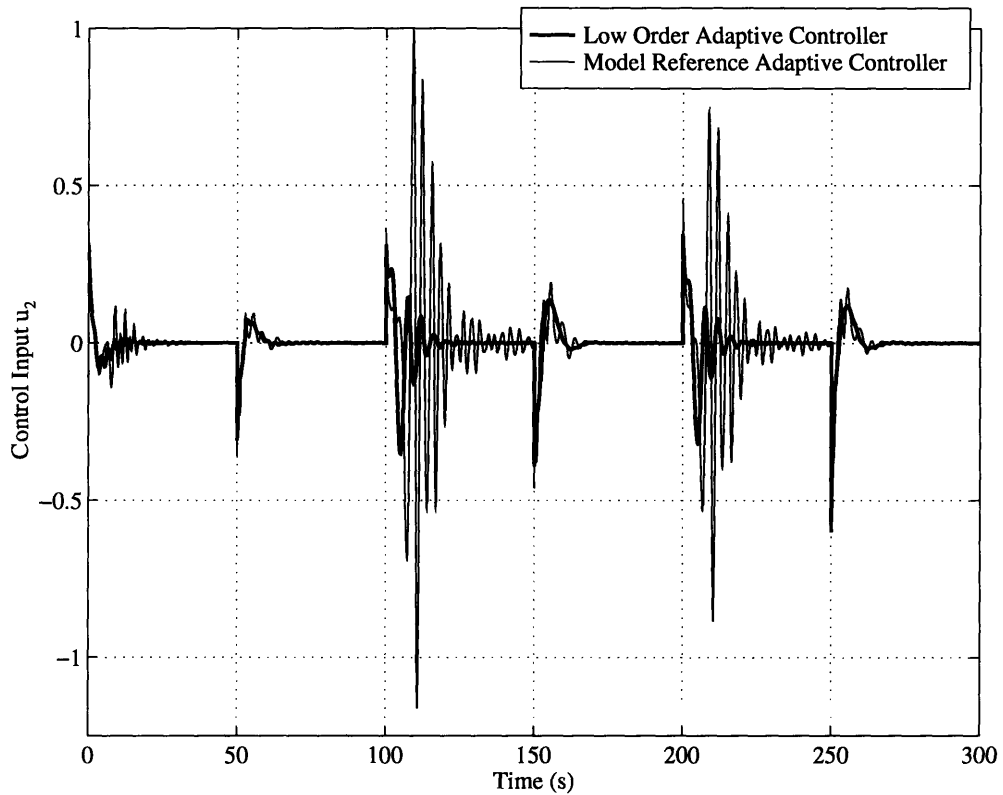


Figure 5-8: Comparison of the low order adaptive controller with a MRAC scheme. Control input u_2 for a tracking example. For $t < 100s$, the control input of the MRAC is more oscillatory than the control input of the low order controller although this is in part due to the choice of the initial gains for the MRAC design. When the parameter error is introduced at $t = 100s$, the MRAC control input is much more oscillatory and larger in magnitude than the low order control input.

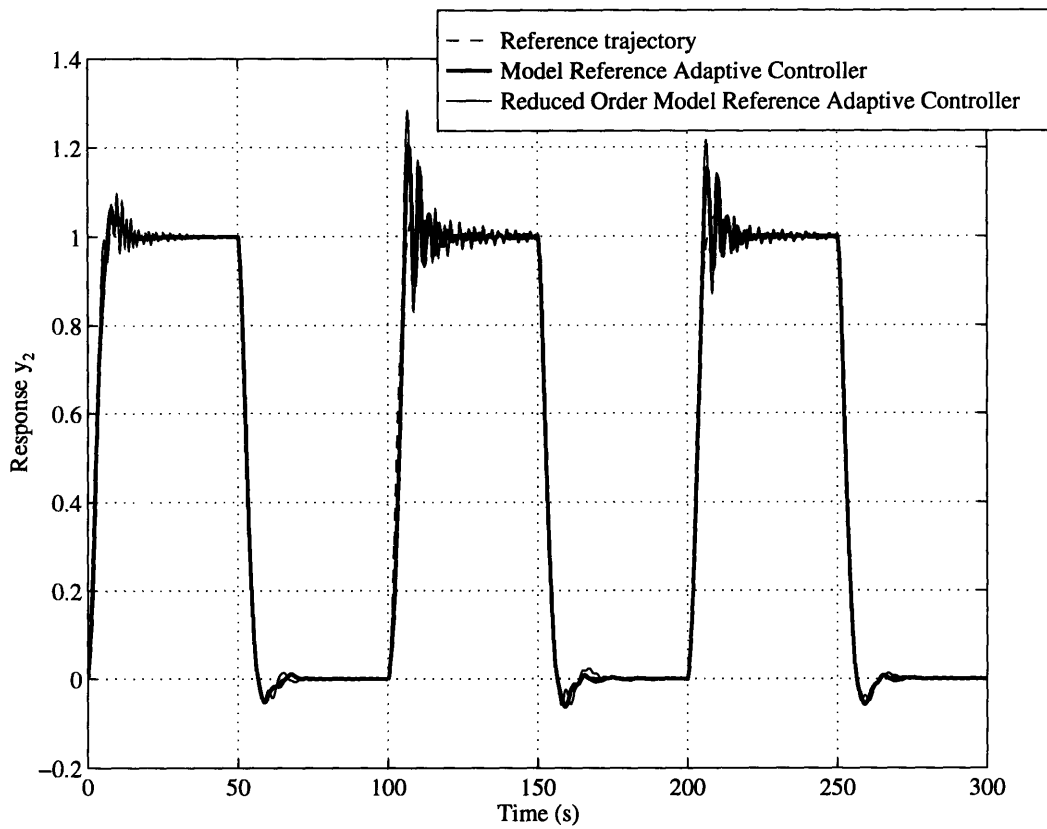


Figure 5-9: Comparison of a MRAC scheme with a reduced order MRAC. Response at y_2 for a tracking example. The reduced order MRAC gives a much more oscillatory response than a (full order) MRAC.

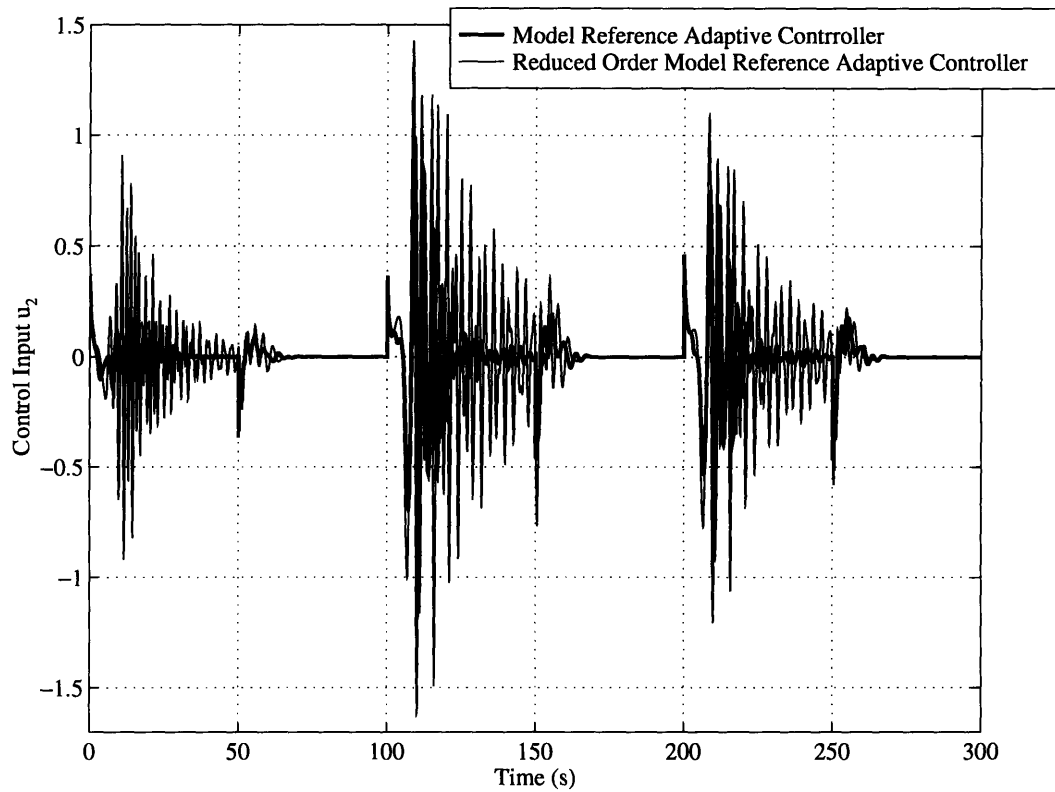


Figure 5-10: Comparison of a MRAC scheme with a reduced order MRAC. Control input u_2 for a tracking example. The control input coming from the reduced order MRAC is larger and more oscillatory than that of the (full order) MRAC.

5.2.6 Disturbance Rejection Example

It is the objective of this example to illustrate how persistent low frequency sinusoidal disturbances acting on a flexible structure can be rejected at the measured outputs. In this example the focus will be on the change in the frequency in the input disturbance, although the same control strategy can be used if parametric modeling errors or on-line parameter changes are present as well. Disturbance rejection can be accomplished regardless of how many dominant modes relative to the number of in- and outputs are present in the structure. As a sample problem we choose $m_i = 1$ ($i = 1, \dots, 5$), $k = 1$ and $c = 0.01$ which results in 5 dominant modes for two colocated actuator sensor pairs at x_1 and x_5 . The external sinusoidal disturbance $d = \sin(\omega_d t)$ enters at x_3 . The nominal modal frequencies are given by $\omega = 0.28, 0.83, 1.31, 1.68$ and 1.92 rad/s. This system exhibits most of the properties of a large flexible structure; it is of high order, and has closely packed modes. The nominal value of the input frequency was chosen to be $\omega_d = 1$ rad/s. The perturbed value of the input frequency was chosen to be $\omega_d = 1.1$ rad/s.

To accomplish exact disturbance rejection, following the discussion in section 3.2.2, the compensator is augmented with an internal model of the disturbance. The fixed compensator is given by

$$G_c = \frac{s + a_o}{s + b_o} \frac{s^2 + 2\zeta_z \omega_z s + \omega_z^2}{s^2 + \omega_d^2} I_{2 \times 2}.$$

Since ω_d is uncertain, in the adaptive controller it will be estimated on-line. $G_c(s)$ is parameterized in a form suitable for adaptation using Theorem 4 as

$$G_c(s) = (I - \Theta_1(sI + \Lambda)^{-1}L)^{-1}$$

where

$$\Lambda = \begin{bmatrix} a_o I_{2 \times 2} & & \\ & 0_{2 \times 2} & -I_{2 \times 2} \\ (a_o - b_o) I_{2 \times 2} & \omega_z^2 I_{2 \times 2} & 2\zeta_z \omega_z I_{2 \times 2} \end{bmatrix} \quad L = \begin{bmatrix} I_{2 \times 2} \\ 0_{2 \times 2} \\ I_{2 \times 2} \end{bmatrix}$$

$$\Theta_1 = [(a_o - b_o)I_{2 \times 2} \quad (\omega_z^2 - \omega_d^2)I_{2 \times 2} \quad 2\zeta_z \omega_z I_{2 \times 2}].$$

The initial gains of the adaptive controller have been chosen to correspond to those of the underlying fixed controller which is designed using the nominal model and using the nominal value of the disturbance input frequency, $\omega_d = 1$ rad/s. The corresponding zero pair is chosen close to the nominal disturbance frequency, $\zeta_z = 0.1$ and $\omega_z = 1$ rad/s. Hence, $\Theta_1(1,3)(t=0) = \Theta_1(2,4)(t=0) = 0$. Since the SPR property of $W_m(s)$ holds for reasonably large parameter changes, a_o and b_o can be chosen *a priori*, and were fixed at $a_o = 0.2$ rad/s and $b_o = 1.2$ rad/s. A feedback gain that assures that $W_m(s)$ is SPR is given by $\Theta_o = -10I_{2 \times 2}$. The adaptive laws are given by Theorem 4. The adaptation gain was chosen as $\Gamma_1 = 0.1I_{2 \times 2}$.

Simulation results are shown in Figs. 5-11–5-16. When the structure is excited by the nominal input frequency of $\omega_d = 1$ rad/s, both the (matched) fixed controller and the adaptive controller give a similar response (Fig. 5-11). The rejection of the disturbance is achieved for both controllers with almost identical control inputs (Fig. 5-12). Most interesting is the time-history of the compensator parameters. Due to the effect of initial conditions, the parameters first diverge from their desired value, but as the excitation persists the parameters eventually come close to the desired values (Fig. 5-13). When the input frequency is perturbed to $\omega_d = 1.1$ rad/s, the now mismatched fixed controller does a poor job at rejecting the disturbance, the adaptive controller recovers in a very reasonable time period (Fig. 5-14). This recovery is achieved with a control input apparently no different than that of the fixed controller (Fig. 5-15). In this case, the compensator gain converges to a new value (Fig. 5-16). It should be noted that although the rejection at the measured outputs is very good, the other masses are still excited and the disturbance rejection at those locations is not that good (Fig. 5-17).

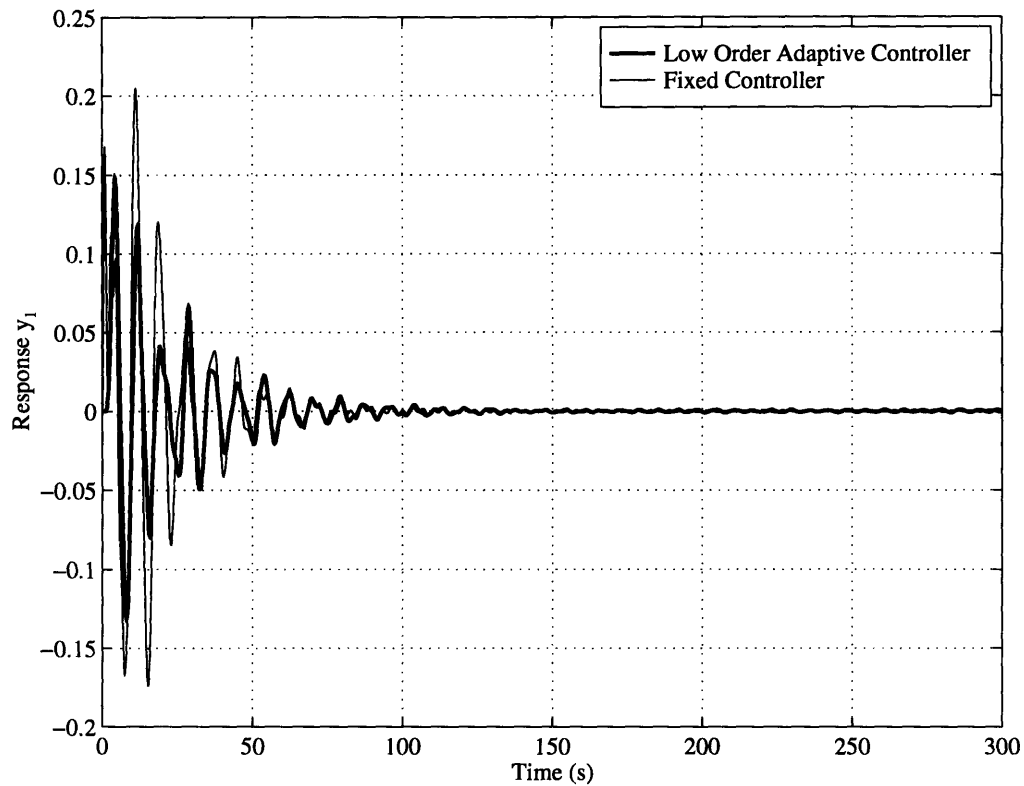


Figure 5-11: Comparison of the low order adaptive controller with the underlying fixed controller. Plant output y_1 for a disturbance rejection example. The fixed controller is matched to the disturbance frequency at $\omega_d = 1$ rad/s. The adaptive and fixed controller give the same performance.

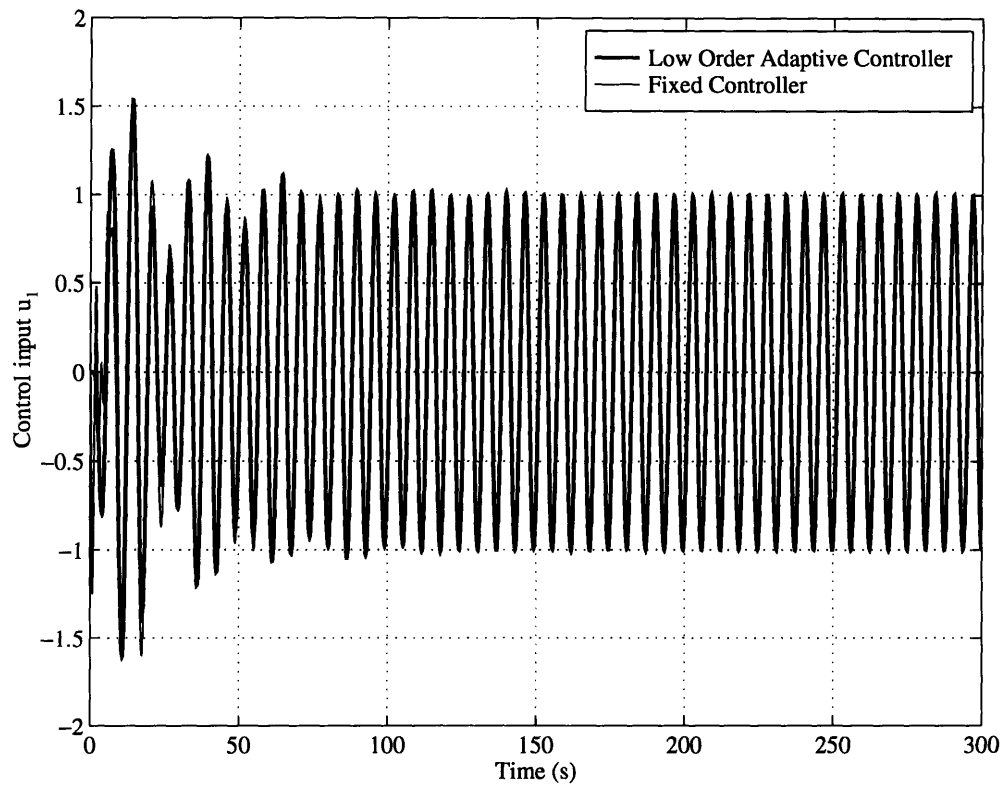


Figure 5-12: Comparison of the low order adaptive controller with the underlying fixed controller. Control input u_1 for a disturbance rejection example. The matched fixed controller and the adaptive controller generate almost identical control inputs.

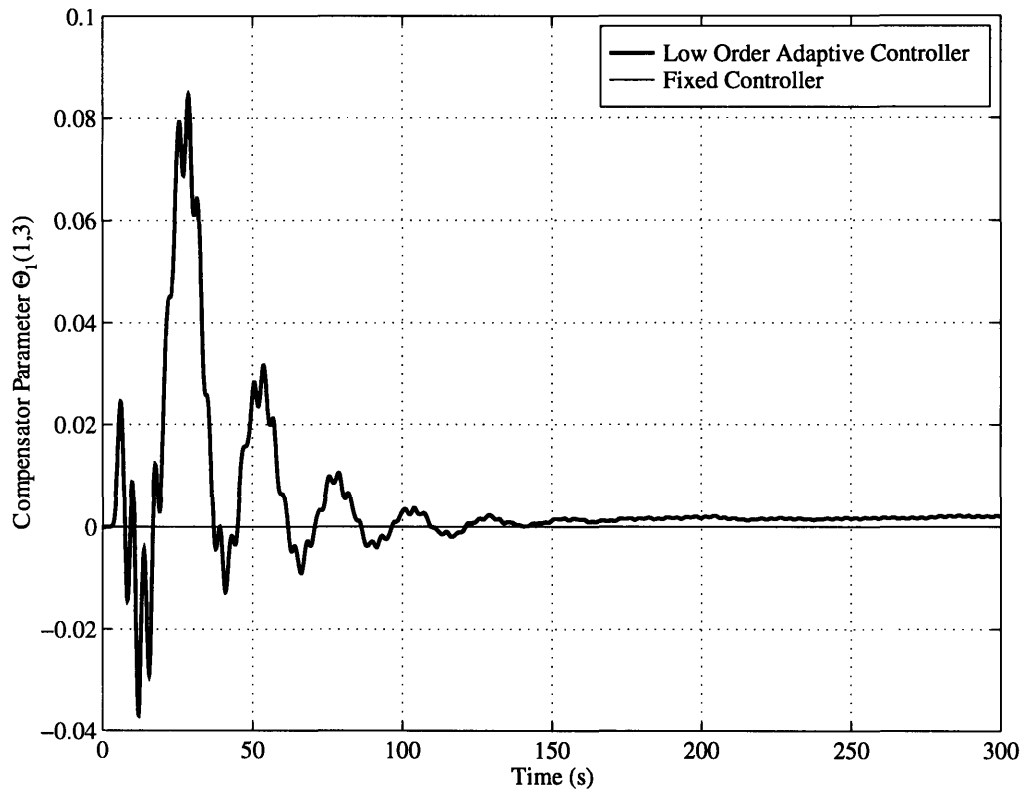


Figure 5-13: Comparison of the low order adaptive controller with the underlying fixed controller. Compensator parameter $\Theta_1(1,3)$ for a disturbance rejection example. For $t < 150s$ the changes in the control parameter are due to initial condition effects.

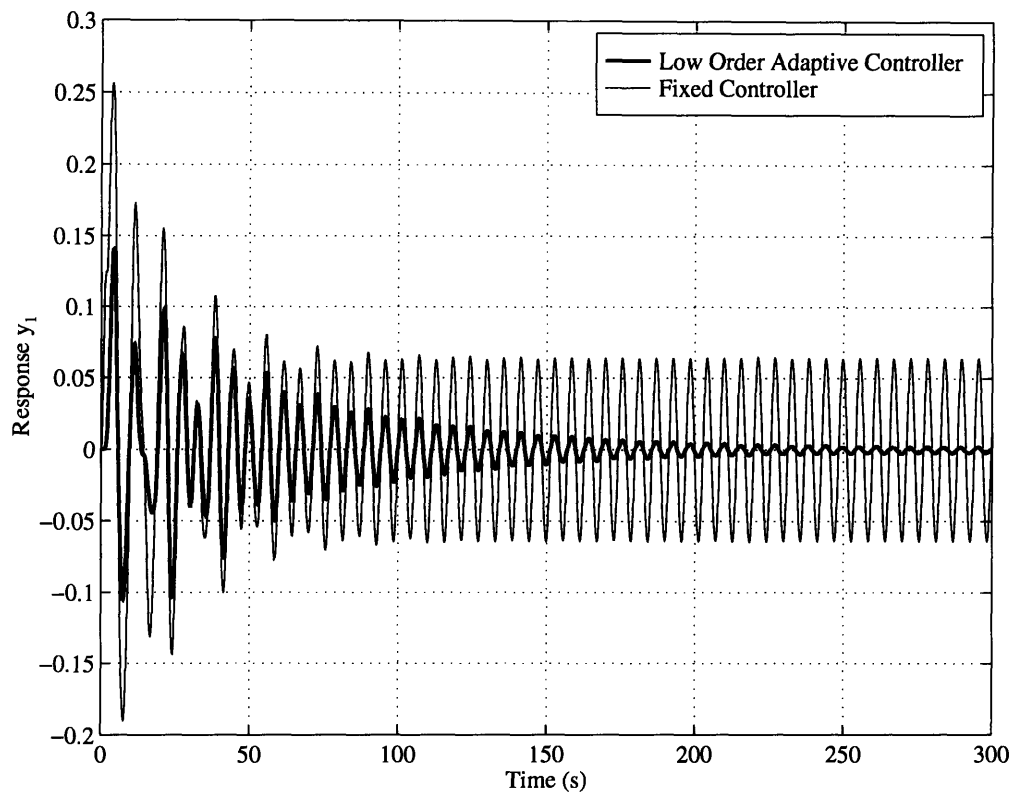


Figure 5-14: Comparison of the low order adaptive controller with the underlying fixed controller. Plant output y_1 for a disturbance rejection example. The disturbance input frequency is perturbed to $\omega_d = 1.1$ rad/s. The mismatched fixed controller results in poor disturbance rejection. The adaptive controller recovers with very reasonable transients for y_1 .

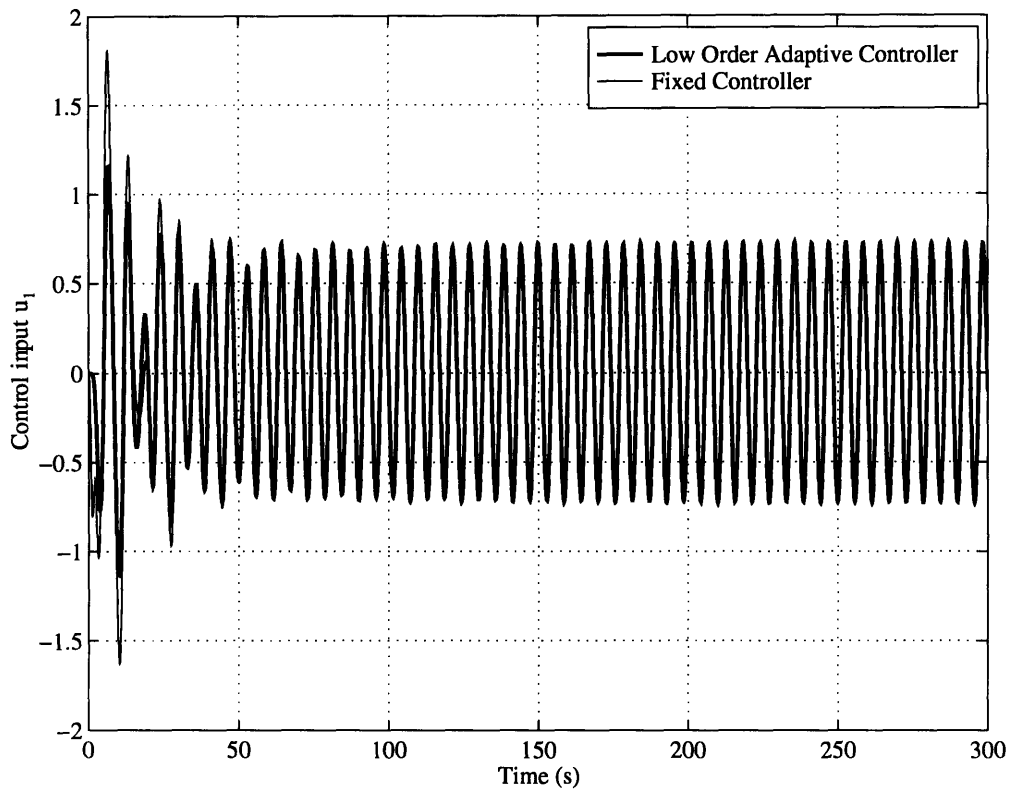


Figure 5-15: Comparison of the low order adaptive controller with the underlying fixed controller. Control input u_1 for a disturbance rejection example. The adaptive control input is very reasonable despite the non-linear terms in the control law. (Although not clear from the figure, the magnitude of the adaptive control input is slightly larger than that of the fixed control input, the frequency of both control inputs is the same).

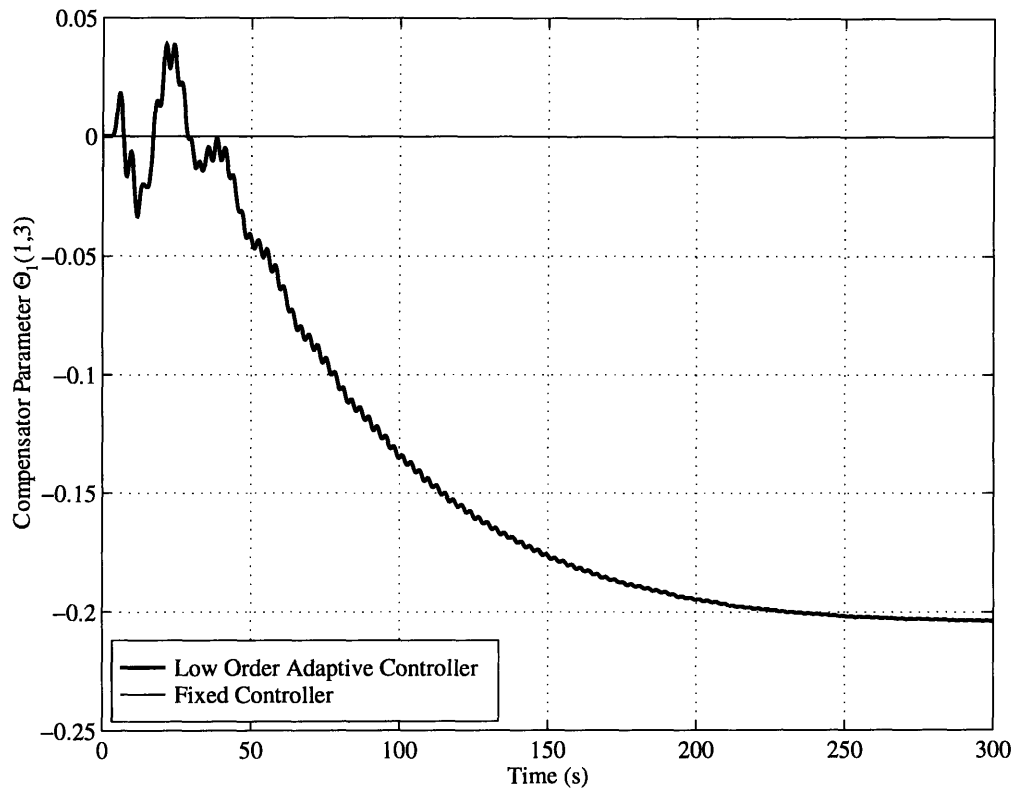


Figure 5-16: Comparison of the low order adaptive controller with the underlying fixed controller. Compensator parameter $\Theta_1(1,3)$ for a disturbance rejection example. The mismatch in the initial compensator parameter causes the parameter to converge to a new value such that disturbance rejection is achieved.

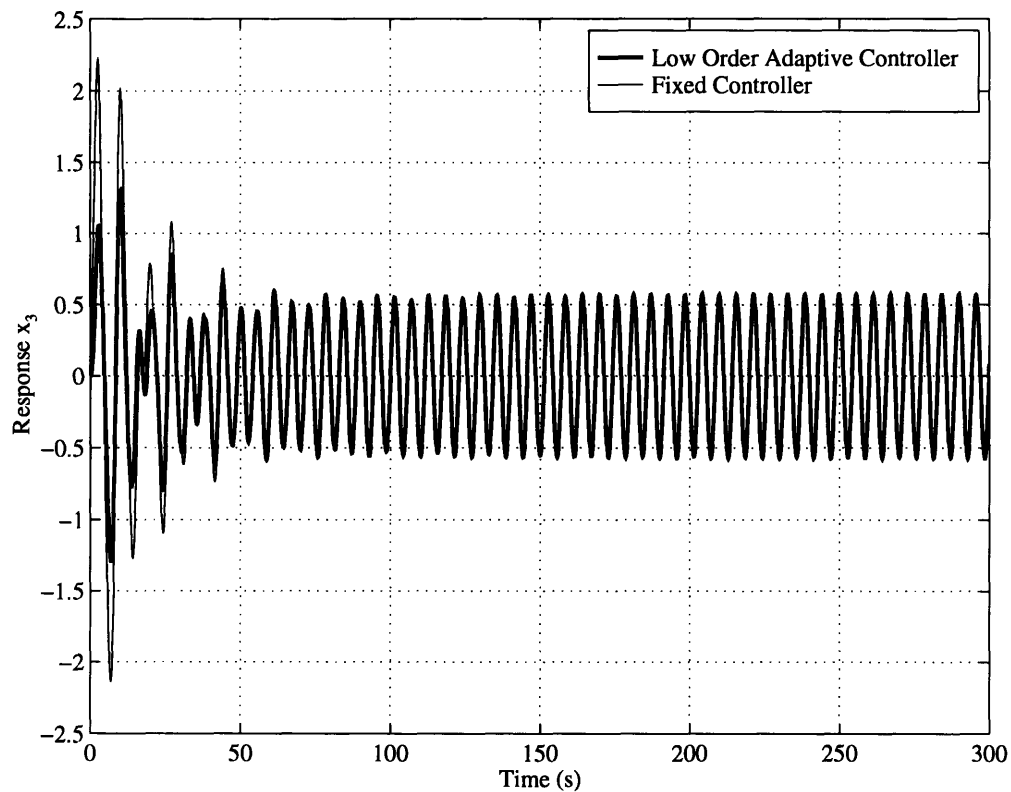


Figure 5-17: Comparison of the low order adaptive controller with the underlying fixed controller. Plant response at x_3 for a disturbance rejection example. Despite the good disturbance rejection at the actuator-sensor locations, the rejection at the other locations is poor for both the adaptive and (mismatched) fixed controller.

5.2.7 Unmodeled Dynamics Example

In section 5.2.3 the dynamic model of a flexible structure was discussed. The main idea there was that if colocated actuators and sensors are used, assumptions (A1), (A2) and (A3) required for application of the low order adaptive controller are met. Under these assumptions, in sections 5.2.5 and 5.2.6 the controller was applied to a sample structure to meet certain performance objectives. Naturally, these experiments were performed under ideal circumstances. When a controller is applied to a real physical plant, unmodeled phenomena such as fast actuator dynamics, small computational time delays, small gain non-linearities and a small dislocation of actuator and sensor may be present. Also, other exogenous inputs such as measurement noise and high frequency disturbances may be present. For the adaptation to remain stable in the presence of these unmodeled phenomena, the robustified adaptive controller presented in section 4.3 was developed. Specifically, the robustified controller was developed with in mind the presence of fast actuator dynamics, and small high frequency external disturbances.

The purpose of this example is to show, qualitatively, that the robustified adaptive controller presented in Theorem 4.3 results in bounded loop signals when the unmodeled actuator dynamics is excited by a (high frequency) external disturbance. For comparison the unaltered low order adaptive controller and the underlying fixed controller is used. Also, for ease of exposition, a singlevariable, low order dynamic system was considered. A mass-spring-damper oscillator with nominal mass $m = 1$, nominal stiffness $k = 1$ and $c = 0.01$ was chosen as a sample system. Similar to section 5.2.5, the reference trajectory was of third order with an almost pole-zero cancellation at $s = -a_o = -0.1$ rad/s resulting in a good tracking controller if all parameters were known. The complex pole pair was chosen at frequency $\omega_m = 1$ rad/s and damping ratio $\zeta = 0.707$. An actuator was modeled as a first order system with unity DC-gain and a corner frequency at $\alpha = 20$ rad/s. The initial feedback gains were chosen as $\Theta_o = -10$ and $\Theta_1 = -9.9$ resulting in a well damped closed loop plant pole ($\omega_{cl} = 1.11$ rad/s, $\zeta_{cl} = 0.5$). The parameter values of the nominal plant

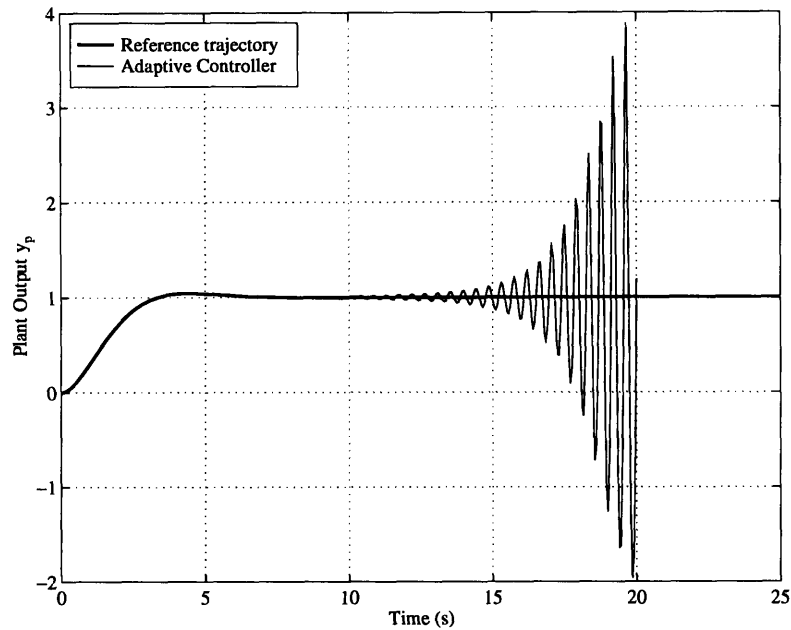
and the initial gains were used to compute the feedforward gain Θ_m . These values were used as the initial values for both the robustified adaptive controller (as given in Theorem 6), and the unaltered adaptive controller (as given in Theorem 4). For both adaptive controllers, all gains were adjusted on-line using high adaptation gains, $\Gamma_m = 10$ and $\Gamma_o = \Gamma_1 = 5$. Naturally, the benefit of using high adaptation gains is good tracking performance when parametric uncertainties occur. The disadvantage of using high adaptation gains is higher and more oscillatory control inputs, and that unmodeled dynamic effects increase with time more rapidly. The filter parameters were chosen as $a = 1$ rad/s and $\Lambda = a_o = 0.1$ rad/s. The additional leakage-term σ in Theorem 6 was chosen as $\sigma = 0.1$ rad/s. Following the construction in [53], based on the actual plant (including actuator dynamics) and the initial values of the control gains, a worst case output disturbance was chosen to be a sinusoid of frequency $\omega_d = 14.05$ rad/s and amplitude $A_d = 0.01$. The actual measurement used for feedback is given by $y(t) = y_p(t) + A_d \sin(\omega_d t)$ where y_p is the actual plant response. Under these conditions, the adaptive controller can become unstable for a nonzero, constant reference input chosen as $r(t) \equiv 1$.

The control objective is to track an up-and-down reference signal with intervals of 50s. At $t = 100s$, an on-line parametric uncertainty is introduced by doubling the mass m . At $t = 200s$, the external high frequency disturbance exciting the unmodeled dynamics is removed. Note that this control objective is similar to the one posed in section 5.2.5. In this case however, a worst case external disturbance is also entering the system and unmodeled actuator dynamics is present as well. In other words, in this example the control objective is to achieve robust tracking performance; in a worst case scenario, tracking of a low frequency signal despite parametric uncertainty as well as attenuation of a high frequency disturbance despite unmodeled dynamics should be achieved.

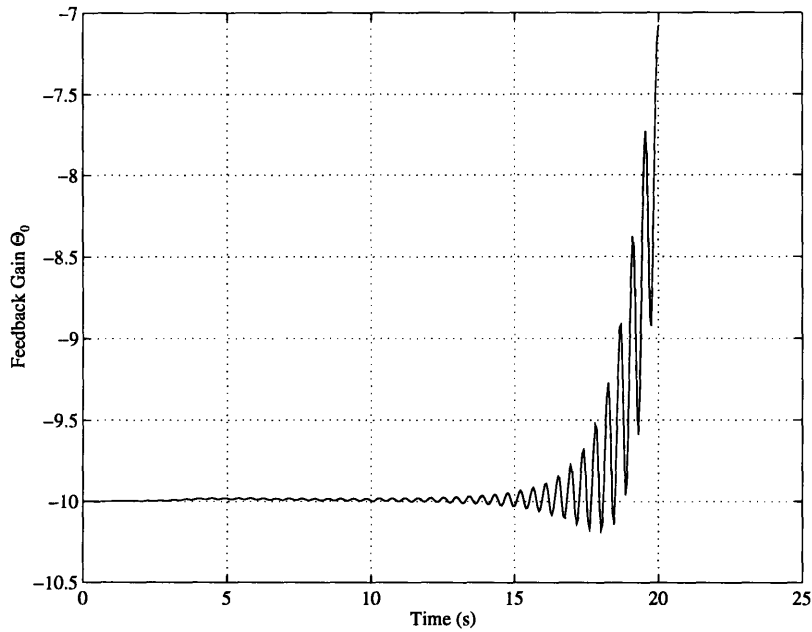
In designing the fixed controller, it was assumed that the nominal plant (excluding actuator dynamics) was well known. Following the remarks in section 4.3, this prior information was used in designing the modified adaptive controller as well. The benefit of using this prior information is that it can increase the size of the allowable

unmodeled dynamics. The anticipated parametric uncertainty in the plant parameters were captured in the modified adaptive controller by choosing $\theta_{max}^* = 5$.

Simulation results are shown in Figs. 5-18–5-20. Without any modification of the adaptive law, the control parameters drift and the plant output diverges (Fig. 5-18). With the robustified adaptive controller, a bounded plant output is obtained (Fig. 5-19(b)). Note that the output disturbance of magnitude 0.01 is considerably amplified at the output to almost 2, this is an amplification factor of almost 200 (Fig. 5-19(b)). This is a disconcerting result, since the underlying fixed controller exhibits very good disturbance attenuation at ω_d . When the reference input is changed at $t = 50s$, the amplification vanishes ($50s < t < 100s$). This makes sense, as a nonzero reference input is needed to achieve the amplification of the disturbance [53]. At $t = 100s$, when a parametric uncertainty and a step change are introduced, the fixed controller shows considerable overshoot while the adaptive controller results in good tracking ($100s < t < 120s$). The high frequency disturbance is still amplified in the robustified adaptive controller ($120s < t < 150s$). However, since the worst case disturbance frequency ω_d is now mismatched to the plant parameters (frozen at $t = 100s$), the amplification is significantly less. When the external disturbance is removed at $t = 200s$, the modified adaptive controller achieves good tracking, despite the presence of unmodeled dynamics, whereas the fixed controller shows a large overshoot. The robustified adaptive controller achieves boundedness of signals through a projection of the adaptive parameters (Fig. 5-20). Comparison of the control input for the fixed and robustified adaptive controller for $t < 50s$ shows that the adaptive control input is 800 times larger than the fixed control input when the actuator dynamics are excited ($t < 50s$).

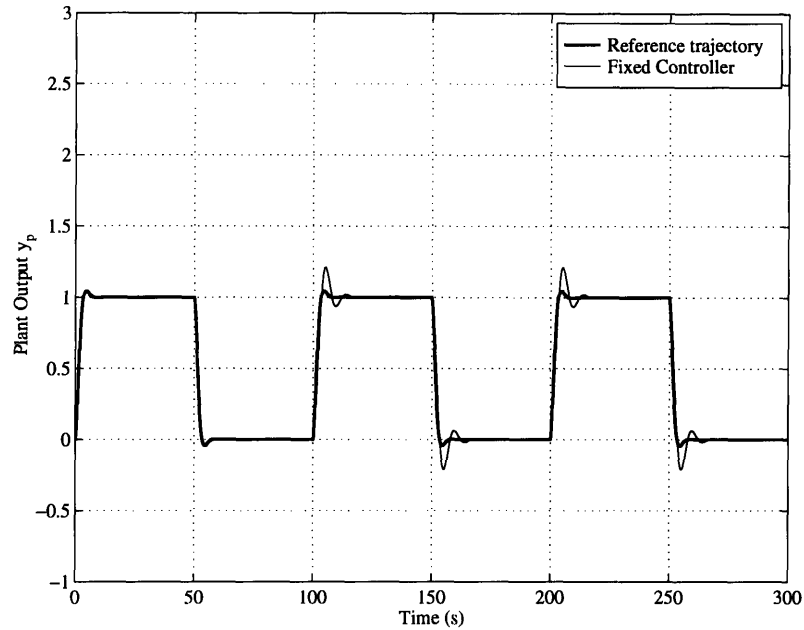


(a) Adaptive controller plant response for a robust tracking example.

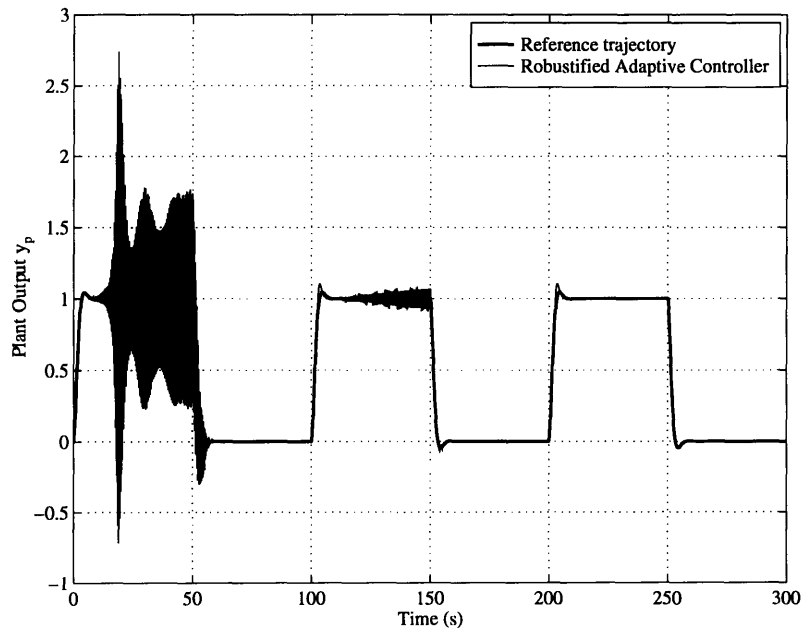


(b) Adaptive controller feedback gain Θ_0 for a robust tracking example.

Figure 5-18: Response of the unaltered adaptive controller. The response of the matched, unaltered adaptive controller appears fine for $t < 10$ s. Due to the excited unmodeled dynamics the feedback gain Θ_0 starts to drift, and the output error starts to diverge ($t > 10$ s). The other control gains change in a similar manner. The simulation was terminated at $t = 20$ s.



(a) Fixed controller plant response for a robust tracking example.



(b) Robustified adaptive controller plant response for a robust tracking example.

Figure 5-19: The robustified adaptive controller results in a bounded but large tracking error when matched to the actual plant ($t < 50s$). On the other hand, the matched fixed controller exhibits good disturbance attenuation ($t < 50s$). When a parametric uncertainty is introduced ($t = 100s$), the robustified adaptive controller results in good tracking but worsening disturbance attenuation ($120s < t < 150s$). The mismatched fixed controller results in a large overshoot ($t = 100s$), but good disturbance attenuation. When the external disturbance is removed ($t > 200s$), the robustified adaptive controller shows good tracking despite the presence of the unmodeled actuator dynamics.

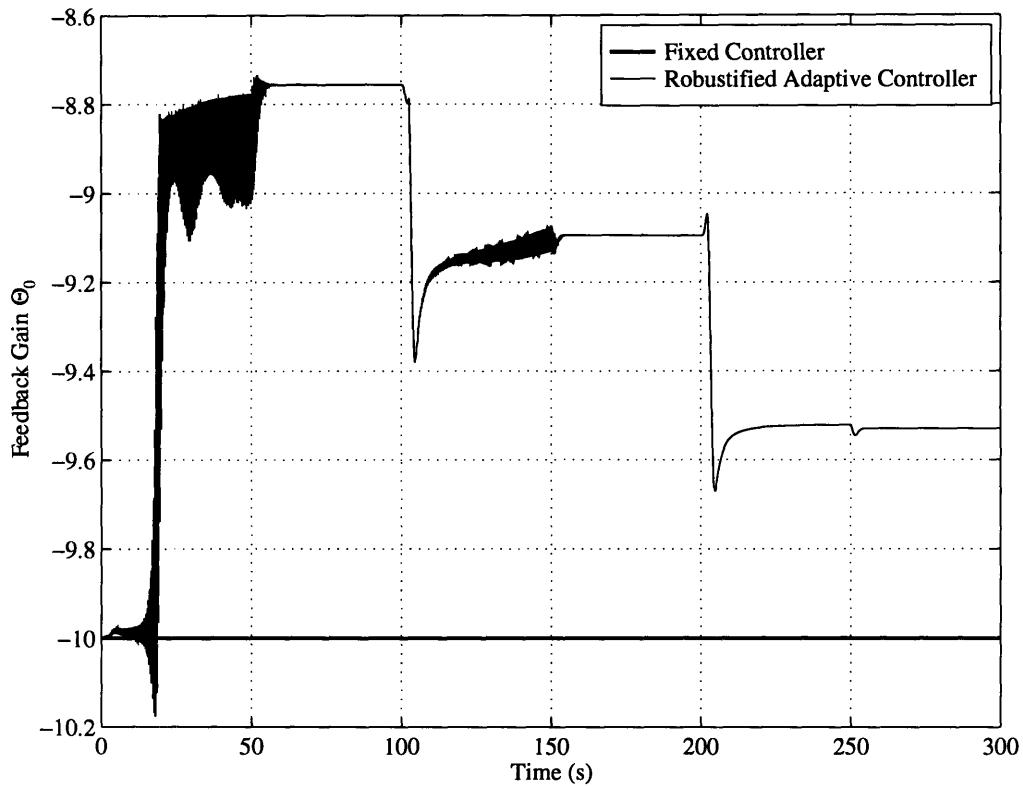


Figure 5-20: Feedback gain Θ_0 for a robust tracking example. Due to the excitation of unmodeled dynamics, the feedback control parameter Θ_0 in the robustified adaptive controller drifts until it reaches a bound determined by θ_{max}^* ($t < 200s$). When the external disturbance is absent, the parameter converges such that the tracking objective is realized ($t > 200s$). The other control gains change in a similar manner.

5.2.8 Discussion

In this section the low order adaptive controller was applied to lightly damped flexible structures. Three control objectives were considered: tracking, disturbance rejection and robust tracking. To accomplish these control objectives, different control parameters were tuned on-line. To achieve tracking, only Θ_m was adjusted (Fig. 5-2). To achieve disturbance rejection, only elements of Θ_1 were adjusted. In the robust tracking example, all control parameters were tuned on-line (i.e. Θ_m , Θ_o and Θ_1 were all time-varying). In what follows the simulation results for each of the control objectives are discussed.

In section 5.2.5 the adaptive controller has been shown to result in good tracking performance in the presence of on-line introduced parametric changes in the system dynamics. This was accomplished for a two-input two-output flexible structure with two dominant modes using a low order multivariable adaptive controller. Comparisons with multivariable MRAC schemes showed that the low order adaptive controller was the better controller, either from the viewpoint of controller order or from the viewpoint of tracking performance. A full order MRAC showed tracking performance comparable to that of the low order adaptive control scheme, for both schemes the tracking error converged to zero after continued excitation. However, the order of the MRAC was almost three times higher than the order of the low order adaptive controller. A reduced order MRAC was used for comparison as well. The reduced order MRAC and the low order controller had a comparable number of controller states. However, in the reduced order MRAC case the tracking error showed more high frequency components, and the control input was much more oscillatory. This may be because the reduced order MRAC destabilizes the higher frequency modes, making them more dominant in the closed loop input-output map. A rigorous analysis that explains the behavior of the reduced order MRAC scheme requires the use of the desired control parameters. Unfortunately, a state-space solution to determine these parameters is not available in the literature. Naturally, it would be desirable to control flexible systems with more dominant modes than control inputs. With

the controller presented in this thesis, this would be possible by augmenting the compensator with additional zeros placed in the vicinity of selected modes so that they become weakly observable/controllable in the closed loop input-output map at the expense of increasing the order of the controller.

In section 5.2.6 the low order adaptive controller was used for rejecting a sinusoidal input disturbance of unknown frequency acting on a flexible structure. Excellent disturbance rejection was obtained using very reasonable control inputs. No assumptions regarding the number of dominant modes relative to the number of inputs and outputs were needed. This approach to (adaptive) disturbance rejection is well known, see [24, 47] for example. However, the controllers proposed in [24, 47] are of very high order when applied to this sample problem. It should be noted that the disturbance rejection approach presented in this thesis can deal with narrow band disturbances quite effectively, although vibrations at points other than the sensor locations are not necessarily attenuated. Broadband disturbance attenuation, for systems where many modes affect the performance, require other feedback methods where sufficient damping is added to the modes.

Finally, in section 5.2.7, the tracking performance of the adaptive controller in the presence unmodeled dynamics and external disturbances was illustrated. As the theory presented in section 4.3 suggested, a bounded response is obtained. Unfortunately, for this example, the tracking error is extremely large. Also, the control inputs are unacceptable. Three remedies are suggested for this problem: (1) One remedy may be to constrain the magnitude of the control input, and modify the control inputs accordingly [30]. The benefit of this modification is twofold. First, the control input would now be physically realizable. Second, qualitatively, for a stable plant a smaller control input may result in a smaller tracking error. (2) When only Θ_m was adjusted on-line, and Θ_o and Θ_1 were fixed, high frequency disturbance attenuation comparable to that of the underlying fixed controller was obtained, as well as tracking when the parametric error was introduced. Therefore, when in the range of expected parameter variations $W_m(s)$ is SPR for fixed Θ_o and Θ_1 , adjusting only Θ_m seems a robust adaptive control approach. (3) There is a tradeoff between the size of θ_{max}^*

and the amplification of the high frequency disturbance. If θ_{max}^* is small, less amplification is obtained. Hence, the smaller θ_{max}^* can be chosen using prior information on the parameter uncertainty, the better the controller will perform.

In conclusion, it should be kept in mind that the robust tracking example was constructed by choosing the input frequency ω_d to create the worst possible amplification of loop signals. In practice, such an external signal may not always be present for all time and the responses presented here may never occur.

5.3 Control of an unstable Combustion System

5.3.1 Introduction

In this section the application of the low order adaptive controller to a combustion process is discussed. This section is organized as follows. In section 5.3.2 the use of active control in combustion is motivated. In section 5.3.3 the constitutive relations describing the combustion process are given, and the finite element solution of these relations is presented. In Appendix A the discretization of these constitutive laws is given. In section 5.3.3, assumptions (A1), (A2) and (A3) required for application of the low order adaptive controller are discussed as well. In section 5.3.4 a sample system is described and simulation results are presented. A discussion of the results is given in section 5.3.5.

5.3.2 Motivation

In this section we will discuss an application in the area of power generation. Examples of power generation systems are propulsion systems such as rocket motors and jet engines, and combustion devices such as utility boilers and furnaces. The two major issues in power generation are efficiency, and emission. The performance in terms of efficiency and emission is determined by the underlying process, combustion. Many issues are of importance in the design of a well controlled combustion process as to achieve high efficiency and low emission. One phenomenon that can severely degrade the efficiency and emission of a combustor is combustion instability. Combustion instability manifests itself by large, growing pressure fluctuations that eventually settle into a limit cycle. This condition is tied to increased emission and undesirable increased heat transfer, and requires increased design specifications of components for a given life expectancy of the combustor. Combustion instability mechanisms are very system dependent, and it is perhaps impossible to develop a general model of the combustion process that captures all these phenomena. As a result, any stability problems only appear first in the testing phase. The instability problems

are typically combatted by identifying the cause of the instability, and then making the necessary design modifications. These modifications are for example changes in the flame holder geometry, the addition of acoustic dampers, and changes in the dimensions of the combustion chamber. However, these changes may not always be successful. For example, an acoustic damper can be implemented by perforating the cooling liner close to the flame holder [65]. By tuning the size of the holes and cavity in the liner, the acoustic damping can be maximized for a particular unstable mode. However, the effectiveness of the damping liner decreases significantly for frequencies below $1000Hz$, and devices of this type are almost impossible to implement for lower frequencies because of constraints on the allowable volume of the cavity.

Another way to prevent combustion instability is through active control. A survey of active control methods for combating combustion instabilities can be found in [41]. There are many system dependent issues when selecting the appropriate active control method for an unstable combustion process. A very important issue is the selection of the actuators and sensors used for control. The actuators used can be divided into three groups. In the first group the actuator changes the pressure field directly, an example of such an actuator is a loudspeaker [25, 52]. In the second group the gas flow inside the combustor is changed, for example by changing the flow at the inlet [12]. In the third group the combustion process is changed by changing the air-fuel ratio of the mixture to be burned [11, 22, 37]. The effectiveness of these actuation types depends on the actuator bandwidth and authority relative to the combustion dynamics. Two types of sensors are typically used for determining the state of the combustion process, pressure sensors [11, 12, 22, 25, 52] and flame emission sensors [11, 37, 51]. Pressure sensors are for example high bandwidth condenser microphones. A flame emission sensor is typically a photodiode generating a signal that depends on the intensity of Chemiluminescence of the flame. The output of a flame emission sensor is therefore directly related to heat release. However, a flame emission sensor requires optical access to the flame and may therefore not be practical.

Active control of combustion instability has been attempted before. In [25] a phase-lead controller cascaded with various filters is used to stabilize the combustion

process. The control gains are determined experimentally. In a theoretical study, [21] discusses the use of a PI-controller. In this case the control gains are selected such that the controlled unstable mode is least sensitive to a loop time delay. An adaptive control approach is discussed in [11]. The controller is based on the anti-sound concept, where fluctuations created by an actuator are superimposed on the combustion oscillations. The adaptive rule in this case is based on a least squares algorithm. Stability of the controller is not discussed. Both emission and pressure measurements are inputs to the adaptive algorithm, the control output is a change in the air-fuel ratio. Much of the work done in the active control of combustion instability has been experimental because of the lack of a fundamental model that shows the interaction between the pressure perturbations in the combustor and the flame dynamics. Recently, such a fundamental model has been developed in [2]. This model gives a complete description of the combustion process and explains the instability phenomenon and will be used in part here.

5.3.3 Dynamic Model

In this section the model of the unstable combustion process is presented. First, a simplified one-dimensional model of the combustion process is given. Next, the fundamental laws describing the one-dimensional fluid flow and the flame dynamics are presented. Since the fundamental equations have the form of partial differential equations, a finite dimensional solution to these equations is derived. It should be noted that the formulation and derivation of the combustion instability model is not a contribution of this thesis, but is taken from [2]. The finite element discretization of the partial differential equations is quite different from the approach taken in [2] where an assumed mode solution is used.

Combustion systems can have quite complex three dimensional geometries. However, the instability phenomenon that is considered here is dominated by the flow in the radial direction. The combustor is therefore modeled as a long, slender duct. The duct is either closed at the left end and open at the right end (Fig. 5-21) or open at both ends. We will consider the first type of boundary condition, the same

approach can be applied to the latter. Along the duct, at a distance x_o , a flame holder is mounted. A mix of fuel and air enters the duct at the upstream end with a flow rate determined by a compressor, the mixture is ignited when passing the flame holder, and exits at the downstream end as a burned gas at atmospheric pressure. For controlling the pressure in the duct a loudspeaker will be used. The loudspeaker can be either end-mounted or side-mounted at a distance x_a along the duct. In both cases a microphone is mounted at x_s , the output of the microphone is a measure of the pressure. Here a closed open combustor with an end-mounted loudspeaker will be considered (Fig. 5-21).

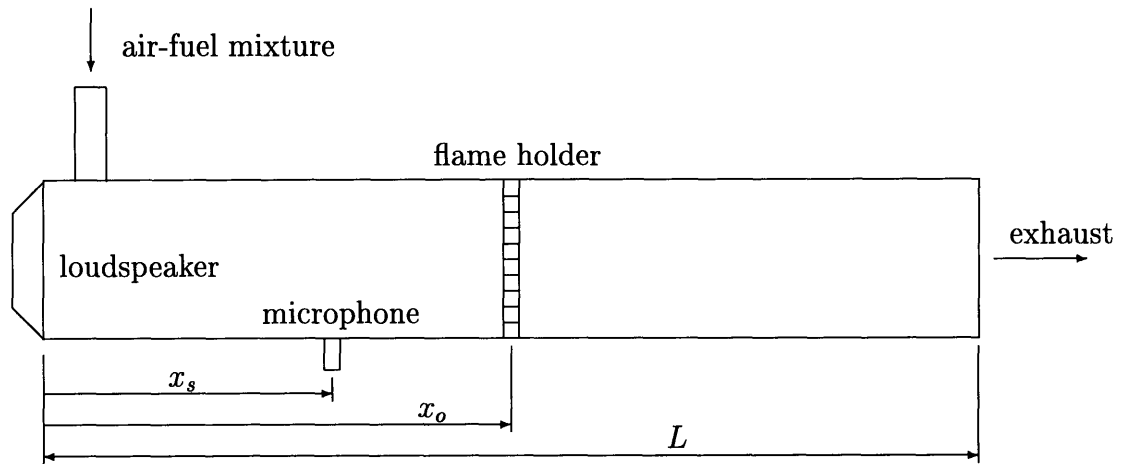


Figure 5-21: Combustion system with end-mounted loudspeaker.

The dynamics of a fluid flow is governed by a set of coupled partial differential equations describing a highly nonlinear system. Starting from the conservation of mass, the Euler equation and the energy equation, it is shown in [2] that for the one-dimensional model considered, the governing equations can be simplified to a set of equations describing the steady flow and a perturbation of the flow. In deriving this model it is assumed that the fluid flow is one-dimensional and laminar, and that viscosity effects are negligible. The mean flow is (piecewise) constant along the duct, and perturbations of the system variables from the mean are small. Heat is localized at one location (x_o) and this heat is transferred to the flow only i.e. conductivity and

<i>Symbol</i>	<i>Description</i>	<i>Units</i>
ρ	Density	$kg\ m^{-3}$
u, v	Flow velocity	$m\ s^{-1}$
p	Pressure	$N\ m^{-2}$
$q, \text{ or } q_o$	Heat generated	$J\ s^{-1}\ m^{-3}, \text{ or } J\ s^{-1}\ m^{-2}$
γ	Ratio of specific heats	–
\overline{M}	Mach number	–
\bar{c}	Velocity of sound	$m\ s^{-1}$
s_u	Burning velocity	$m\ s^{-1}$
e	Internal energy	$J\ kg^{-1}$
R	Gas constant	$N\ m\ kg^{-1}\ ^\circ K^{-1}$
T	Temperature	$^\circ K$
h	Enthalpy	$J\ kg^{-1}$

Table 5.3: List of Symbols.

radiation effects are negligible. The fluid is assumed to behave as a perfect gas. For reference, most of the symbols used are given in Table 5.3. A system variable $a(x, t)$ (such as flow velocity or pressure) is separated into its mean part \bar{a} and its perturbed part a' as $a(x, t) = \bar{a}(x) + a'(x, t)$. Below first the equations for the steady flow are presented, followed by the equations that describe the perturbed flow.

When the mach number of the mean flow $\overline{M} = \frac{\bar{u}}{\bar{c}} < 1$, it can be shown that the change in mean pressure \bar{p} along the duct, and across the flame holder is negligible [2, 36]. However, \bar{p} and \bar{u} will have a significant step change at x_o . Let the upstream mean variable \bar{a} be denoted by \bar{a}_1 , and let the downstream mean variable be denoted by \bar{a}_2 . \bar{p} , \bar{u}_1 , $\bar{\rho}_1$ and \bar{c}_1 are known quantities, the objective is to find the values for the downstream variables. The temperature in the combustion chamber is related to the temperature in the premixing chamber by

$$T_2 = R_T T_1$$

where R_T is the temperature ratio. R_T is determined experimentally [2, 36]. Since

the conservation of mass for the steady flow is given by

$$\frac{d(\bar{\rho} \bar{u})}{dx} = 0,$$

it follows that

$$\bar{u}_2 = \frac{\bar{\rho}_1 \bar{u}_1}{\bar{\rho}_2}.$$

The equation of state for an ideal gas gives $\bar{p} = \bar{\rho}_1 RT_1 = \bar{\rho}_2 RT_2$ so that

$$\bar{p} = \frac{\bar{\rho}_1}{R_T}.$$

Also, since

$$\bar{p} = \frac{\bar{c}_1^2 \bar{\rho}_1}{\gamma} = \frac{\bar{c}_2^2 \bar{\rho}_2}{\gamma},$$

it follows that

$$\bar{c}_2 = \bar{c}_1 \sqrt{\frac{\bar{\rho}_1}{\bar{\rho}_2}}.$$

This completes the description of the mean flow.

The equations describing the perturbed flow are given by

$$\frac{\partial^2 p'}{\partial t^2} + (\bar{u}^2 - \bar{c}^2) \frac{\partial^2 p'}{\partial x^2} + 2\bar{u} \frac{\partial^2 p'}{\partial x \partial t} = (\gamma - 1) \left[\frac{\partial q'}{\partial t} + \bar{u} \frac{\partial q'}{\partial x} \right]. \quad (5.5)$$

$$\frac{\partial p'}{\partial t} + \bar{u} \frac{\partial p'}{\partial x} + \gamma \bar{p} \frac{\partial u'}{\partial x} = (\gamma - 1) q'. \quad (5.6)$$

Eq. (5.5) is known as a wave equation, and is obtained by linearizing the Euler equation around an operating point (\bar{p}, \bar{u}_1) . Eq. (5.6) is essentially the linearized energy equation. Eqs. (5.5) and (5.6) describe the dynamics of the fluid flow in terms of pressure perturbations and flow velocity perturbations. More importantly, Eqs. (5.5) and (5.6) show how the acoustic dynamics is excited by the generated heat q' . The heat is generated at the interface of the air-fuel mixture and the exhaust. In [2] a model of the flame has been developed by looking at the energy exchange mechanism at this interface more closely. The idea behind this model is that the perturbation in the velocity of the flow causes the flame area to change. Since the heat

generated is proportional to the surface area of the flame, $q'_o(t) = q'(x_o, t)$ increases with $u'_o(t) = u'(x_o, t)$. When no flow velocity perturbation is present, the flame area will decrease since then the flame will burn inward. For a flame holder consisting of a perforated plate of area A_f with a total of n_f flame holes each of radius r_f , the change in heat generated can be described quantitatively by

$$\dot{q}'_o(t) = -\alpha_2 q'_o(t) + \alpha_1 u'_o(t), \quad (5.7)$$

where $u'_o(t) = u'(x_o, t)$, and

$$\alpha_1 = \alpha_2 \bar{\rho} h \frac{n_f \pi r_f^2}{A_f}, \quad \alpha_2 = \frac{2s_u}{r_f},$$

h is the enthalpy of the air-fuel mixture, and s_u the burning velocity of the flame. The perturbed system dynamics is completely described by Eqs. (5.5)–(5.7).

To complete the model, a solution to Eqs. (5.5)–(5.7) is needed. For this purpose a finite element discretization of Eqs. (5.5) and (5.6) was performed. The procedure for the discretization is outlined in Appendix A.2 and Appendix A.4. In what follows, first the finite dimensional model in case no mean heat and no mean flow is presented and used to explain the instability mechanism. Then the complete finite dimensional model with mean heat and mean flow effects included is presented, and used to verify assumptions (A1), (A2) and (A3).

In case no mean heat and no mean flow is present, the combustor dynamics over a selected bandwidth can be described by, from Eqs. (A.25)–(A.27), (Fig. 5-22):

$$\begin{aligned} M\ddot{P}(t) + B_{pqd}\alpha_1 a_o C_{qpd}\dot{P}(t) + KP(t) &= -B_{pqd}(\gamma - 1)\alpha_3 q'_o(t) + B_{pcu}\bar{\rho} \bar{c}^2 \dot{u}_c(t) \\ \dot{q}'_o(t) &= -\alpha_3 q'_o(t) - \alpha_1 \frac{1}{\gamma \bar{p}} C_{qpd}\dot{P}(t) \\ p'_s(t) &= C_{cp}P(t). \end{aligned} \quad (5.8)$$

In Eq. (5.8), P denotes the vector with nodal pressures. q_o is the heat generated by the flame. $p'_s(t)$ is the (perturbed) pressure measurement obtained from the loudspeaker, and $u_c(t)$ is the velocity of the loudspeaker diaphragm. M is a symmetric,

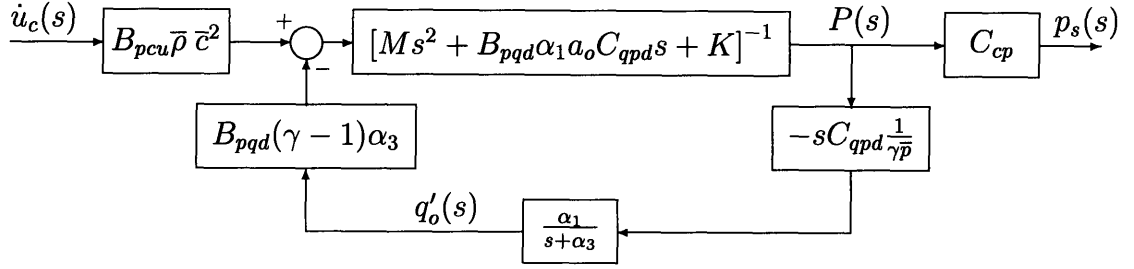


Figure 5-22: Block diagram of Combustor Dynamics with no mean heat and no mean flow effects.

positive definite, dimensionless matrix. K is also symmetric, positive definite, and has the units of \bar{c}^2 . In order to interpret Eq. (5.8), the following simplification will be made. For typical combustor parameters, the corner frequency of the flame dynamics, $\alpha_3 = \alpha_2 - \alpha_1 a_o > 0$, is much lower than the modal frequencies characterized by M and K . Furthermore, the DC-gain of the flame dynamics, $\frac{\alpha_1}{\alpha_3}$, is small compared to the DC-gain of the acoustic dynamics, characterized by K . Therefore, from a systems point of view, in the frequency range of the acoustic modes the model is very well approximated by

$$\begin{aligned} M\ddot{P}(t) + B_{pqd}\alpha_1 a_o C_{qpd}\dot{P}(t) + KP(t) &= B_{pcu}\bar{\rho}\bar{c}^2\dot{u}_c(t) \\ p'_s(t) &= C_{cp}P(t). \end{aligned} \quad (5.9)$$

From Eq. (5.9) it can be seen when open loop acoustic modes are unstable. Namely, the modal form of Eq. (5.9) is given by

$$\begin{aligned} \ddot{\eta}(t) + \Phi^T B_{pqd}\alpha_1 a_o C_{qpd}\Phi\dot{\eta}(t) + \text{diag}(\omega_i^2)\eta(t) &= \Phi^T B_{pcu}\bar{\rho}\bar{c}^2\dot{u}_c(t) \\ p'_s(t) &= C_{cp}\Phi\eta(t) \end{aligned} \quad (5.10)$$

where Φ contains the undamped, unforced modeshapes characterized by M and K . From Eq. (5.10) it is seen that all modes are coupled through the (non-diagonal) damping matrix, $\mathcal{C} = \Phi^T B_{pqd}\alpha_1 a_o C_{qpd}\Phi$. In case the model contains one mode only, \mathcal{C} is a scalar and $\Phi^T B_{pqd}$ corresponds to the mode evaluated at $x = x_o$. For example,

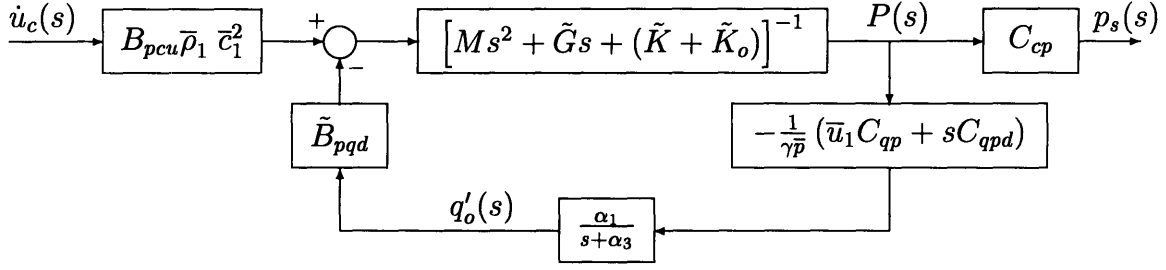


Figure 5-23: Block diagram of Combustor Dynamics including mean heat and mean flow effects.

for the closed open combustor (Fig. 5-21), if the model contains the fundamental mode only, then $\Phi B_{pqd} = \cos(\frac{\pi x_o}{2L})$. $C_{qpd}\Phi$ corresponds to the integral of the mode evaluated at $x = x_o$. For the lowest mode, this implies that $C_{qpd}\Phi = \int_0^{x_o} \cos(\frac{\pi x}{2L}) dx = \frac{2L}{\pi} \sin(\frac{\pi x_o}{2L})$. If the product of these two terms is positive, positive damping is obtained, and the mode is stable and *vice versa*. The fundamental mode in the above example is therefore always stable. This observation corresponds with the conclusion in [2]. When multiple modes are present, using a Lyapunov stability argument, a sufficient condition for open loop stability of all modes is $C_{qpd}(x_o)B_{pqd}(x_o) > 0$ ⁴. Whether or not this condition is satisfied depends on the location of the flame x_o , which is typically determined by combustor design constraints.

When mean heat and mean flow are present, the combustor dynamics is described by, from Eq. (A.36), (Fig. 5-23):

$$\begin{aligned}
 M\ddot{P} + \tilde{G}\dot{P} + (\tilde{K} + \tilde{K}_o)P &= -\tilde{B}_{pqd}q'_o + B_{pcu}\bar{\rho}_1\bar{c}_1^2\dot{u}_c + B_{pcv}k_{uv}\bar{\rho}_a\bar{c}_a^2\dot{u}_c \\
 \dot{q}'_o &= -\alpha_3q'_o - \alpha_1\left(\frac{1}{\gamma\bar{p}}C_{qpd}\dot{P} + \frac{\bar{u}_1}{\gamma\bar{p}}C_{qp}P\right) \\
 p'_s &= C_{cp}P.
 \end{aligned} \tag{5.11}$$

Comparing Eq. (5.11) to Eq. (5.9), the introduction of mean flow and mean heat has introduced two additional terms to the acoustic dynamics, G and \tilde{K}_o , where

⁴Choose $V = \frac{1}{2}\dot{P}^T M \dot{P} + \frac{1}{2}P^T K P$, then $\dot{V} = -P^T B_{pqd}\alpha_1 a_o C_{qpd}P$. The result follows by noting that $rank(B_{pqd}C_{qpd}) = 1$ and $\bar{\lambda}(B_{pqd}C_{qpd}) = \bar{\lambda}(C_{qpd}B_{pqd})$.

$\tilde{G} = G + B_{pqd}\alpha_1 a_o C_{qpd}$. G is a gyroscopic term due to mean flow, and is skew symmetric. \tilde{K}_o is due to additional feedback effects of the flame. It is worth noting that if $\bar{u}_1 \rightarrow 0$, then Eq. (5.11) reduces to Eq. (5.8). Similar to the case where no mean heat and no mean flow was present, the flame dynamics feedback loop described by α_1 and α_3 has a negligible effect on the acoustic dynamics. Therefore, from a systems point of view, the system dynamics can be described by:

$$\begin{aligned} M\ddot{P} + (G + B_{pqd}\alpha_1 a_o C_{qpd})\dot{P} + (\tilde{K} + \tilde{K}_o)P &= B_{pcu}\bar{\rho}_1\bar{c}_1^2\dot{u}_c \\ p'_s &= C_{cp}P, \end{aligned} \quad (5.12)$$

In what follows, assumptions (A1), (A2) and (A3) for the system described by Eq. (5.12) are discussed. Since the original system in Eq. (5.11) is only a small perturbation of the system described by Eq. (5.12), the conclusions made based on Eq. (5.12) will hold for Eq. (5.11) as well. First, since Eq. (5.12) is of the same form as Eqs. (5.1) and (5.2) and since M is positive definite, assumptions (A1) and (A3) are satisfied if a colocated actuator and sensor are used. Since Eq. (5.12) represents a discretization of a continuous system, assumptions (A1) and (A3) will hold as well when a small dislocation between the actuator and sensor exists. Assumption (A2) is much more difficult to verify than in the case of flexible structures. This is in part due to the nontrivial structure of the damping matrix $C = G + B_{pqd}\alpha_1 a_o C_{qpd}$. The approach taken here to verify assumption (A2) was through extensive numerical computation of the system zeros for reasonable ranges of the system parameters. Below the conclusions of these computations are discussed qualitatively for the premixed laminar combustor with closed-open boundary conditions (Fig. 5-21). Typical pole-zero plots show that the low frequency system zeros are minimum phase for dislocations between the actuator and sensor of upto 25% of the combustor length (Fig. 5-24). For small dislocations between the actuator and sensor, the well known pole zero interleaving as they occur in flexible structures, is maintained. When the non-colocation between actuator and sensor is increased further, the zeros move past the associated poles which, for a selected bandwidth, implies a loss in relative degree.

No real zero pairs (stable and unstable) are obtained. This corresponds to results obtained for wave equations with no damping terms [42]. A change in the operating point, i.e. a change in the mean flow and the mean heat, results in the same pole zero patterns, with the imaginary parts of the poles and zeros changed only. (This observation can be explained intuitively from the structure of G , which is skew-symmetric). The conclusion that can be drawn from these computation studies is that the system described by Eq. (5.12) satisfies assumption (A2) for realistic values of the system parameters. Naturally, in practice these parameters are known to within a certain range only.

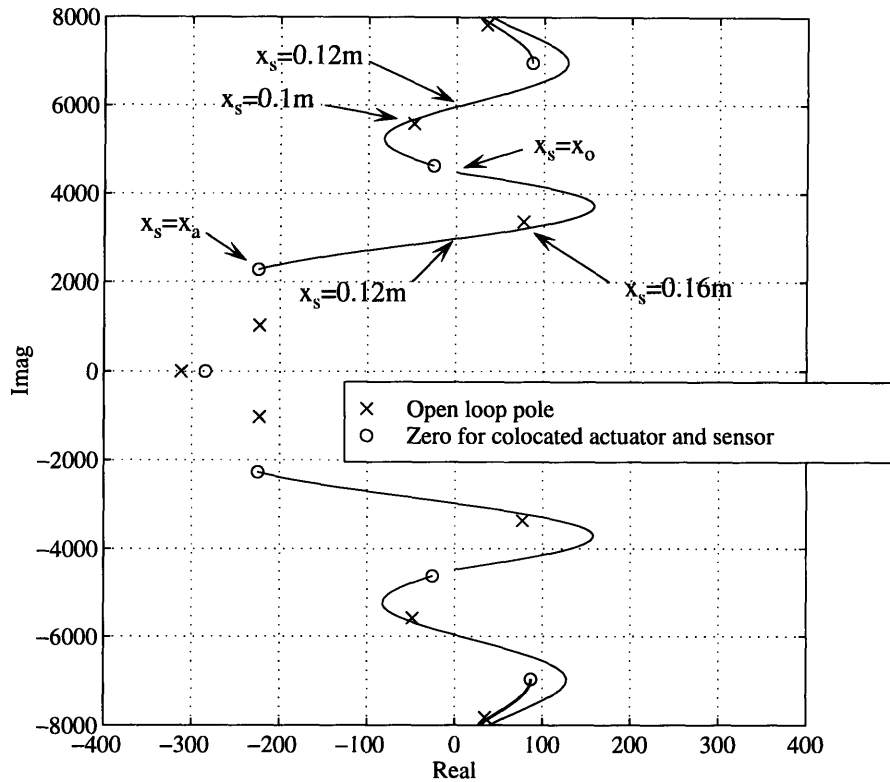


Figure 5-24: Locus of the system zeros with varying sensor location. The sensor is collocated with the actuator at $x_s = 0$, and then moved to $x_s = x_o = 0.24m$. The low frequency zero becomes unstable if the dislocation is larger than $0.12m$. An almost pole zero cancellation occurs at $x_s = 0.16m$. Physically, this location corresponds a node of the second mode which lies at $x = \frac{L}{3} = 0.16m$ and makes the second mode unobservable from this sensor location. When $x_s \rightarrow x_o$ the low frequency zero approaches the imaginary axis, but now from the unstable side.

parameter	value
L	0.48 m
x_o	0.24 m
x_s	0.1 m
n_f	80
A_f	$16 \times 10^{-4} \text{ m}^2$
r	$0.75 \times 10^{-3} \text{ m}$
s_u	0.4 ms^{-1}
γ	1.4
h	$2.563 \times 10^6 \text{ Jkg}^{-1}$
$\bar{\rho}$	1 kgm^{-3}
\bar{c}	350 ms^{-1}
$\bar{\rho}_1$	1 kgm^{-3}
\bar{u}_1	230 mls^{-1} or 0.14 ms^{-1}
\bar{c}_1	350 ms^{-1}
R_T	1.8

Table 5.4: System parameters for the Combustion Example.

5.3.4 Example

In this section a sample combustor will be given and a case will be made for the use of adaptive control in actively controlling combustion instabilities. The control objective is clear from the onset, it is desired to stabilize the unstable mode(s) without destabilizing other, open loop stable modes. The sample combustor that will be considered here is a premixed, laminar combustor with closed open boundary conditions (Fig. 5-21). The parameters that characterize the combustor were taken from [2, 52] (Table 5.4).

The finite element discretization as discussed in section 5.3.3 and Appendix A was performed. 48, 3-node elements were used. This mesh results in smooth low frequency modeshapes, and is sufficient to obtain an accurate model in the selected frequency range. It should be apparent that these finite element parameters result in a 96 mode model. Close inspection of these modes reveals a total of 48 stable modes and 48 unstable modes, alternating stable and unstable along the imaginary axis. Two steps have to be undertaken to make this model physically more realistic, and computationally feasible. First, in a real physical combustor only a few, low frequency

modes are unstable. The higher, theoretically unstable modes are still present but are in practice open-loop stable due to the presence of (as of yet unmodeled) passive damping mechanisms such as notches or damping resonators. Therefore, to obtain a physically realistic model, these higher modes should have added passive damping. In this example a case will be considered where the second mode is the only unstable mode, the passive damping for the higher modes was implemented through modal damping for the acoustic modes with uniform modal damping coefficient $\zeta = 0.0075$. The resulting modal damping coefficients in the presence of the flame dynamics for the lowest six modes are shown in Table 5.5. Second, for control simulation purposes, the model has to be accurate up to 4 to 10 times the desired closed loop bandwidth. In this case, as it is desired to stabilize the unstable mode, the desired bandwidth is about 3400 rad/s. In the simulations, a model fidelity of 10 times the desired closed loop control bandwidth was chosen. This implies that 15 modes need to be included in the model. Using a mode superposition technique, the full order model with 96 modes was reduced to a 15 mode model. This technique is presented in detail in Appendix A.3 and A.4. The frequency response plot shows that of these 15 modes, about 5 are dominant (modes 1, 2, 4, 5 and 6) (Fig. 5-25).

mode number i	ω_i (rad/s)	ζ_i (Theory)	ζ_i (Corrected)
1	1050	0.21	0.21
2	3371	-0.023	-0.023
3	5584	0.0086	0.0161
4	7828	-0.0044	0.0031
5	10059	0.0027	0.0102
6	12299	-0.0018	0.0057

Table 5.5: Modal frequencies and damping ratios for the lowest six modes in the Combustion Example.

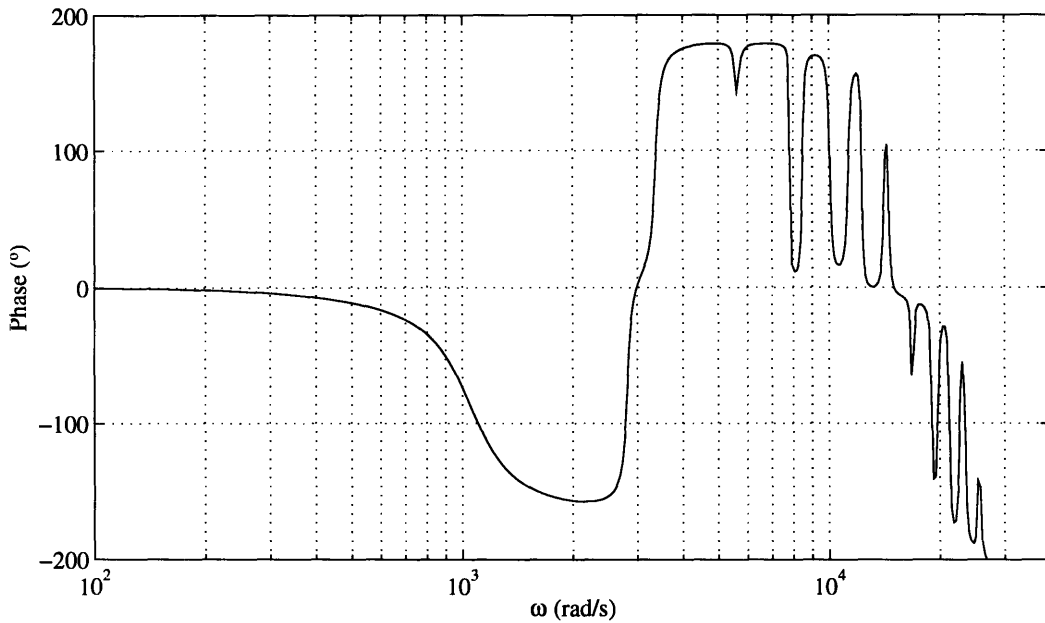
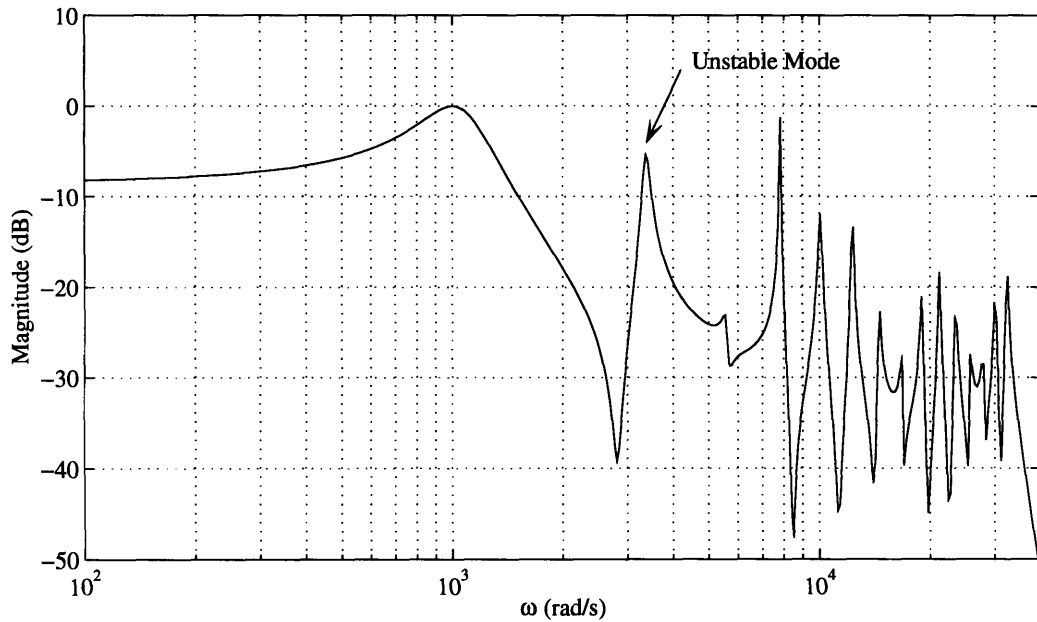


Figure 5-25: Frequency response plot of the sample Combustor ($\bar{u}_1 = 0$). Of the 15 modes, modes 1, 2, 4, 5 and 6 are dominant. The third mode is almost canceled due to the placement of the microphone on a node of the third mode. Since the second mode is unstable, an additional phase lead of 180° around $\omega_2 = 3371$ rad/s occurs. The alternating pole zero pattern is maintained upto about $\omega = 10^4 - 2 \cdot 10^4$ rad/s, In this frequency range a zero-pole-pole-zero pattern appears causing the 180° roll-off in this region.

In what follows, a case for the use of adaptive control in combustion stabilization is made, and illustrated for the numerical example. The need for the use of adaptive control is twofold. First, the system parameters are not precisely known; i.e. the plant structure is well modeled, but is uncertain in the parameters. Few fixed control strategies exist that can deal with this parametric uncertainty elegantly and still result in non-conservative performance. Second, not only are the system parameters unknown, they may change on-line. Specifically, the model relies on the fact that the mean flow and mean heat are constant. These however may vary during the operation of the combustor due to a change in power demand for example. Adaptive control can take care of both concerns, parametric uncertainty and a change in operating conditions, simultaneously. From a systems point of view, the uncertainty in the parameters causes uncertainty in the locations of the poles and zeros (Fig. 5-26). That such uncertainties can be reduced through the use of feedback is well known [17]. To illustrate this, a fixed controller was designed and the sensitivity of the poles and zeros was examined. The fixed controller was designed following the discussion in section 3.2.1. A phase-lead compensator was used augmented with a complex pole-zero pair such that a low feedback gain is needed to stabilize the combustor. The compensator transfer function is given by

$$G_c(s) = 3.25 \frac{s + 3500}{s + 4500} \frac{s^2 + 800s + 2000^2}{s^2 + 1200s + 3000^2}. \quad (5.13)$$

The uncertainty in the closed loop pole-zero locations is less than in the open loop case (Fig. 5-26).

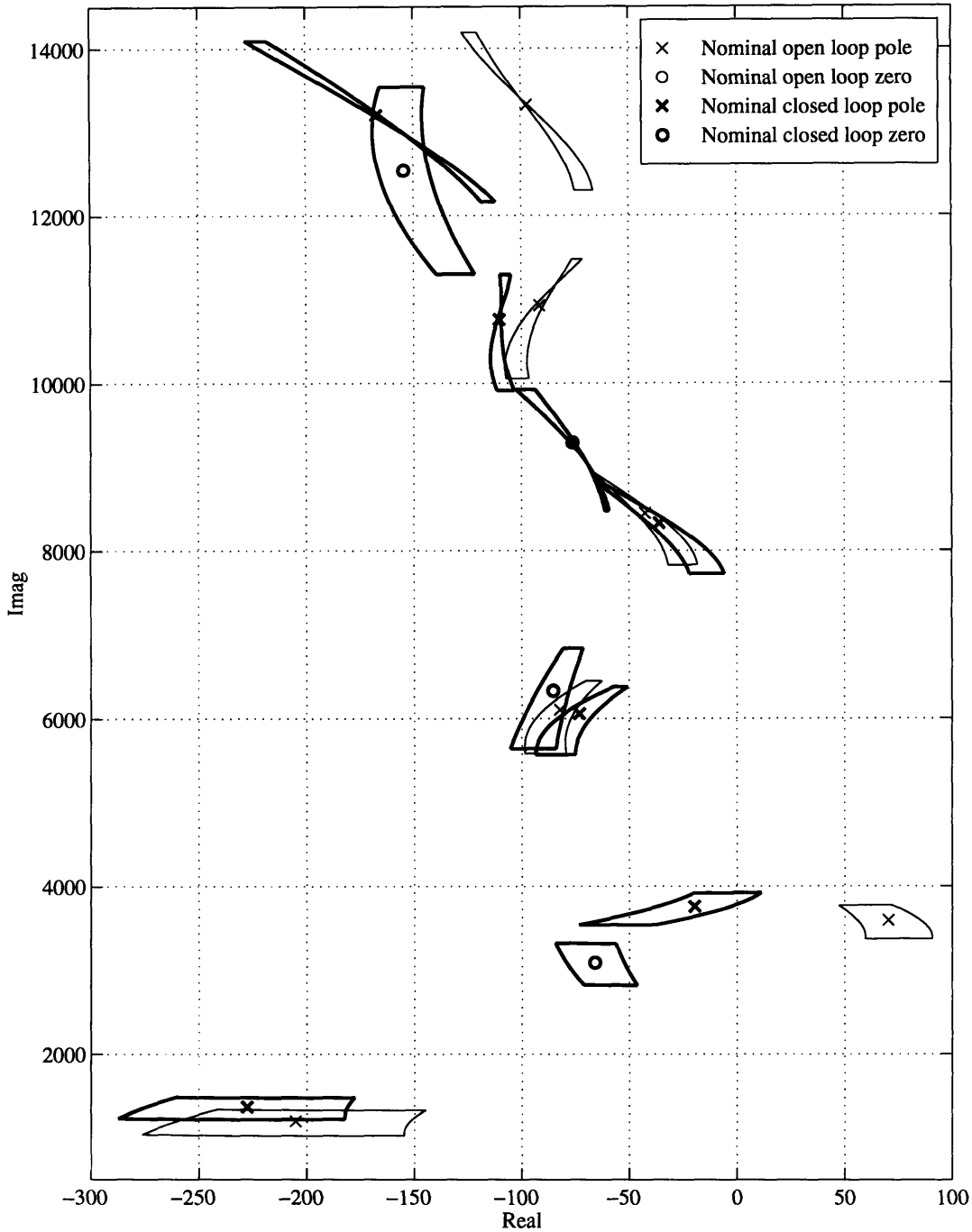


Figure 5-26: Uncertainty in the combustor pole-zero locations due to parametric uncertainty ($2 \leq h \leq 3 [\times 10^6 \text{ Jkg}^{-1}]$) and uncertainty in the operating point ($0 \leq \bar{u}_1 \leq 230 [\text{mls}^{-1}]$). Comparison between the open loop sensitivity and the closed loop sensitivity. The graph illustrates that feedback, although low gain, reduces the uncertainty in the pole and zero locations.

The scenario that was considered in the simulations is when the fixed compensator (as in Eq. (5.13)) does not stabilize the unstable modes for all possible, physically realistic parameter values (as in Fig. 5-26). Note that for a fixed control design, the closed loop can be further desensitized by simply increasing the gain in $G_c(s)$. However, the extend to which this gain can be increased is uncertain and increasing it too much result in excitation of unmodeled dynamics. It is precisely this uncertainty that the adaptive controller will accommodate. In the adaptive control design, to tune the feedback gain on-line, the adaptation gain for $\Theta_o \in \mathbb{R}$ is chosen as $\Gamma_o = 10^5$. Furthermore, to accommodate for uncertainties in the imaginary part of the poles and zeros, $\Theta_1 \in \mathbb{R}^{1 \times 3}$ is tuned on-line with $\Gamma_1 = 10^9$. Based on the nominal parameter values the filter was chosen as $a = 1000$ rad/s. The input filter is chosen as

$$\Lambda_1 = \begin{bmatrix} 4500 & & \\ & 0 & 1 \\ & -2000^2 & -800 \end{bmatrix}, \quad L = \begin{bmatrix} 1 \\ 0 \\ 1 \end{bmatrix}.$$

The initial parameter values $\Theta_o(t = 0)$ and $\Theta_1(t = 0)$ were chosen such that the initial adaptive controller corresponds to the fixed control design with the compensator as in Eq. (5.13). The initial condition of the combustor was set by exciting the first two modes as $\eta_1(t = 0) = \eta_2(t = 0) = 10$ Pa and $\dot{\eta}_1(t = 0) = \dot{\eta}_2(t = 0) = 0$.

The simulation results for a worst case operating point and parameter uncertainty are shown in Figs. 5-27–5-29. The adaptive controller results in a stable response whereas the fixed controller response is unstable (Fig. 5-27). The adaptive stabilization is achieved using an initially larger control input due to the presence of adaptation terms in the adaptive control law (Fig. 5-28). The stabilization is essentially the result of increasing the feedback gain judiciously on-line (Fig. 5-29). To show that the adaptive controller results in stabilization for a wide range of operating points, simulations were performed for \bar{u}_1 varying between 0 and 230 ml/s. The results are shown in Figs. 5-30–5-32. The adaptive controller shows uniform stabilization, whereas the fixed controller is stable in only a small region (Fig. 5-30).

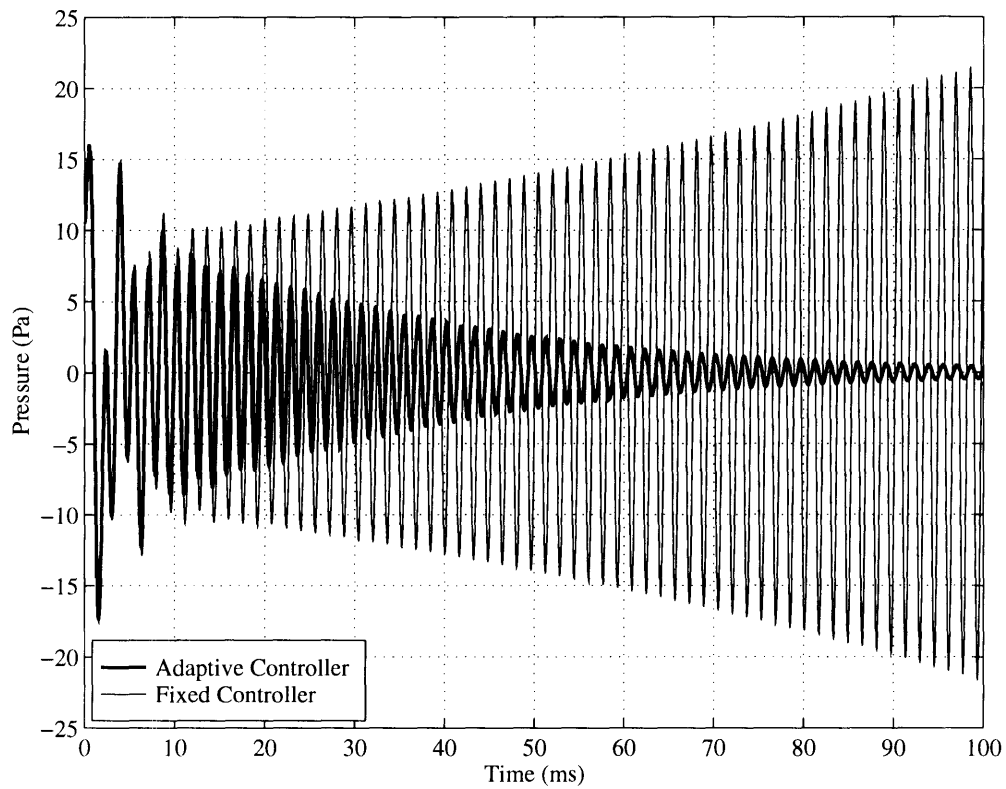


Figure 5-27: Combustion example, $h = 3 \times 10^6 \text{ J/kg}$ and $\bar{u}_1 = 230 \text{ ml/s}$. Comparison of the plant response using the adaptive and the fixed controller. The fixed controller is unstable, the adaptive controller establishes a stable response.

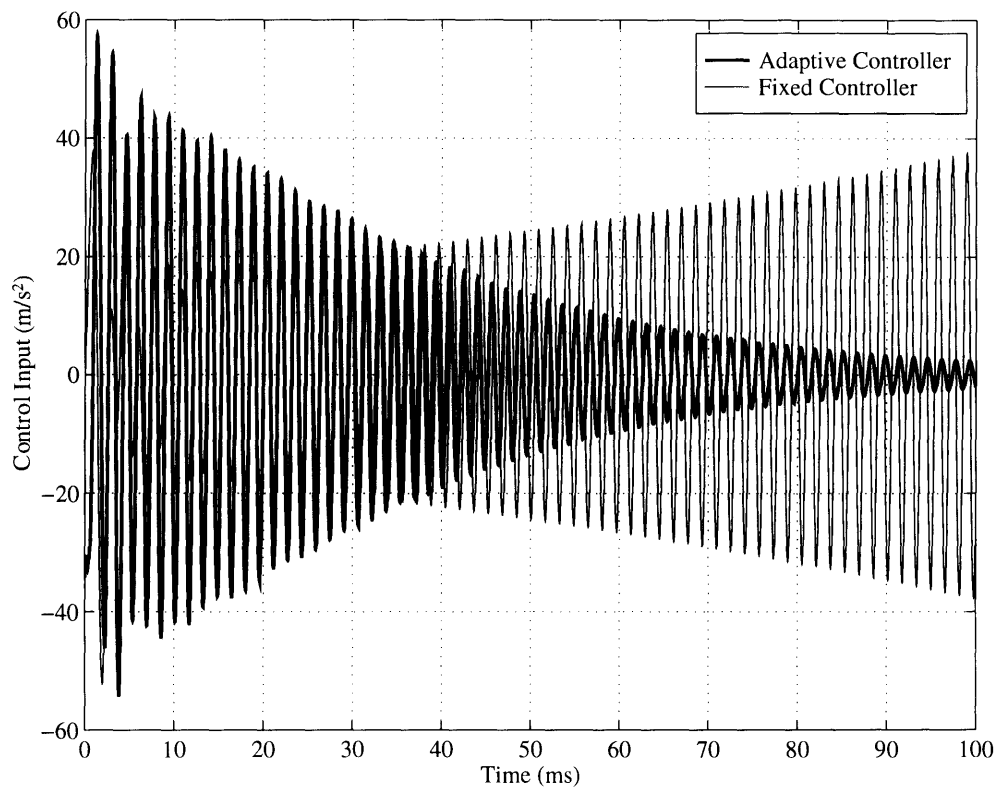


Figure 5-28: Combustion example. Comparison of the control input using the adaptive and the fixed controller. Due to high adaptation gains, the control input for the adaptive controller is higher between $t = 0$ ms and $t = 40$ ms.

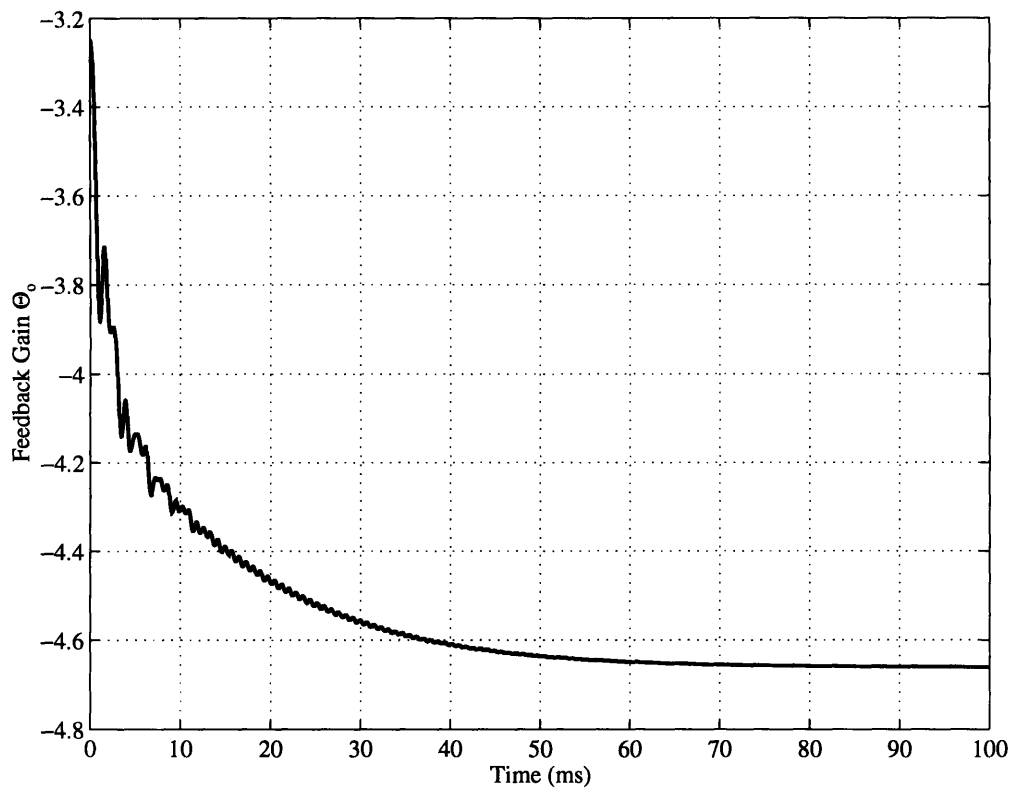
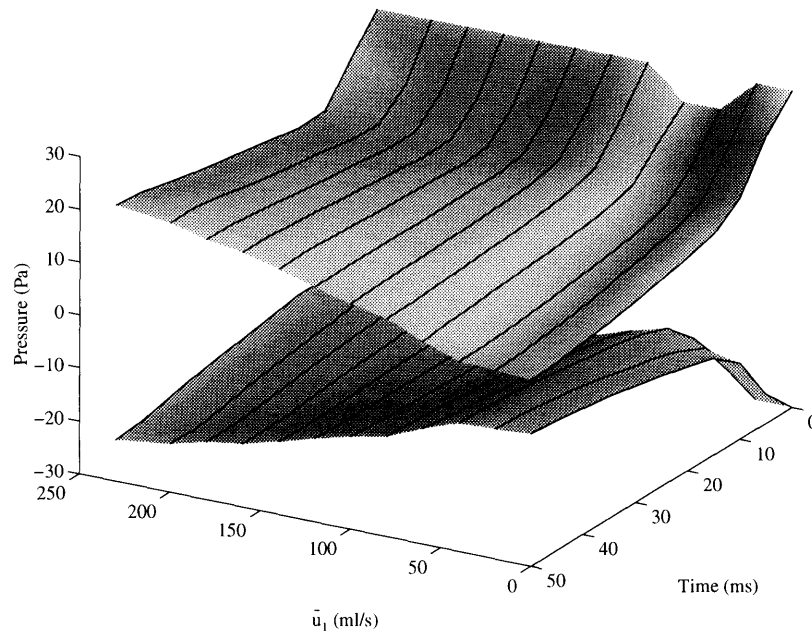
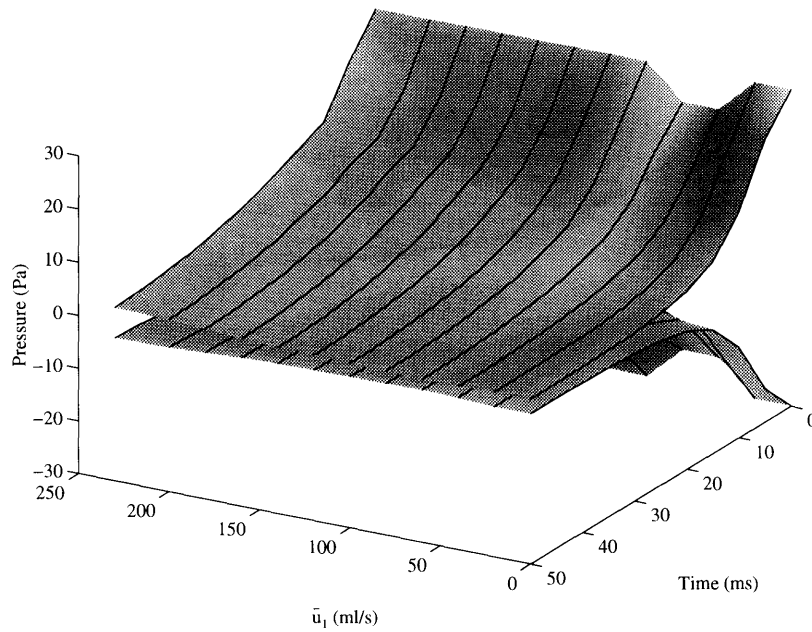


Figure 5-29: Combustion example. Time history of the feedback gain Θ_o . The initial value of Θ_o corresponds to that of the fixed controller.

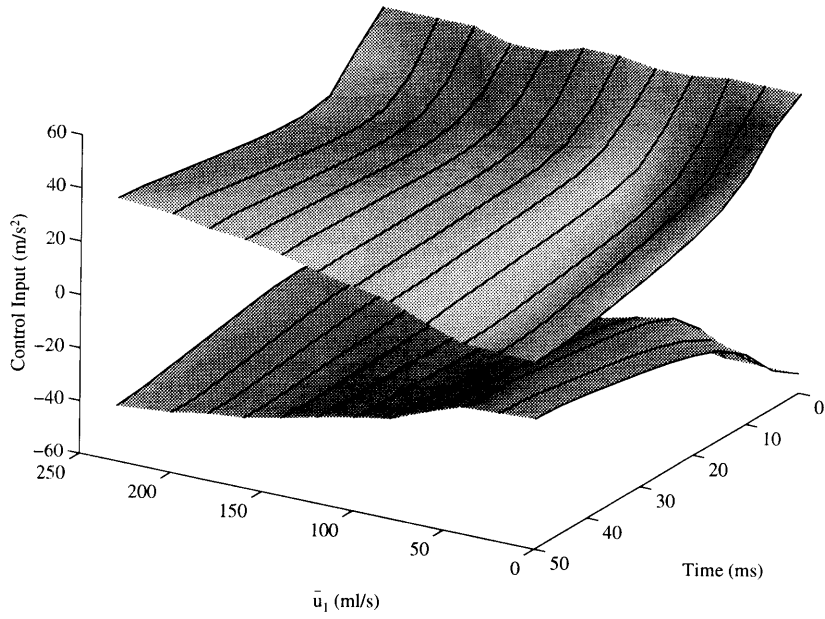


(a) Fixed controller plant response.

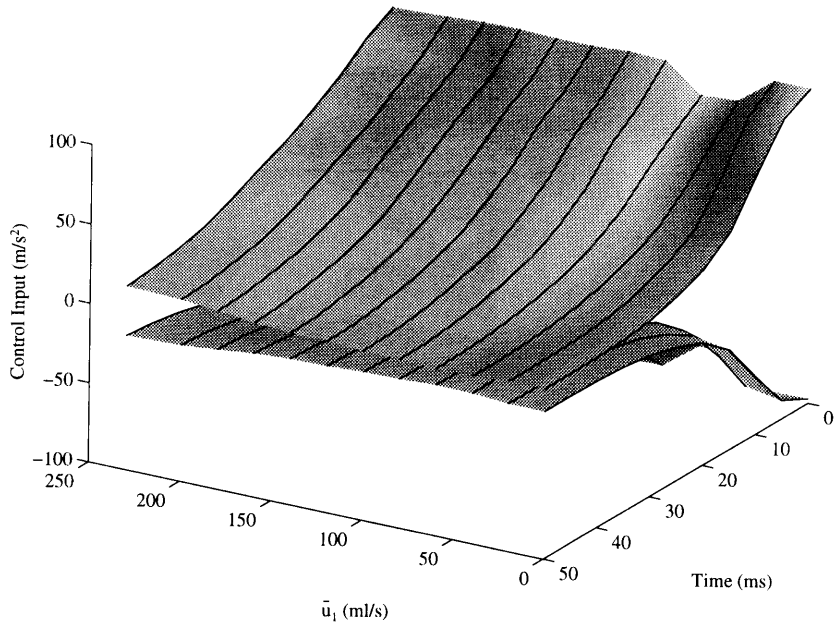


(b) Adaptive controller plant response.

Figure 5-30: Combustion example. Maximum value of the pressure for different values of mean flow.



(a) Fixed control input.



(b) Adaptive control input.

Figure 5-31: Combustion example. Maximum value of the control input for different values of mean flow.

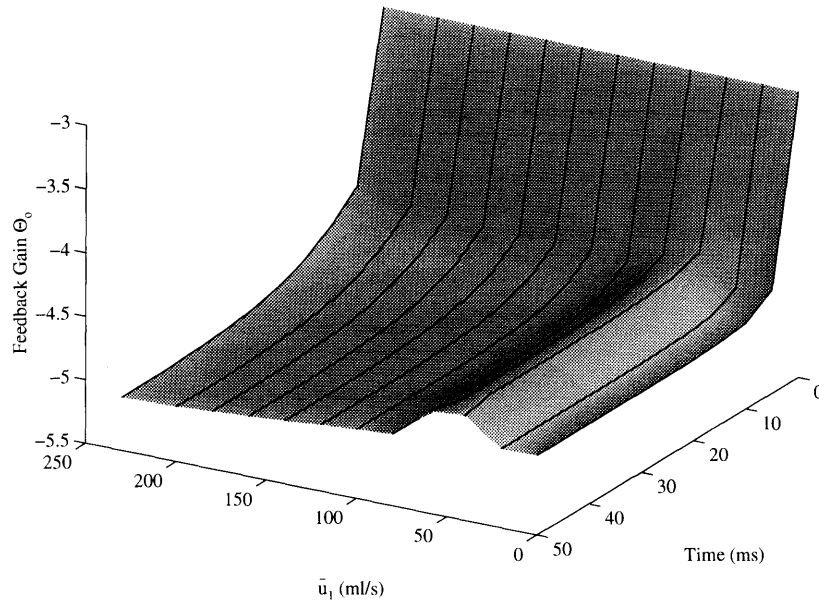


Figure 5-32: Combustion example. Time history of the feedback gain Θ_o for different values of mean flow.

5.3.5 Discussion

In this section the low order adaptive controller was applied to an unstable combustion process. Using a non-colocated actuator-sensor pair, a model was derived that includes the first 15 pressure modes. For realistic values of the model parameters, this model satisfied assumption (A2), i.e. the system was minimum phase. In the lower frequency range the model satisfied assumptions (A1) and (A3) as well. The control objective was to stabilize the unstable mode in the presence of parametric modeling errors and changes in the operating point. The low order adaptive controller was shown to result in satisfactory stabilization over a range of parametric uncertainties and operating points.

In an actual physical experiment it is advisable to use lower adaptation gains than the ones used in the simulations presented here. This is because, ideally, the on-line tuning of the gains should be driven by a possible instability only. In the simulations presented here, even if the conditions are such that the underlying closed loop system is stable, the feedback gains increase. This effect can be diminished by reducing the

adaptation gain. In the simulations presented here, a high adaptation gain was used to achieve stabilization within a computationally tractable time. Also, in practice, environment noise will excite the acoustic modes. This noise can destabilize the adaptive controller. However, using a standard dead-zone modification in the adaptive law stabilization can still be achieved [47].

The combustion example presented here is a SISO example. The adaptive control theory presented in this thesis provides the basis for extending the adaptive stabilization approach to MIMO situations as well. For example, in case the combustor is of larger size, more unstable modes will be present in the lower frequency range. Although by careful compensator design the combustor can be stabilized using one actuator sensor pair, a more robust approach would be the use of multiple loudspeaker/microphone pairs. Specifically, an effective control design is obtained by using as many control inputs as there are unstable modes.

5.4 Summary

In this Chapter two examples of the use of the low order adaptive controller were given. Using an academic example of a flexible structure, the controller was shown to result in good tracking performance and good disturbance rejection. The contribution of these examples is that they show how control objectives can be realized in the presence of large parametric uncertainty using a practically feasible multivariable adaptive controller. Tracking in the presence of unmodeled dynamics and parametric uncertainty was examined as well. Bounded signals were obtained, tracking performance was not satisfactory however.

A truly physical example was provided in the adaptive control of an unstable combustion process. Over a range of unknown operating points, the adaptive controller was shown to stabilize the combustion process. The contribution of this example is that it shows how adaptive control techniques can be used systematically in a practically important problem.

Chapter 6

Conclusion

This thesis contributes to the theory of adaptive control as well as in the area of the application of adaptive control. First, this thesis provides a theory for the design adaptive controllers whose stability does not depend on the order of the plant. This is achieved by limiting the minimum row relative degrees in the plant transfer function matrix to be either one or two. The resulting controller is of lower order and complexity than most other multivariable adaptive control schemes. Since in a real physical system the assumptions made in designing the adaptive controller are not always met at higher frequencies, a robust adaptive controller is developed as well. When unmodeled dynamics are excited and using this controller, bounded loop signals are obtained.

Second, since the control method does not require the order of the plant to be known, it is well suited for the control of distributed systems using multiple inputs and outputs. Two applications are considered: flexible structures and combustion. In an academic example of a flexible structure, using colocated actuators and sensors, it is shown that tracking is achieved in the presence of parametric uncertainties. Attenuation of poorly known bandlimited disturbances can be realized as well. In an example of an unstable combustion process it is shown that unstable pressure modes are stabilized in the presence of parametric uncertainties and changes in the operating point.

We will now focus on future research directions. Naturally, further relaxation of the assumptions made regarding the plant to be controlled is desirable. Specifically, elegant adaptive control strategies that can deal with non-minimum phase zeros are of interest when controlling flexible structures. For example, structures that contain bending modes and that use sufficiently non-colocated actuator sensor pairs will have low frequency non-minimum phase real zeros. In this case, because of the structural limitations imposed by non-minimum phase zeros on the tracking performance, a control approach different from model-following will have to be used. Also, since positive realness does not allow non-minimum phase zeros, adaptive rules based on other principles than positivity have to be found.

Another open research direction is the design of adaptive controllers in the presence of unmodeled dynamics. One can view the adaptive control approach discussed in this thesis as the adaptive control of plants which contain non-negligible unmodeled dynamics. In this thesis, it has been shown how to deal elegantly with dynamics that do not change the relative degree of the input-output map. Results were also obtained in the case where unmodeled dynamics change the relative degree. However, simulation results showed that when these unmodeled dynamics are excited, bad high-frequency disturbance attenuation is obtained. This bad high-frequency behavior is in part inherent to the adaptive laws used. On the other hand, to a certain extent this behavior may be due to the fact that the underlying fixed controller does not roll-off. However, such a feature is desirable from a stability-robustness point of view. The development of adaptive algorithms that provide controller roll-off in a systematic way may yield interesting robustness results.

The distributed systems that were considered in this thesis contain many modes inside the desired bandwidth. In many instances, all of these modes will contribute in some way to a performance criterion. The criteria considered in this thesis were all measurable on-line, as we considered regulation, tracking and disturbance attenuation at the measured outputs. However, in some cases it is desirable to consider performance criteria that are not directly measurable. For example, in the application of an unstable combustion process it is desirable not only to stabilize the unstable

modes but also to minimize the energy contained in all modes when excited by process noise. Current adaptive control methods cannot deal with such performance criteria well. The development of a theory that can deal with not directly on-line measurable performance criteria in the presence of parameter uncertainty may lead to practically important adaptive control strategies.

References

- [1] B. D. O. Anderson and John B. Moore. *Optimal Control: Linear Quadratic Methods*. Prentice Hall, Englewood Cliffs, N. J., 1990.
- [2] A.M. Annaswamy, M. Fleifil, Z. Ghoniem, and A.F. Ghoniem. A feedback model of thermoacoustic instability in combustion processes. Technical Report 9502, Adaptive Control Laboratory, MIT, Cambridge, MA, submitted for publication to *Journal of Fluid Mechanics*, 1995.
- [3] J.N. Auburn. Theory of the control of structures by low-authority controllers. *Journal of Guidance and Control*, 3(5):444–451, 1980.
- [4] R. Bakker and A.M. Annaswamy. Simple multivariable adaptive control with application to flexible structures. In *Proceedings of the ACC*, Baltimore, MD, 1994.
- [5] R. Bakker and A.M. Annaswamy. Low order multivariable adaptive control with application to flexible structures. *Automatica*, Accepted for Publication, 1995.
- [6] R. Bakker and A.M. Annaswamy. Stability and robustness properties of a simple adaptive controller. *IEEE Transactions on Automatic Control*, Accepted for Publication, 1995.
- [7] I. Bar-kana and H. Kaufman. Simple adaptive control of large flexible space structures. *IEEE Transactions on Aerospace and Electronic Systems*, 29(4), 1993.
- [8] I. Bar-kana, H. Kaufman, and M. Balas. Model reference adaptive control of large structural systems. *Journal of Guidance and Control*, 6(2):112–118, 1983.
- [9] K.-J. Bathe. *Finite Element Procedures in Engineering Analysis*. Prentice-Hall, Englewood Cliffs, 1982.
- [10] R. J. Benhabib, R.P. Iwens, and R.L. Fackson. Stability of large space structure control systems using positivity concepts. *Journal of Guidance and Control*, 4(5):487–494, 1981.
- [11] G. Billoud, M.A. Galland, C. Huynh Huu, and S. Candel. Adaptive active control of combustion instabilities. *Combust. Sci. and Tech.*, 81:257–283, 1992.

- [12] G.J. Bloxside, A.P. Dowling, N. Hooper, and P.J. Langhorne. Active control of reheat buzz. *AIAA Journal*, 26(7), July 1988.
- [13] M. Corless. Adaptive control of a class of nonlinearly perturbed linear systems of relative degree two. *Systems & Control Letters*, 21:59–64, 1993.
- [14] M. A. Dahleh and I.J. Diaz-Bobillo. *Control of uncertain systems. A linear programming approach*. Prentice-Hall, Englewood Cliffs, NJ, 1995.
- [15] M. de Mathelin and M. Bodson. Multivariable model reference adaptive control without constraints on the high-frequency gain matrix. *Automatica*, 31:597–604, 1995.
- [16] C. A. DeSoer and Y. T. Wang. Linear time-invariant robust servomechanism problem: A self-contained exposition. In C. T. Leondes, editor, *Control and Dynamical Systems: Advances in Theory and Application*, volume 16, pages 81–129. Academic Press, 1980.
- [17] J. C. Doyle, B. A. Francis, and A. R. Tannenbaum. *Feedback Control Theory*. Macmillan, 1992.
- [18] L. Dugard and J.M. Dion. Direct adaptive control for linear multivariable systems. *International Journal of Control*, 42(6):1251–1281, 1985.
- [19] H. Elliott and W.A. Wolovich. Parameter adaptive control of linear multivariable systems. *IEEE Transactions on Automatic Control*, 27:340–352, 1982.
- [20] B.A. Francis and W.M. Wonham. The internal model principle of control theory. *Automatica*, 12(5):457–465, 1976.
- [21] Y-T. Fung and V. Yang. Active control of nonlinear pressure oscillations in combustion chambers. *Journal of Propulsion and Power*, Vol. 8, No. 6:1282–1289, 1992.
- [22] Y.-T. Fung, V. Yang, and A. Sinha. Active control of combustion instabilities with distributed actuators. *Combust. Sci. and Tech.*, 78:217–245, 1991.
- [23] F. R. Gantmakher. *Theory of Matrices*, volume 1. Chelsea Publishing Co., New York, 1959.
- [24] G. C. Goodwin and K. S. Sin. *Adaptive Filtering, Prediction, and Control*. Prentice-Hall, 1984.
- [25] A. Gulati and R. Mani. Active control of unsteady combustion-induced oscillations. *Journal of Propulsion and Power*, 8(5):1109–1115, 1992.
- [26] A. Ilchman. Non-identifier based high-gain adaptive control. In *Lecture Notes in Control and Information Sciences*, volume 189. Springer-Verlag, 1993.

- [27] P. Ioannou. Reply to comments on the robust stability analysis of adaptive controllers using normalizations. *IEEE Transactions on Automatic Control*, 35:1184, 1990.
- [28] S.M. Joshi and P.G. Maghami. Robust dissipative compensators for flexible spacecraft control. *IEEE Transactions on aerospace and electronic systems*, 28(3), 1992.
- [29] T. Kailath. *Linear Systems*. Prentice-Hall, Englewood Cliffs, NJ, 1980.
- [30] S.P. Kárason. Adaptive control in the presence of input constraints. Master's thesis, M.I.T., Cambridge, MA., 1993.
- [31] H. Kaufman and G. W. Neat. Asymptotically stable multiple-input multiple-output direct model reference adaptive controller for processes not necessarily satisfying a positive real constraint. *International Journal of Control*, 58(5):1011–1031, 1993.
- [32] B. Kouvaritakis and A.G.J. MacFarlane. Geometric approach to analysis and synthesis of system zeros: Part 1. Square systems. *International Journal of Control*, 23(2):149–166, 1976.
- [33] B. Kouvaritakis and U. Shaked. Asymptotic behaviour of root-loci of linear multivariable systems. *International Journal of Control*, 23(3):297–340, 1976.
- [34] J. M. Krause, P. P. Khargonekar, and G. Stein. Robust adaptive control: Stability and asymptotic performance. *IEEE Transactions on Automatic Control*, 37(3):316–331, 1992.
- [35] I.D. Landau. *Adaptive Control*. Marcel Dekker, Inc., New York, 1979.
- [36] W. Lang, T. Poinsot, and S. Candel. Active control of combustion instability. *Combustion and Flame*, 70:281–289, 1987.
- [37] P.J. Langhorne, A.P. Dowling, and N. Hooper. Practical active control system for combustion oscillations. *Journal of Propulsion and Power*, 6(3):324–333, 1990.
- [38] R. Lozano-Leal and S.M. Joshi. Strictly positive real transfer functions revisited. *IEEE Transactions on Automatic Control*, 35(11):1243–1245, 1990.
- [39] A.G.J. MacFarlane and I. Postlethwaite. The generalized nyquist stability criterion and multivariable root loci. *International Journal of Control*, 25(1):81–127, 1977.
- [40] D. G. MacMartin and S. R. Hall. Control of uncertain structures using an H_∞ power flow approach. *Journal of Guidance and Control*, 14(3):521–530, 1991.
- [41] K.R. McManus, T. Poinsot, and S.M. Candel. A review of active control of combustion instabilities. *Progress in energy and combustion science*, 19(1):1–30, 1993.

- [42] D. K. Miu. Physical interpretation of transfer function zeros for simple control systems with mechanical flexibilities. *ASME Journal of Dynamic Systems, Measurement, and Control*, 113:419–424, September 1991.
- [43] A.S. Morse. A three-dimensional universal controller for the adaptive stabilization of any strictly proper minimum phase system with relative degree not exceeding two. *IEEE Transactions on Automatic Control*, 30:1188–1191, 1985.
- [44] I. H. Mufti. Model reference adaptive control of large structural systems. *Journal of Guidance and Control*, 10(5):507–509, 1987.
- [45] Y. Mutoh and R. Ortega. Interactor structure estimation for adaptive control of discrete-time multivariable nondecouplable systems. *Automatica*, 29(3):635–647, 1993.
- [46] S. M. Naik, P.R. Kumar, and B. E. Ydstie. Robust continuous-time adaptive control by parameter projection. *IEEE Transactions on Automatic Control*, 37(2):182–197, 1992.
- [47] K. S. Narendra and A. M. Annaswamy. *Stable Adaptive Systems*. Prentice-Hall, Inc., Englewood Cliffs, N.J., 1988.
- [48] K.S. Narendra and J.H. Taylor. *Frequency Domain Criteria for Absolute Stability*. Academic Press, New York, 1973.
- [49] R. W. Newcomb. *Linear Multiport Synthesis*. McGraw-Hill, New York, 1966.
- [50] M.J. O’Brien and J.R. Broussard. Feedforward control to track the output of a forced model. In *Proceedings of the IEEE CDC*, 1978.
- [51] T.P. Parr, E. Gutmark, D.M. Hanson-Parr, and K.C. Schadow. Feedback control of an unstable ducted flame. *Journal of Propulsion and Power*, 9(4):529–535, 1993.
- [52] T. Poinot, F. Bourienne, S. Candel, and E. Esposito. “Suppression of combustion instabilities by active control”. *Journal of Propulsion and Power*, 5(1):14–20, 1989.
- [53] C. Rohrs, L. Valavani, M. Athans, and G. Stein. Robustness of continuous-time adaptive control algorithms in the presence of unmodeled dynamics. *IEEE Transactions on Automatic Control*, 30:881–889, 1985.
- [54] U. Shaked and E. Soroka. On the stability robustness of the continuous-time LQG optimal control. *IEEE Transactions on Automatic Control*, 30:1039–1043, 1985.
- [55] R.P. Singh. *Stable Multivariable Adaptive Control Systems*. PhD thesis, Yale University, 1985.

- [56] R.P. Singh and K.S. Narendra. Prior information in the design of multivariable adaptive controllers. *IEEE Transactions on Automatic Control*, 29:1108–1111, December 1984.
- [57] J.-J. E. Slotine and W. Li. *Applied Nonlinear Control*. Prentice Hall, Englewood Cliffs, NJ, 1991.
- [58] G. Tao and P.A. Ioannou. Strictly positive real matrices and the Lefschetz-Kalman-Yakubovich lemma. *IEEE Transactions on Automatic Control*, 33(12):1183–1185, 1988.
- [59] G. Tao and P.A. Ioannou. Stability and robustness of multivariable adaptive control schemes. *Control and Dynamic Systems: Advances in Theory and Applications*, 53:99–124, 1993.
- [60] M. Vidyasagar. *Nonlinear Systems Analysis*. Prentice Hall, 2nd edition, 1993.
- [61] P.G. Voulgaris, M.A. Dahleh, and L.S. Valavani. Robust adaptive control: a slowly varying systems approach. *Automatica*, 30:1455–1461, 1994.
- [62] S.R. Weller and G.C. Goodwin. Hysteresis switching adaptive control of linear multivariable systems. *Automatica*, 39(7), 1994.
- [63] J. T. Wen. Time domain and frequency domain conditions for strict positive realness. *IEEE Transactions on Automatic Control*, 33(10):988–992, 1988.
- [64] T. Williams. Transmission zero bounds for large space structures, with applications. *Journal of Guidance and Control*, 12(1):33–38, 1989.
- [65] E. E. Zukoski. Afterburners. In Gordon C. Oates, editor, *The aerothermodynamics of aircraft gas turbine engines*, chapter 21, pages 42–48. Air Force Aero Propulsion Laboratory, Report No. AFAPL-TR-78-52, 1978.

Appendix A

Discretization of the Combustor Equations

A.1 Introduction

In this Appendix the finite element discretization of the fundamental laws that describe the unstable, perturbed combustion process is presented in detail. First, in Appendix A.2 the discretization is performed for the case that no mean flow and no mean heat is present. Next, in section A.3 the order of the finite element model is reduced to include a physically reasonable number of modes. Finally, in section A.4 the results are given for the case that mean flow and mean heat are present.

A.2 Discretization

When no mean heat and no mean flow is present, Eqs. (5.5) and (5.6) reduce to

$$\frac{\partial^2 p'}{\partial t^2} - \bar{c}^2 \frac{\partial^2 p'}{\partial x^2} = (\gamma - 1) \frac{\partial q'}{\partial t} \quad (\text{A.1})$$

$$\frac{\partial p'}{\partial t} + \gamma \bar{p} \frac{\partial u'}{\partial x} = (\gamma - 1) q'. \quad (\text{A.2})$$

In what follows, $p'(x, t)$ in Eq. (A.1) is solved first, $u'(x, t)$ is then found through direct integration of Eq. (A.2). Eq. (A.1) can be rewritten as

$$\bar{c}^2 \frac{\partial^2 p'}{\partial x^2} = -f^B \quad (\text{A.3})$$

where

$$f^B = (\gamma - 1) \frac{\partial q'}{\partial t} - \frac{\partial^2 p'}{\partial t^2}. \quad (\text{A.4})$$

f^B is a forcing term that acts inside the fluid body. The essential boundary condition is given by

$$p'(L, t) = 0 \quad (\text{A.5})$$

since at the outlet $\bar{p} = p$. The natural boundary condition due to an end-mounted loudspeaker follows from Eq. (A.2), evaluated at $x = 0$,

$$\begin{aligned} \frac{\partial p'}{\partial x}(0, t) &= -\bar{\rho} \frac{\partial u'}{\partial t}(0, t) - \bar{\rho} \bar{u} \frac{\partial u'}{\partial x}(0, t) \\ &= -\bar{\rho} \dot{u}_c(t), \end{aligned} \quad (\text{A.6})$$

where $\dot{u}_c(t) = \frac{\partial u'}{\partial t}(0, t)$. The natural boundary condition due to a side-mounted loudspeaker can not be derived from the one dimensional flow dynamics. However, considering the Euler equation in the radial direction and incorporating the transducer modeling considerations, the natural boundary condition for a side-mounted loudspeaker is given by

$$\frac{\partial p'}{\partial x}(x_a^+, t) = \frac{\partial p'}{\partial x}(x_a^-, t) - k_{uv} \bar{\rho} \dot{v}_c(t), \quad (\text{A.7})$$

where v_c is the velocity of the loudspeaker diaphragm. k_{uv} is a dimensionless attenuating factor which depends on the flow characteristics and the radial dimensions of the combustor. Eq. (A.7) says that the side-mounted loudspeaker affects the pressure gradient at $x = x_a$.

Eqs. (A.3)–(A.7) specify the solution of $p'(x, t)$. Below we will derive a finite dimensional fit in x to p' using a finite element discretization. Similar to the principle

of virtual work, we multiply Eq. (A.3) with an admissible virtual pressure $\delta p'$ and integrate from 0 to L ,

$$\int_0^L \left(\bar{c}^2 \frac{\partial^2 p'}{\partial x^2} + f^B \right) \delta p' dx = 0. \quad (\text{A.8})$$

Note that

$$\frac{\partial}{\partial x} \left(\frac{\partial p'}{\partial x} \delta p' \right) = \frac{\partial^2 p'}{\partial x^2} \delta p' + \frac{\partial p'}{\partial x} \frac{\partial \delta p'}{\partial x},$$

so that Eq. (A.8) can be written as

$$\int_0^L \left(\bar{c}^2 \left[\frac{\partial}{\partial x} \left(\frac{\partial p'}{\partial x} \delta p' \right) - \frac{\partial p'}{\partial x} \frac{\partial \delta p'}{\partial x} \right] + f^B \delta p' \right) dx = 0. \quad (\text{A.9})$$

We have that

$$\begin{aligned} & \int_0^L \frac{\partial}{\partial x} \left(\frac{\partial p'}{\partial x} \delta p' \right) dx \\ &= \int_0^{x_a} \frac{\partial}{\partial x} \left(\frac{\partial p'}{\partial x} \delta p' \right) dx + \int_{x_a}^L \frac{\partial}{\partial x} \left(\frac{\partial p'}{\partial x} \delta p' \right) dx \\ &= \frac{\partial p'}{\partial x} \delta p' \Big|_0^{x_a^-} + \frac{\partial p'}{\partial x} \delta p' \Big|_{x_a^+}^L \\ &= -\frac{\partial p'}{\partial x} \delta p'(0, t) + \left(\frac{\partial p'}{\partial x}(x_a^-, t) - \frac{\partial p'}{\partial x}(x_a^+, t) \right) \delta p'(x_a, t) + \frac{\partial p'}{\partial x} \delta p'(L, t) \\ &= \bar{\rho} \dot{u}_c \delta p'_o + k_{uv} \bar{\rho} \dot{v}_c \delta p'_a \end{aligned} \quad (\text{A.10})$$

where $\delta p'_o = \delta p'(0, t)$, and $\delta p'_a = \delta p'(x_a, t)$. The last equality in Eq. (A.10) follows from the natural boundary conditions given by Eqs. (A.6) and (A.7), and the fact that $\delta p'$ is an admissible variation, i.e. $\delta p'(L, t) = 0$. Using Eq. (A.10), it follows that Eq. (A.9) can be written as

$$\bar{c}^2 \int_0^L \frac{\partial p'}{\partial x} \frac{\partial \delta p'}{\partial x} dx = \int_0^L f^B \delta p' dx + \bar{\rho} \bar{c}^2 \dot{u}_c \delta p'_o + k_{uv} \bar{\rho} \bar{c}^2 \dot{v}_c \delta p'_a. \quad (\text{A.11})$$

We will divide the duct into N elements, Eq. (A.11) can then be rewritten as a sum

of integrations over the length of all elements,

$$\sum_{m=1}^N \bar{c}^2 \int_{L^{(m)}} \frac{\partial p'^{(m)}}{\partial x} \frac{\partial \delta p'^{(m)}}{\partial x} dx = \sum_{m=1}^N \int_{L^{(m)}} f^B{}^{(m)} \delta p'^{(m)} dx + \bar{\rho} \bar{c}^2 \dot{u}_c \delta p'_o + k_{uv} \bar{\rho} \bar{c}^2 \dot{u}_c \delta p'_a. \quad (\text{A.12})$$

In the finite element method, the pressure in the m^{th} element is approximated by

$$p'^{(m)}(x, t) = H^{(m)}(x)P(t) \quad (\text{A.13})$$

where $H^{(m)}$ is the pressure interpolation matrix for the m^{th} element, and P is an n -dimensional vector with nodal pressures. Similarly, the admissible pressure variations are interpolated as

$$\delta p'^{(m)}(x, t) = H^{(m)}(x)\hat{P}(t) \quad (\text{A.14})$$

where \hat{P} is the vector with nodal pressure variations. If o denote the number of nodes per elements, then $H^{(m)}(x)$ is of the form

$$H^{(m)}(x) = [0 \quad \dots \quad 0 \quad h_1^{(m)}(x) \quad \dots \quad h_o^{(m)}(x) \quad 0 \quad \dots \quad 0].$$

The one-dimensional interpolation functions h_i^m chosen depend on the number of nodes o per element. For example, 2, 3 or 4 node elements can be used. For 2 node elements, linear interpolation functions would be used, for 3 node elements quadratic interpolation functions would be used [9]. For the variation $\delta p'_o$ and $\delta p'_a$ we have, respectively,

$$\delta p'_o = H^{(1)}(x=0)\hat{P}(t), \quad (\text{A.15})$$

$$\delta p'_a = H^{(m_a)}(x_a)\hat{P}(t), \quad (\text{A.16})$$

where m_a denotes the element in which x_a lies. We will develop an iso-parametric finite element discretization in which the pressure gradient is interpolated as

$$\frac{\partial p'^{(m)}(x, t)}{\partial x} = B^{(m)}(x)P(t)$$

$$\frac{\partial \delta p^{(m)}(x, t)}{\partial x} = B^{(m)}(x) \hat{P}(t) \quad (\text{A.17})$$

where $B^{(m)}(x) = \frac{d}{dx} H^{(m)}(x)$.

Substituting Eqs. (A.13)–(A.17) into Eq. (A.12) results in

$$\hat{P}^T(t) K P(t) = \hat{P}^T(t) F^B(t) + \hat{P}^T(t) F^S(t) \quad (\text{A.18})$$

where

$$\begin{aligned} K &= \sum_m K^{(m)}, & K^{(m)} &= \bar{c}^2 \int_{L^{(m)}} B^{(m)T}(x) B^{(m)}(x) dx, \\ F^B(t) &= \sum_m F^{(m)B}(t), & F^{(m)B}(t) &= \int_{L^{(m)}} H^{(m)T}(x) f^{B(m)}(x, t) dx, \\ F^S(t) &= F_u^S(t) + F_v^S(t), & F_u^S(t) &= B_{pcu} \bar{\rho} \bar{c}^2 \dot{u}_c(t), & B_{pcu} &= H^{(1)T}(0), \\ F_v^S(t) &= B_{pcv} k_{uv} \bar{\rho} \bar{c}^2 \dot{v}_c(t), & B_{pcv} &= H^{(m_a)T}(x_a). \end{aligned}$$

We now choose the nodal variations as $\hat{P} = e_i$ for $i = 1, \dots, n$, where e_i is a basis vector in \mathbb{R}^n . Combining the resulting n equations we obtain

$$K P(t) = F^B(t) + F^S(t). \quad (\text{A.19})$$

Substituting for the body forcing term in Eq. (A.4), we find that Eq. (A.19) can be written as

$$M \ddot{P}(t) + K P(t) = F^q(t) + F^S(t), \quad (\text{A.20})$$

where M is given by

$$M = \sum_m M^{(m)}, \quad M^{(m)} = \int_{L^{(m)}} H^{(m)T}(x) H^{(m)}(x) dx,$$

and the forcing function due to heat generation is given by

$$F^q(t) = (\gamma - 1) \sum_m \int_{L^{(m)}} H^{(m)T}(x) \frac{\partial q(x, t)}{\partial t} dx.$$

For the system we are considering, the heat generated is localized to $x = x_o$ so that

$$q(x, t) = \delta(x - x_o)q'_o(t)$$

where $\delta(\cdot)$ is the Dirac impulse function, and q'_o is the heat generated per unit area given in Eq. (5.12). Hence, for localized heat generation, $F^q(t)$ can be simplified as

$$F^q(t) = B_{pqd}(\gamma - 1)q'_o(t) \quad B_{pqd} = H^{(m_o)^T}(x_o)$$

where m_o denotes the element in which x_o lies. P is an n dimensional vector containing the modal pressures. Let P_i be the i^{th} component of P , and let P be ordered such that P_1 corresponds to the pressure for the node at $x = 0$, and P_n corresponds to the pressure for the node at $x = L$. The essential boundary condition given by Eq. (A.5) prescribes that $P_n = 0$. Eq. (A.20) can therefore be reduced by one degree of freedom by eliminating the last row and last column. To avoid proliferation of notation we will assume that this reduction has been performed, and that the resulting P is n dimensional.

We will use the solution for $p(x, t)$ to find the solution for $u'_o(t)$ in Eq. (5.7). The essential boundary condition for $u'(x, t)$ is given by

$$u'(0, t) = 0. \quad (\text{A.21})$$

Since $\bar{p} \neq 0$ we have from Eq. (A.2)

$$\frac{\partial u'}{\partial x} = \frac{1}{\gamma\bar{p}} \left[(\gamma - 1)q' - \frac{\partial p'}{\partial t} \right].$$

Integrating this equation from $x = 0$ to L , with the interpolation of $p'(x, t)$ given by Eq. (A.13) and using Eq. (A.21), results in

$$\begin{aligned} u'_o(t) &= u'(0, t) + a_o \int_o^{x_o} q'(x, t) dx - \frac{1}{\gamma\bar{p}} \int_o^{x_o} \frac{\partial p'}{\partial t} dx \\ &= a_o q'_o(t) - \frac{1}{\gamma\bar{p}} C_{qpd} \dot{P}(t), \end{aligned}$$

where

$$a_o = \frac{\gamma - 1}{\gamma \bar{p}}, \quad C_{qpd} = \sum_{m=1}^{m_o-1} \int_{L^{(m)}} H^{(m)}(\xi) d\xi + \int_{\frac{(m_o-1)}{N}L}^{x_o} H^{(m_o)}(\xi) d\xi.$$

Summarizing the results of this section, the finite element discretization of the governing partial differential equations is given by

$$M\ddot{P}(t) + KP(t) = B_{pqd}(\gamma - 1)\dot{q}'_o(t) + B_{pcu}\bar{\rho}\bar{c}^2\dot{u}_c(t) + B_{pcv}k_{uv}\bar{\rho}\bar{c}^2\dot{v}_c(t) \quad (\text{A.22})$$

$$u'_o(t) = a_o q'_o(t) - \frac{1}{\gamma \bar{p}} C_{qpd} \dot{P}(t) \quad (\text{A.23})$$

$$\dot{q}'_o(t) = -\alpha_2 q'_o(t) + \alpha_1 u'_o(t). \quad (\text{A.24})$$

These equations can be simplified by eliminating u'_o . Substituting Eq. (A.23) into Eq. (A.24) we find

$$\dot{q}'_o(t) = -\alpha_3 q'_o(t) - \alpha_1 \frac{1}{\gamma \bar{p}} C_{qpd} \dot{P}(t), \quad (\text{A.25})$$

where

$$\alpha_3 = \alpha_2 - \alpha_1 a_o.$$

Substituting Eq. (A.25) into Eq. (A.22) results in

$$\begin{aligned} M\ddot{P}(t) + B_{pqd}\alpha_1 a_o C_{qpd} \dot{P}(t) + KP(t) = \\ -B_{pqd}(\gamma - 1)\alpha_3 q'_o(t) + B_{pcu}\bar{\rho}\bar{c}^2\dot{u}_c(t) + B_{pcv}k_{uv}\bar{\rho}\bar{c}^2\dot{v}_c(t). \end{aligned} \quad (\text{A.26})$$

The pressure perturbation at the microphone location x_s is given by

$$p'_s(t) = H^{(m_s)}(x_s)P(t) = C_{cp}P(t), \quad (\text{A.27})$$

where x_s lies in element m_s . Eqs. (A.25), (A.26) and (A.27) completely specify the input–output dynamics of the system.

A.3 Reduced Mode Superposition

In the previous section we derived a finite dimensional representation of the system dynamics. The order of the system described by Eq. (A.26) is too high for several reasons. First, the modal frequencies and mode shapes computed at high frequencies are inaccurate by the very nature of finite element analysis, and should therefore not be excited in a realistic dynamic model. Second, the frequency range spanned by all n modes is a much larger frequency range than we are interested in from the viewpoint of controller bandwidth, and frequency content of external disturbances. Typically the model is required to be accurate to within 4 to 10 times the controller bandwidth. Hence, the presence of higher modes in the model is undesirable and a lower order model for the system dynamics described by Eqs. (A.25), (A.26) and (A.27) should be obtained. The added advantage of such a lower order model is that it is suitable to be used in a model based control method.

Based on computational considerations, a technique frequently employed in dynamic finite element analysis is to reduce the order of the governing equations by reducing the number of modes considered in a mode superposition solution. The number of modes retained is typically chosen to include all modes whose frequencies lie below 4 to 10 times the highest frequency expected in the external forcing terms. The non retained modes are not excited and their dynamic contribution is therefore discarded. The static contribution of the non retained modes is incorporated through what is known as a static correction. In this section we will apply this technique to the system described by Eqs. (A.25), (A.26) and (A.27).

An accurate model of the system in the frequency range of interest may be determined by looking at the open loop mode shapes ϕ_i ($i = 1, \dots, n$) found as the solution of the generalized eigenvalue problem

$$K\phi_i = M\omega_i^2\phi_i. \quad (\text{A.28})$$

Having determined the required number of elements N , the number retained modes p and the number of non retained modes ($n - p$), a low order dynamic model can

be obtained as described below. A full mode superposition solution of Eq. (A.25) is found by setting

$$P = \Phi \eta$$

where $\Phi = [\phi_1 \ \phi_2 \ \dots \ \phi_n]$ is the solution to Eq. (A.28), and η is the vector with modal coordinates. The eigenvectors are normalized such that

$$\Phi^T M \Phi = I, \quad \Phi^T K \Phi = \Omega^2,$$

where $\Omega = \text{diag}(\omega_1, \omega_2, \dots, \omega_n)$. We will order the modal frequencies in ascending order, $\omega_1 \leq \omega_2 \leq \dots \leq \omega_n$, and order the eigenvectors ϕ_i ($i = 1, \dots, n$) correspondingly. The modal decomposition can then be partitioned as

$$P = [\Phi_r \ \Phi_{nr}] \begin{bmatrix} \eta_r \\ \eta_{nr} \end{bmatrix} \quad (\text{A.29})$$

where $\eta_r : \mathbb{R}^+ \rightarrow \mathbb{R}^p$ is the vector with modal coordinates of the retained modes, and $\eta_{nr} : \mathbb{R}^+ \rightarrow \mathbb{R}^{(n-p)}$ is the vector of modal coordinates of the non retained modes. Substituting the decomposition given by Eq. (A.29) into Eq. (A.26), and premultiplying with Φ^T , results in

$$\begin{aligned} & \begin{bmatrix} I_p & 0 \\ 0 & I_{(n-p)} \end{bmatrix} \begin{bmatrix} \ddot{\eta}_r \\ \ddot{\eta}_{nr} \end{bmatrix} + \begin{bmatrix} \Phi_r^T \\ \Phi_{nr}^T \end{bmatrix} B_{pqd} \alpha_1 a_o C_{qpd} [\Phi_r \ \Phi_{nr}] \begin{bmatrix} \dot{\eta}_r \\ \dot{\eta}_{nr} \end{bmatrix} + \begin{bmatrix} \Omega_r^2 & 0 \\ 0 & \Omega_{nr}^2 \end{bmatrix} \begin{bmatrix} \eta_r \\ \eta_{nr} \end{bmatrix} = \\ & - \begin{bmatrix} \Phi_r^T B_{pqd} \\ \Phi_{nr}^T B_{pqd} \end{bmatrix} (\gamma - 1) \alpha_3 q'_o + \begin{bmatrix} \Phi_r^T B_{pcu} \\ \Phi_{nr}^T B_{pcu} \end{bmatrix} \bar{\rho} \bar{c}^2 \dot{u}_c + \begin{bmatrix} \Phi_r^T B_{pcv} \\ \Phi_{nr}^T B_{pcv} \end{bmatrix} k_{uv} \bar{\rho} \bar{c}^2 \dot{v}_c, \end{aligned} \quad (\text{A.30})$$

where $\Omega_r = \text{diag}(\omega_1, \omega_2, \dots, \omega_p)$ and $\Omega_{nr} = \text{diag}(\omega_{p+1}, \omega_2, \dots, \omega_n)$. For Eqs. (A.25) and (A.27) we have

$$\dot{q}'_o = -\alpha_3 q'_o - \alpha_1 \frac{1}{\gamma \bar{\rho}} C_{qpd} [\Phi_r \ \Phi_{nr}] \begin{bmatrix} \dot{\eta}_r \\ \dot{\eta}_{nr} \end{bmatrix}, \quad (\text{A.31})$$

$$p'_s = C_{cp} [\Phi_r \ \Phi_{nr}] \begin{bmatrix} \eta_r \\ \eta_{nr} \end{bmatrix}. \quad (\text{A.32})$$

Based on the considerations discussed in the beginning of this section, we assume that the non retained modes are not excited. Hence

$$\ddot{\eta}_{nr}(t) \equiv 0, \quad \text{and} \quad \dot{\eta}_{nr}(t) \equiv 0. \quad (\text{A.33})$$

Note however that we will still incorporate the static contribution of the non retained modes in the analysis. The reduced model is found by substituting Eq. (A.33) into Eqs. (A.30), (A.31) and (A.32) and eliminating η_{nr} . The result, in first order control form, is given by

$$\begin{aligned} \dot{x}_r &= A_r x_r - B_{rq} q'_o + B_{rcu} \dot{u}_c + B_{rcv} \dot{v}_c \\ \dot{q}'_o &= -\alpha_3 q'_o - \alpha_1 C_{qr} x_r \\ \dot{p}'_s &= C_{sr} x_r - D_{sq} q'_o + D_{scu} \dot{u}_c + D_{scv} \dot{v}_c \end{aligned}$$

where

$$\begin{aligned} x_r &= \begin{bmatrix} \eta_r \\ \dot{\eta}_r \end{bmatrix}, \\ A_r &= \begin{bmatrix} 0 & I_p \\ -\Omega_r^2 & -\Phi_r^T B_{pqd} \alpha_1 a_o C_{qpd} \Phi_r \end{bmatrix}, \\ B_{rq} &= \begin{bmatrix} 0 \\ \Phi_r^T B_{pqd} \end{bmatrix} (\gamma - 1) \alpha_3, \\ B_{rcu} &= \begin{bmatrix} 0 \\ \Phi_r^T B_{pcu} \end{bmatrix} \bar{\rho} \bar{c}^2, \\ B_{rcv} &= \begin{bmatrix} 0 \\ \Phi_r^T B_{pcv} \end{bmatrix} k_{uv} \bar{\rho} \bar{c}^2, \\ C_{qr} &= \left[0 \quad \frac{1}{\gamma \bar{\rho}} C_{qpd} \Phi_r \right], \\ C_{sr} &= \left[C_{cp} \Phi_r \quad -C_{cp} \Phi_{nr} \Omega_{nr}^{-2} \Phi_{nr}^T B_{pqd} \alpha_1 a_o C_{qpd} \Phi_r \right], \\ D_{sq} &= C_{cp} \Phi_{nr} \Omega_{nr}^{-2} \Phi_{nr}^T B_{pqd} (\gamma - 1) \alpha_3, \\ D_{scu} &= C_{cp} \Phi_{nr} \Omega_{nr}^{-2} \Phi_{nr}^T B_{pcu} \bar{\rho} \bar{c}^2, \\ D_{scv} &= C_{cp} \Phi_{nr} \Omega_{nr}^{-2} \Phi_{nr}^T B_{pcv} k_{uv} \bar{\rho} \bar{c}^2. \end{aligned}$$

A.4 Mean Heat and Mean Flow

In the solution of the fundamental laws in section A.2 we assumed that $\bar{u} = 0$ and $\bar{q} = 0$. We will now rederive the solution of Eqs. (5.5) and (5.6) in the case that these mean variables are not zero. Specifically, we will consider the case that $\bar{M} < 1$. With $\bar{M} < 1$, Eq. (5.5) can be written as

$$\frac{\partial^2 p'}{\partial t^2} - \bar{c}^2 \frac{\partial^2 p'}{\partial x^2} + 2\bar{u} \frac{\partial^2 p'}{\partial x \partial t} = (\gamma - 1) \left[\frac{\partial q'}{\partial t} + \bar{u} \frac{\partial q'}{\partial x} \right]. \quad (\text{A.34})$$

The essential boundary condition is

$$p'(L, t) = 0.$$

The natural boundary condition in case of an end-mounted loudspeaker is given by

$$\begin{aligned} \frac{\partial p'(0, t)}{\partial x} &= -\bar{\rho}_1 \frac{\partial u'(0, t)}{\partial t} - \bar{\rho}_1 \bar{u}_1 \frac{\partial u'(0, t)}{\partial x} \\ &= -\bar{\rho}_1 \dot{u}_c(t), \end{aligned} \quad (\text{A.35})$$

where we assumed that the second term in Eq. (A.35) is negligible. This assumption is reasonable since at $x = 0$ the mean flow enters radially. The natural boundary condition in case a side-mounted loudspeaker is used is given by

$$\frac{\partial p'}{\partial x}(x_a^+, t) = \frac{\partial p'}{\partial x}(x_a^-, t) - k_{uv} \bar{\rho} \dot{v}_c(t),$$

where we neglect the effect of \bar{u} on the radial pressure distribution at $x = x_a$. Multiplying Eq. (A.34) with an admissible pressure and integrating from 0 to L results in

$$\int_0^L \left(\bar{c}^2 \frac{\partial^2 p'}{\partial x^2} - 2\bar{u} \frac{\partial^2 p'}{\partial x \partial t} + f^B \right) \delta p' dx = 0$$

where

$$f^B = (\gamma - 1) \left[\frac{\partial q'}{\partial t} + \bar{u} \frac{\partial q'}{\partial x} \right] - \frac{\partial^2 p'}{\partial t^2}.$$

A finite element discretization similar to the one performed in section A.2 can be carried out. However, since \bar{u} and \bar{c} are not constant over the entire duct, different elements have to be used for $x < x_o$ and $x > x_o$. The following result is obtained:

$$\begin{aligned}
M\ddot{P} + \tilde{G}\dot{P} + (\tilde{K} + \tilde{K}_o)P &= -\tilde{B}_{pqd}q'_o + B_{pcu}\bar{\rho}_1\bar{c}_1^2\dot{u}_c + B_{pcv}k_{uv}\bar{\rho}_a\bar{c}_a^2\dot{u}_c \\
\dot{q}'_o &= -\alpha_3q'_o - \alpha_1\left(\frac{1}{\gamma\bar{p}}C_{qpd}\dot{P} + \frac{\bar{u}_1}{\gamma\bar{p}}C_{qp}P\right) \\
p'_s &= C_{cp}P,
\end{aligned} \tag{A.36}$$

where $\bar{\rho}_a = \bar{\rho}(x_a)$ and $\bar{c}_a = \bar{c}(x_a)$. The matrices and vectors are defined as in section A.2. Due to the different element properties used for $x < x_o$ and $x > x_o$ we have

$$\begin{aligned}
\tilde{K} &= \sum_{m=1}^{m_1} K_1^{(m)} + \sum_{m=m_1+1}^N K_2^{(m)}, \\
\tilde{K}_o &= B_{pqd}\alpha_1 a_o \bar{u}_1 C_{qp} + \sum_m K_o^{(m)}, \\
K_1^{(m)} &= \bar{c}_1^2 \int_{L^{(m)}} B^{(m)T}(x) B^{(m)}(x) dx, \\
K_2^{(m)} &= \bar{c}_2^2 \int_{L^{(m)}} B^{(m)T}(x) B^{(m)}(x) dx, \\
K_o^{(m)} &= H^{(m)T}(x_o) \left[\bar{c}_2^2 B^{(m_1+1)}(x_o) - \bar{c}_1^2 B^{(m_1)}(x_o) \right],
\end{aligned}$$

where m_1 is the element directly to the left of x_o . The transport effect of the mean flow, and the destabilizing effect of the flame feedback, is expressed by

$$\begin{aligned}
\tilde{G} &= G + B_{pqd}\alpha_1 a_o C_{qpd}, \\
G &= \sum_{m=1}^{m_1} G_1^{(m)} + \sum_{m=m_1+1}^N G_2^{(m)}, \\
G_1^{(m)} &= 2\bar{u}_1 \int_{L^{(m)}} H^{(m)T}(x) B^{(m)}(x) dx, \\
G_2^{(m)} &= 2\bar{u}_2 \int_{L^{(m)}} H^{(m)T}(x) B^{(m)}(x) dx,
\end{aligned}$$

and

$$B_{pq} = B^{(m_1+1)T}(x_o),$$

$$\begin{aligned}\tilde{B}_{pqd} &= B_{pqd}(\gamma - 1)\alpha_3 + B_{pq}(\gamma - 1)\bar{u}_2, \\ C_{qp} &= \sum_{m=1}^{m_1} \int_{L^{(m)}} B^{(m)}(\xi) d\xi.\end{aligned}$$

The reduced order model of the full order model described by Eq. (A.36) can be derived as follows. Let $\tilde{\Phi}$ denote the eigenvectors of the generalized eigenvalue problem

$$\tilde{K}\tilde{\Phi} = M\tilde{\Phi}\tilde{\Omega}^2.$$

Using the frequencies $\tilde{\Omega}$ and modeshapes $\tilde{\Phi}$, the model reduction method outlined in section A.3 can be carried out for the system described by Eq. (A.36). The result is:

$$\begin{aligned}\dot{x}_{rm} &= A_{rm}x_{rm} - B_{rmq}q'_o + B_{rmcu}\dot{u}_c + B_{rmcv}\dot{v}_c \\ \dot{q}'_o &= -\alpha_3q'_o - \alpha_1(C_{qrm}x_{rm} - D_{qq}q'_o + D_{qcu}\dot{u}_c + D_{qcv}\dot{v}_c) \\ \dot{p}'_s &= C_{srm}x_{rm} - D_{sqm}q'_o + D_{scum}\dot{u}_c + D_{scvm}\dot{v}_c\end{aligned}$$

where

$$\begin{aligned}x_{rm} &= \begin{bmatrix} \eta_r \\ \dot{\eta}_r \end{bmatrix}, \\ A_{rm} &= \begin{bmatrix} 0 & I_p \\ -\tilde{\Omega}_r^2 - \tilde{\Phi}_r^T(\tilde{K}_o - \tilde{K}_o\tilde{\Phi}_{nr}\Omega_s^{-2}\tilde{\Phi}_{nr}^T\tilde{K}_o)\tilde{\Phi}_r & -\tilde{\Phi}_r^T\tilde{G}\tilde{\Phi}_r \end{bmatrix}, \\ B_{rmq} &= \begin{bmatrix} 0 \\ \tilde{\Phi}_r^T(I - \tilde{K}_o\tilde{\Phi}_{nr}\Omega_s^{-2}\tilde{\Phi}_{nr}^T)\tilde{B}_{pqd} \end{bmatrix}, \\ B_{rmcu} &= \begin{bmatrix} 0 \\ \tilde{\Phi}_r^T(I - \tilde{K}_o\tilde{\Phi}_{nr}\Omega_s^{-2}\tilde{\Phi}_{nr}^T)B_{pcu} \end{bmatrix} \bar{\rho}_1 \bar{c}_1^2, \\ B_{rmcv} &= \begin{bmatrix} 0 \\ \tilde{\Phi}_r^T(I - \tilde{K}_o\tilde{\Phi}_{nr}\Omega_s^{-2}\tilde{\Phi}_{nr}^T)B_{pcv} \end{bmatrix} k_{uv}\bar{\rho}_a \bar{c}_a^2, \\ C_{qrm} &= \frac{1}{\gamma\bar{p}} [\bar{u}_1 C_{qp}(I - \tilde{\Phi}_{nr}\Omega_s^{-2}\tilde{\Phi}_{nr}^T\tilde{K}_o)\tilde{\Phi}_r \quad C_{qpd}(I - \tilde{\Phi}_{nr}\Omega_s^{-2}\tilde{\Phi}_{nr}^T\tilde{G})\tilde{\Phi}_r], \\ D_{qq} &= \frac{\bar{u}_1}{\gamma\bar{p}} C_{qp}\tilde{\Phi}_{nr}\Omega_s^{-2}\tilde{\Phi}_{nr}^T\tilde{B}_{pqd}, \\ D_{qcu} &= \frac{\bar{u}_1}{\gamma\bar{p}} C_{qp}\tilde{\Phi}_{nr}\Omega_s^{-2}\tilde{\Phi}_{nr}^T B_{pcu}\bar{\rho}_1 \bar{c}_1^2,\end{aligned}$$

$$\begin{aligned}
D_{qcv} &= \frac{\bar{u}_1}{\gamma \bar{p}} C_{qp} \tilde{\Phi}_{nr} \Omega_s^{-2} \tilde{\Phi}_{nr}^T B_{pcv} k_{vu} \bar{\rho}_a \bar{c}_a^2, \\
C_{srm} &= [C_{cp} (I - \tilde{\Phi}_{nr} \Omega_s^{-2} \tilde{\Phi}_{nr}^T \tilde{K}_o) \tilde{\Phi}_r \quad -C_{cp} \tilde{\Phi}_{nr} \Omega_s^{-2} \tilde{\Phi}_{nr}^T \tilde{G} \tilde{\Phi}_r], \\
D_{sqm} &= C_{cp} \tilde{\Phi}_{nr} \Omega_s^{-2} \tilde{\Phi}_{nr}^T \tilde{B}_{pqd}, \\
D_{scum} &= C_{cp} \tilde{\Phi}_{nr} \Omega_s^{-2} \tilde{\Phi}_{nr}^T B_{pcu} \bar{\rho}_1 \bar{c}_1^2, \\
D_{scvm} &= C_{cp} \tilde{\Phi}_{nr} \Omega_s^{-2} \tilde{\Phi}_{nr}^T B_{pcu} k_{uv} \bar{\rho}_a \bar{c}_a^2,
\end{aligned}$$

and

$$\begin{aligned}
\tilde{G} &= \tilde{G} + \tilde{K}_o \tilde{\Phi}_{nr} \Omega_s^{-2} \tilde{\Phi}_{nr}^T \tilde{G} \\
\Omega_s^2 &= \tilde{\Omega}_{nr}^2 + \tilde{\Phi}_{nr}^T (\tilde{K}_o + B_{pqd} \alpha_1 a_o \bar{u}_1 C_{qp}) \tilde{\Phi}_{nr},
\end{aligned}$$

Ω_s is assumed to be invertible.

4538-1